



**UNIVERSITY of the  
WESTERN CAPE**

**NON-INVASIVE CHARACTERIZATION OF UNSATURATED ZONE TRANSPORT IN  
DRY COAL ASH DUMPS: A CASE STUDY OF TUTUKA, SOUTH AFRICA**

by

**Innocent Muchingami**

A Thesis submitted in fulfilment of the requirements of the degree of  
UNIVERSITY of the  
WESTERN CAPE  
**Doctor of Philosophy**

in the

**Department of Earth Sciences**

**Faculty of Natural Sciences**

Supervisors:

**Professor Y. Xu**

**Doctor J. M. Nel**

**October 2013**

**DECLARATION**

I, Innocent Muchingami declare that **NON-INVASIVE CHARACTERIZATION OF UNSATURATED ZONE TRANSPORT IN DRY COAL ASH DUMPS: A CASE STUDY OF TUTUKA, SOUTH AFRICA** is my own work, that it has not been submitted before for any degree or examination in any other university, and that all the sources I have used or quoted have been indicated and acknowledged as complete reference.



Innocent Muchingami

October 2013



Signed.....



UNIVERSITY *of the*  
WESTERN CAPE

## ACKNOWLEDGEMENTS

- First and foremost, I would like to thank my Supervisors, Professor Y. Xu and Dr J. M. Nel, for guiding and advising me throughout the course of my studies. Without them this thesis would have never been accomplished. A special mention will go to Dr J. M. Nel for giving me the opportunity to study at UWC.
- I am also very grateful to ESKOM for funding this project as well as allowing me and the UWC Groundwater group permission to access the Tutuka ash dump.
- I am thankful to the Department of Earth Sciences and the division of Post-Graduate studies for their contributions towards building my capacity as a student and making the necessary facilities and structures available that contributed towards finishing this project.
- A big thank to all fellow graduate students, during my study for their friendship, support and encouragement. Names may not be necessary; we walked the journey together, and I learnt a lot from you.
- My heartfelt thanks go to all my family members, and friends for their continual prayers, encouragement, moral support and the faith we kept in each other.
- Above all, I give to God all the praise, glory and adoration. I thank Him for giving me the precious gift of life and giving me the strength to overcome all the challenges which characterized this journey.

## ABSTRACT

The management of the large volumes of solid wastes produced as coal combustion residue is of particular concern due to the presence of leachable metals and salts which may constitute a long term environmental risk and potential contamination of both surface and groundwater systems of the surrounding environment. In order to implement an efficient monitoring scheme and to assess the impact of the ash dump on the hydrologic system, a thorough knowledge on the migration of solutes fluxes in dry ash dumps as well as the controls on the transport of these solutes to the underlying groundwater system is required.

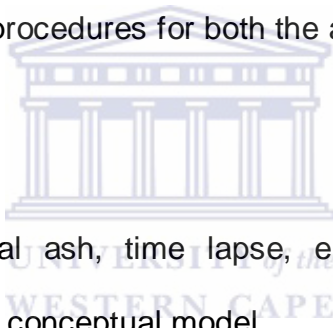
The conventional methods which have been widely used for such applications are centred on extracting and analysing several samples from observation wells are drilled on the dump. This has however created a potentially hazardous situation as the installation of monitoring wells may result in the creation of new fluid pathways and results in further migration of leachates. Nevertheless, non-invasive characterization has often been useful in the determination of subsurface hydraulic properties and is a key step towards the solution of real-life problems in hydrology, hydrogeology and soil science. In contaminant transport non-invasive methods have often proved to be an efficient tool as compared to traditional drilling and sampling techniques which in most cases results in the creation of preferential flow paths and do not allow for the space and time resolution needed for the monitoring of hydrological and environmental processes.

In this context, this study seeks to develop a generic conceptual model for the ash dump through the use of non-invasive geophysical techniques and numerical modelling

techniques at the Tutuka Ash dump, Mpumalanga South Africa. Changes in electrical resistivity were used correlate changes in moisture contents during moisture and salt leachate ingress in ash dumps with a sufficient accuracy. A determination of the suitability of Archie's law to describe the relationship between electrical resistivity and solute transport ash medium was achieved through empirical laboratory experiments. Electrical resistivity tomography was then used as an appropriate tool for the elucidation of potential flow paths and brine dispersion in the ash dump. The flow rates through the ash dump were estimated by considering the rate of brine injection and the distance travelled by the brine plume over the time spanned in time lapse infiltration experiments. Additional geophysical profiles managed to show the lithostratigraphy of underlying hydro-geology, thereby ensuring that the knowledge of the geology can be established without the application of any intrusive methods.

To ensure that development of the conceptual model of the unsaturated zone transport of the ash dump was developed with sufficient accuracy, numerical models were also used to describe solute transport in the vadose zone. The HYDRUS2D numerical package was used simulate the flux dynamics within the unsaturated zone of the coal ash medium, so as to develop a conceptual understanding of water flow and salt transport through the unsaturated zone of the coal ash medium. The results from the study suggested a conceptual solute transport model that consists of a two layers. The upper layer represented the unsaturated zone of the ash dump which was the source of any potential contaminant transport that could be of concern. The lower layer describe the underlying the subsurface environment to the ash dump which include the soil zone, the shallow aquifer and the deep fractured rock aquifer.

To enable this conceptualisation, results from the numerical simulations and geophysical interpretations of the electrical resistivity profiles were the critical components for optimising the site-specific subsurface water flow and solute transport processes, as well as producing the most acceptable conceptualisation of the ash dump system that could be used in hazard assessment and mitigation against potential groundwater pollution. The conceptual models developed in this study proposed an explanation on impact of the ash dump to the hydro-geologic and the eco-hydrologic environment by proposing a scenario of contamination of the underlying ash dump and the existing. In this regard, the study managed to provide important scenarios that may be necessary during mitigation procedures for both the ash dump and the wetland.



**Key words:** non-invasive, coal ash, time lapse, electrical resistivity tomography, numerical models, HYDRUS2D, conceptual model.

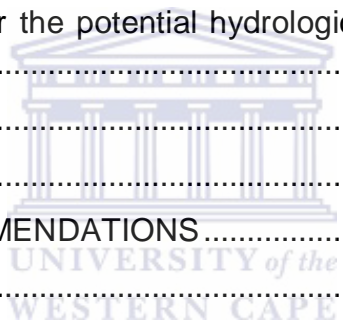
## TABLE OF CONTENTS

DECLARATION .....	i
ACKNOWLEDGEMENTS .....	iii
ABSTRACT.....	iv
LIST OF FIGURES AND PHOTOS .....	x
LIST OF TABLES .....	xiii
CHAPTER 1.....	1
INTRODUCTION.....	1
1.1 Background.....	1
1.2 Tools for simulation of unsaturated transport in ash dumps .....	3
1.3 The scientific problem.....	4
1.4 Research goals .....	5
1.5 Hypothesis .....	6
1.6 Scope of the study .....	6
1.7 Overview of the Thesis .....	7
CHAPTER 2.....	8
THE STUDY AREA .....	8
2.0 Introduction .....	8
2.1 Geographical location and the physical setting of the Tutuka Ash dump .....	8
2.3 The geology and hydrogeology of the study area .....	12
2.4 Ash handling procedure at Tutuka.....	14
2.5 Summary.....	17
CHAPTER 3.....	19
REVIEW OF CONCEPTS AND THEORETICAL BACKGROUND.....	19
3.0 Introduction .....	19
3.1 Thermal electricity generation and formation of coal ash.....	19
3.2 Physio-chemical properties of coal ash .....	25
3.3 Leaching in dry ash dumps .....	32
3.4 Non-invasive characterization .....	36
3.5 Theory of water flux movement in the unsaturated zone .....	39
3.6 Numerical solution for the water flow equation in the unsaturated zone .....	43



3.6.1 Hydrus2d numerical package .....	49
3.7 Theory of Electrical resistivity methods and their application in the monitoring of potential groundwater contamination. ....	54
3.7.1 Electrical properties of earth materials .....	62
3.7.2 Electrical resistivity tomography .....	65
3.7.3 Geophysical inversion of electrical resistivity data.....	68
3.8 Development of conceptual models .....	70
3.9 Summary .....	72
CHAPTER 4.....	73
GEOELECTRICAL CHARACTERISATION OF THE ASH MEDIUM .....	73
4.0 Introduction .....	73
4.1.1 Archie’s law and the physical interpretation of the cementation factor .....	75
4.2 Determination of the cementation factor for coal ash matrix.....	79
4.3 Time lapse infiltration survey using electrical resistivity tomography .....	84
4.2.1 Time lapse results for Site 2 .....	91
4.2.2 Time lapse results for Site 2 .....	96
4.2.3 Conceptual understanding of the infiltration process in the ash dump. ....	100
4.3 Geophysical assessment and Long term monitoring of the ash dump.....	102
4.3.1 Comparison between the 2006 and the 2008 Profiles.....	104
4.3.2 Comparison of the 2008 and the 2010 Profiles .....	108
4.6 Correlation of geophysical results with pre-existing borehole data.....	111
4.7 Summary.....	113
CHAPTER 5.....	116
NUMERICAL SIMULATION OF CONTAMINANT TRANSPORT IN THE UNSATURATED ZONE OF DRY COAL ASH DUMP.....	116
5.1 Introduction .....	116
5.2 Solute flow in the vadose zone of the ash dump .....	117
5.3 Materials and Methodology .....	118
5.3.1 Determination of saturated hydraulic parameters using infiltration methods	119
5.3.2 HYDRUS2D modelling unsaturated zone transport in the unsaturated zone of the ash dump .....	127

5.3.2.1 Model Validation and calibration.....	128
5.4 Long term simulations of solute transport within the ash dump.....	129
5.5 Correlation of Hydrus2D simulations with lithostratigraphic sections of the ash dump.....	138
5.6 Summary.....	142
CHAPTER 6.....	143
A CONCEPTUAL MODEL FOR THE TUTUKA ASH DUMP SITE .....	143
6.1 Introduction .....	143
6.2 Conceptual Model development.....	144
6.2.1 Conceptual understanding of the input and output streams of the ash dump .....	144
6.3 The generalised conceptual model for solute transport at Tutuka ash dump..	148
6.4 Conceptual site model for the potential hydrological interaction between the ash dump and the wetland. ....	152
6.5 Summary.....	155
CHAPTER 7.....	157
CONCLUSIONS AND RECOMMENDATIONS .....	157
7.1 Conclusions.....	157
7.2 Management of Ash Dump.....	160
References .....	163
OUTPUT .....	184
APPENDICES .....	185



## LIST OF FIGURES AND PHOTOS

Figure 2.1. The locality map and the Google base map of the Tutuka Ash dump.....	10
Figure 2.3. The topographical map of the study area.....	12
Photo 2.1. The photographic setting of the Tutuka ash dump showing ash deposition, brine irrigation, and the areal extend of the ash dump.....	16
Figure 3.1. Coal burning and production of fly ash in a dry-bottom utility boiler with electrostatic precipitator (U.S. Department of Transportation, 1998).....	22
Figure 3.2. A conceptual framework for the application of non-invasive techniques in characterizing contaminant transport.....	38
Figure 3.3. Review of various numerical techniques used in the vadose zone flow and transport modelling (Šimůnek 2011).....	44
Figure 3.4. Principle of electrical resistivity measurements C1 and C2 are current electrodes whilst P <sub>1</sub> and P <sub>2</sub> are potential electrodes, .....	61
Figure 3.5. Resistivities of rocks, soils and minerals.....	63
Photo 4.1. The experimental set up for determining the variation of electrical; resistivity (conductivity) with salt and moisture content.....	81
Figure 4.1. Experimental variation of electrical resistivity with moisture / brine content.....	82
Figure 4.2. Basic concept of electrical resistivity subsurface measurement .....	85
Photo 4.2. The SAS 1000 LUND imaging system and the ES 464 switching unit used for the electrical resistivity tomography.....	86
Photo 4.3. A description of the methodology infiltration procedure.....	88
Figure 4.3. Time lapse results for a time lapse Survey for Site 1 .....	92
Figure 4.4. Variation of depth of infiltration with elapsed time.....	94
Figure 4.5. Results of the time lapse infiltration survey results for site 1 after adding more brine.....	95
Figure 4.6. (a) Inverse model resistivity results for the X (North-South direction) of Site 2 and (b) Results of the percentage change in resistivity for the time lapse infiltration survey along the North-South direction (X -axis) of Site 2 .....	98

Figure 4.7. Resistivity model results for the time lapse infiltration survey along the East-West direction (Y-axis) (b) Model results of the percentage changes in resistivity for the time lapse infiltration survey along the East – West (Y) direction of Site 2. ....	99
Figure 4.8. An infiltration conceptual model for the ash dump.....	101
Figure 4.9. Illustration of a computer controlled field data acquisition system using the roll along technique (Adopted from Dahlin, 2001).....	104
Figure 4.10. Comparison of the August 2006 and August 2008 electrical resistivity data sets .....	105
Figure 4.11. Zoomed in section of August 2006 and August 2008 electrical resistivity cross sections highlighting 3 areas where moisture and salt content increased over time.....	107
Figure 4.12. Results of the 2008 and 2010 ERT profiles used to show evidence of potential salt movement within the ash dump.....	109
Figure 4.13. Approximate borehole positions in relation to the electrical resistance profile results. The black line represents the inferred ash/bedrock contact.....	111
Figure 5.1. Principle of infiltration in auger-hole methods (Amoozegar and Warrick, 1986). ....	121
Figure 5.2. The General construction principle of the Guelph infiltrometer used for determining hydraulic conductivity.....	122
Photo 5.1. A photographic summary of the field work done at the study site.....	124
Photo 5.2. Measuring groundwater level at a monitoring borehole A85. The average groundwater level was used as an input parameter for the deep drainage lower boundary condition that was used for the simulations .....	127
Figure 5.3. Results of the HYDRUS2D model using parameters obtained from the time lapse infiltration experiments.....	129
Figure 5.4. The FE- Mesh generated for the plume movement model.....	130
Figure 5.5. Selected pseudo sections for two dimensional solute transport within the ash dump.....	131
Photo 5.3. Field evidence of a saturated bottom layer as a result of accumulation of the solute fluxes. The mechanism of the accumulation is as suggested by the HYDRUS2D models.....	136
Figure 5.6. The Graphic Log and Physical Sample Description of Core AMB81.....	138

Figure 5.7. The Graphic Log and Physical Sample Description of Core AMB82.....140

Figure 6.1. The conceptual diagram of the input and output streams around Tutuka ash deposit.....145

Figure 6.2. Conceptual model of the major hydro-geologic features in the study area.....147

Figure 6.3. Conceptual model for the solute transport of the Tutuka ash dump and its underlying environment.....150

Photo 6.1 Photographic setting of showing the ash dump and the wetland in the eastern side of the study area.....153

Figure 6.4. A site conceptual model describing potential contaminant flow between the ash dump and the wetland.....154



## LIST OF TABLES

Table 3 .1. Typical concentrations of trace elements in pulverized coal ash.....	28
Table 3.2. Nominal chemical composition of pulverized coal ash from Tutuka ash dump.....	29
Table 4.1. Summary of ash and bedrock characteristics at the core sites.....	113
Table 5.1. Results of the moisture content, density and saturated hydraulic conductivities along site 1 geophysics line.....	126



# CHAPTER 1

## INTRODUCTION

### 1.1 Background

As the world population increases, demand for energy supply increases proportionally. Many countries depend on their vast coal deposits for cheap generation of electricity (He and Qin, 2006; Klass, 2003). Combustion of coal for energy generation leads to generation of large volumes of waste products such as coal combustion residues (coal fly ash) and brines (high ionic strength salts effluents). South Africa is largely dependent on the combustion of coal for power generation and uses more than 100 Mt of coal per annum (Willis, 1987).

The management of the large volumes of solid wastes produced as coal combustion residue is of particular concern due to the presence of leachable metals and salts that constitute a long term environmental risk and pose a risk of contaminating both surface and groundwater systems of the surrounding environment. Nevertheless, despite this environmental problem, coal consumption is still growing because of the lack of natural gas and petroleum resources to meet the electricity demands in most developing countries e.g. more than 90% of South Africa's electricity is generated from the combustion of coal that contains approximately 1.2% sulphur (Triester, 2001) and large quantities of coal ash is often produced and disposed in ash dumps. For instance, electricity production in South Africa produces about 27 million tonnes of coal ash annually, of which only about 5 % of the total coal ash produced per year is reused. The large volume of unused fly ash is disposed in most cases to hold ponds, landfills and

slag heaps (Iyer, 2002; Petrik et al., 2003; Joc et al., 2008). The environmental impact of coal ash production has at least two aspects:

- (a) emission and deposition of enormous amounts of coal ash, polluting air, water and soil with ash particles (including the problem of huge ash dumps) and;
- (b) leaching of microelements (including toxic heavy metals), as well as major salts from brine water used for dust suppression.

The question therefore arises as to how best can these dry ash dumps be managed to not only satisfy all legal requirements and possible pressure from social awareness groups, but also, more importantly, prevent, or at least limit, pollution of the natural environment and in particular contamination of groundwater resources.

Hence there is need of implementing a close monitoring mechanism for the environmental impact assessment of the dangers associated with such ash dumps. In this context, the modern approach to environmental issues related to ash disposal is that of pollution prevention and development of appropriate management programs to come out with sustainable coal combustion waste disposal plan (Bishop, 2000).

The key concern for the management of ash disposal sites in the overburden dump is the associated possibility of groundwater contamination. Recent studies have shown that industrial waste disposal sites is the main source of contamination for most utilized aquifers ( e.g. Ramesh et al., 2005). The United States government's Environmental and Protection Agency (EPA, 2003) did an assessment of the risks associated with the disposal of coal combustion waste across the country and reported leaching of elements (e.g. salts, heavy metals) into the surrounding soils and groundwater as one of the dangers associated with ash disposal sites. Potentially toxic elements leached



from fly ash (e.g. in Hajarnavis and Bhide, 1999) can contaminate soils (e.g. in Theis and Richter, 1979), groundwater (e.g. in Theis and Gardner, 1990) and surface waters (e.g. in Mills et al., 1999).

In order to implement an efficient monitoring scheme on potential contaminant transport in and through the ash dump, a thorough knowledge on the migration of solutes fluxes within the dump is required. In fact, sustainable long term ash disposal planning requires a thorough understanding of the migration of both the solute fluxes from the waste disposal sites, as well as the controls on the transport of these solutes through groundwater. The characterization of the dynamics of moisture migration in the unsaturated zone of ash dumps is essential if reliable estimates of the transport of pollutants threatening the underlying groundwater aquifer system are to be made. This therefore necessitates the need for the development of a reliable hydraulic transport model that describes solute transport and leaching processes in the ash dump, so that an understanding of the mobility processes of the leachate as well as the preferred path of the pollution plume can be obtained.

## **1.2 Tools for simulation of unsaturated transport in ash dumps**

Over the years, different methods are applied in the monitoring of fluid migration at waste disposal sites, of which the coal ash dumps are part of. The conventional method that has been widely used for such applications is to extract and analyse several samples from observation wells are drilled on the dump. However, in the implementation of a close monitoring scheme of monitoring fluid migration in ash dumps, the sampling method often present some limitations, such as:

- In dry ash dumps, theory suggests that fluids often move along preferential flow paths, usually caused by the heterogeneity of the medium. Therefore the sampling wells need be placed within these heterogeneities in order to provide accurate information of any contaminant migration.
- When a dense sampling network is required for the monitoring, it means more wells are to be drilled at close range, and thus the costs of implementing the monitoring scheme may become too exorbitant.
- Installation of many wells may result in the creation of new fluid pathways and results in further migration of leachates.

### **1.3 The scientific problem**

There is thus need to demonstrate that use of non-invasive geophysical techniques and numerical modelling techniques is an important tool for analysing complex problems involving water flow and contaminant transport in the unsaturated zone of dry coal ash dumps. These techniques are best known for providing an adequate hydrological description of water flow and contaminant transport in the vadose zone so as to give accurate estimates of the vulnerability of the underlying aquifer system in terms of groundwater contamination.

Historically, the extent to which a full-scale ash dump scenario can be modelled with non-invasive techniques has been limited. It is only relatively recently that the necessary fundamental scientific knowledge and computing power have evolved sufficiently for the development of the relevant modelling frameworks in the form of geophysical tomographies and hydrologic transport models.

While numerical models have been used with success in several contaminant investigations, they have not been frequently used to predict the unsaturated zone transport properties for coal ash medium. In the same way, although geophysical methods, particularly electrical resistivity tomography have been widely used to locate regions of possible contamination and possible contaminant leachate flow paths, they have not been utilised in the determination of unsaturated hydraulic parameters and mapping of potential contaminant transport in dry ash dumps. As such there is need to combine electrical resistivity inverse models and hydrologic models in the characterization of the potential contaminant transport in the coal ash dumps.

#### **1.4 Research goals**

The main goal of the research is to use non- invasive methods in characterizing the unsaturated zone salt transport of coal ash dumps, thereby contributing towards the understanding of moisture and salt transport within the ash dump and its underlying environment.

The specific objectives of the research are:

- To investigate the suitability of using electrical resistivity geophysical methods in characterizing moisture transport through the ash dump.
- To carry out field experiments to determine the unsaturated hydraulic and transport properties of the coal ash medium which will be used as input parameters to hydrological models for unsaturated transport in the ash dump.

- To use techniques of numerical modeling to produce a real time model that characterizes solute transport parameters for the unsaturated zone of the coal ash medium using Hydrus2D model.
- To develop a generic conceptual model for the solute transport between the ash dump and its hydrologic system.

### **1.5 Hypothesis**

The combination of electrical resistivity geophysical modelling and hydrologic modelling will provide a more comprehensive characterization of the unsaturated zone contaminant transport in coal ash dumps.

### **1.6 Scope of the study**

To solve the research problem, electrical resistivity tomography field experiments shall be combined with hydrologic models in order to come up with a precise prediction as well as a comprehensive understanding of and solute transport in dry coal ash dumps. This will involve the establishment of the electrical resistivity parameters of the ash dump so as to establish the use of electrical resistivity geophysical models as a sufficient tool in monitoring moisture occurrence and migration in this medium before 2-dimensional electrical resistivity field experiments are applied to the ash dump in the second stage of the study. The final stage will involve the application of numerical modelling techniques to predict the movement of moisture and solutes through the unsaturated zone of the ash dump, using the field parameters obtained from the geophysical and soil experiments. The results of these will be used to develop a site model for the ash dump transport system.

## 1.7 Overview of the Thesis

Chapter 1 presented the research background and introduced the research problem, as well as to give a proper outline of the research goals. Chapter 2 describes the setting of the study area and the ash dumping procedure at the Tutuka ash dump. It also presents the geographical and the hydro-geological setting of the study area. The relevant background and theoretical aspects of the study tools are presented in Chapter 3. Chapter 4 presents the empirical determination of the cementation factor for the ash medium and also describes the use of electrical resistivity methods in time lapse monitoring moisture movement in the unsaturated zone for coal ash medium. The chapter also presents the results of the geophysical characterisation and long term monitoring of moisture and solute transport through the ash dump. Chapter 5 will describe the use of Hydrus2D numerical model in real time contaminant plume modelling of salt transport in ash dumps. The development of the Site model for the solute transport through the ash dump and its underlying subsurface, together with its evaluation, is presented in Chapter 6. Chapter 7 gives the overall conclusion of the research findings as well as the recommendations for sustainable ash dump management emanating from the research findings.

## CHAPTER 2

### THE STUDY AREA

#### 2.0 Introduction

The hydrologic properties of a landfill or any possible contaminant source are heavily dependent on the physical, geographical and the hydrogeological setting of the environment on which it is located. This chapter gives a detailed description of the physical and geo-hydrological setting of the Tutuka ash dump. It also narrates the lithographic studies which were used to characterise the geological setting of the ash dump.

#### 2.1 Geographical location and the physical setting of the Tutuka Ash dump

Tutuka dry ash dump is located at Tutuka Power Station, 25 km, north-east of the town of Standerton, in the Mpumalanga Province of the Republic of South Africa. The region surrounding the Tutuka site forms part of the Highveld plateau of South Africa with its characteristic flat topography and grasslands, well known for its maize and sunflower agricultural activities.

The area lies in a Savannah type of climate which is characterized by hot and wet summers from September to March and cool and dry winter from April to August. The mean annual rainfall of 620mm rainfall occurs mainly in the summer months from September to March, with the minimum rainfall is experienced in July. It has a warm to cold temperate climate, characterized by two distinct seasonal weather patterns. The main wet season occurs in summer and extends from October to April, contributing to

89.9% of the total rainfall. Most of the heavy rain in the region is associated with thunderstorms. The study area experience a varying temperature range of a summer (October to February) to winter (April to August) range of around 19° C with average temperatures in the contrasting seasons, of 26° C and 8° C .

Small water dams, in the form of a wetland or pond, lies approximately 400 m to the south- east of the ash dump with the other one located less than 30 m north of the ash dump, more clearly delineated together with the small water body in Figure 2.1. The dam is topographically up-gradient from the disposal site and groundwater flow is towards the ash dump.



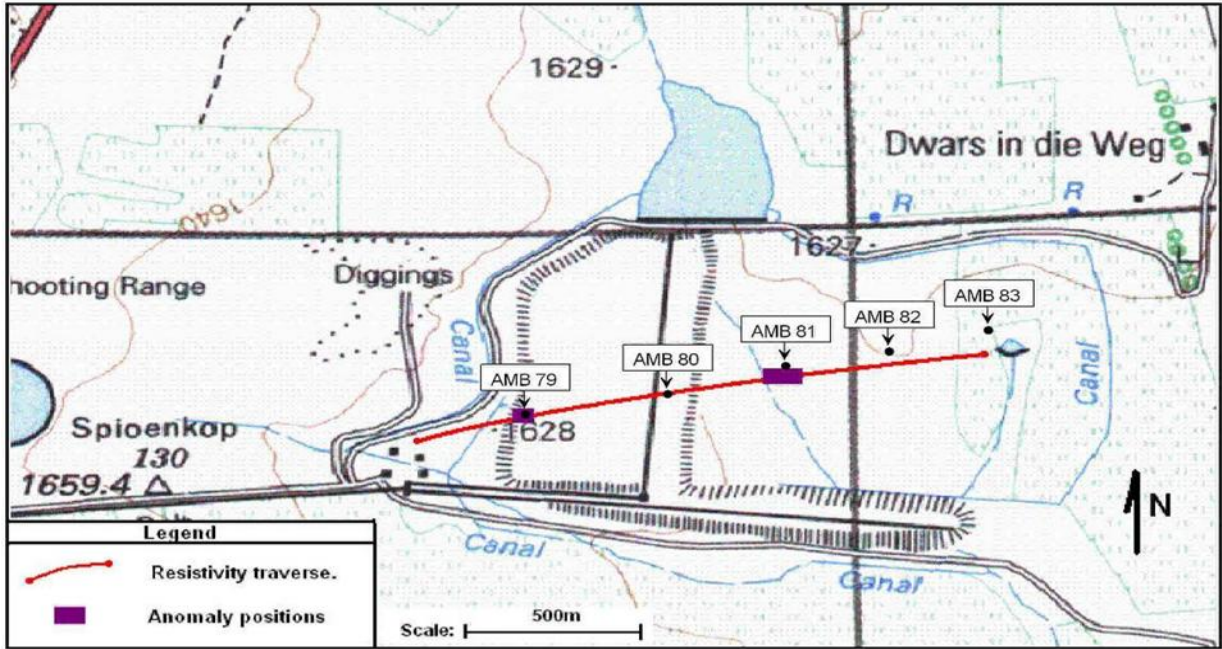


Figure 2.1. The locality map and the Google base map of the Tutuka Ash dump.



### **2.2.1 Topographical description of the study area.**

The Tutuka ash dump occurs within a drainage region that can be sub-divided into secondary drainage regions consisting of smaller streams and creeks. The surface topography of the area is typical of the Mpumalanga Highveld, consisting in the main of a gently undulating plateau. The flood plains of the local streams are at an average elevation of approximately 1600 meters above mean sea level (mamsl). Altitudes varies from + 1675 mamsl at the higher parts to the contour line of the + 1610 mamsl which defines the base of the different Spruit areas. The ash dump area is situated between the contour lines of the 1610 – 1675 mamsl and has been developed upon gradual slopes and a semi-developed drainage system. Figure 2.2 represents the local topography of the area under investigation that was produced using ARCGIS 9.3 software from the Digital Elevation Model (DEM) data obtained from ASTER global satellite. The map was produced using shows the topographical distribution of elevation from the top of the ash dump (red contours) to the wetland area located on the eastern side of the study area.

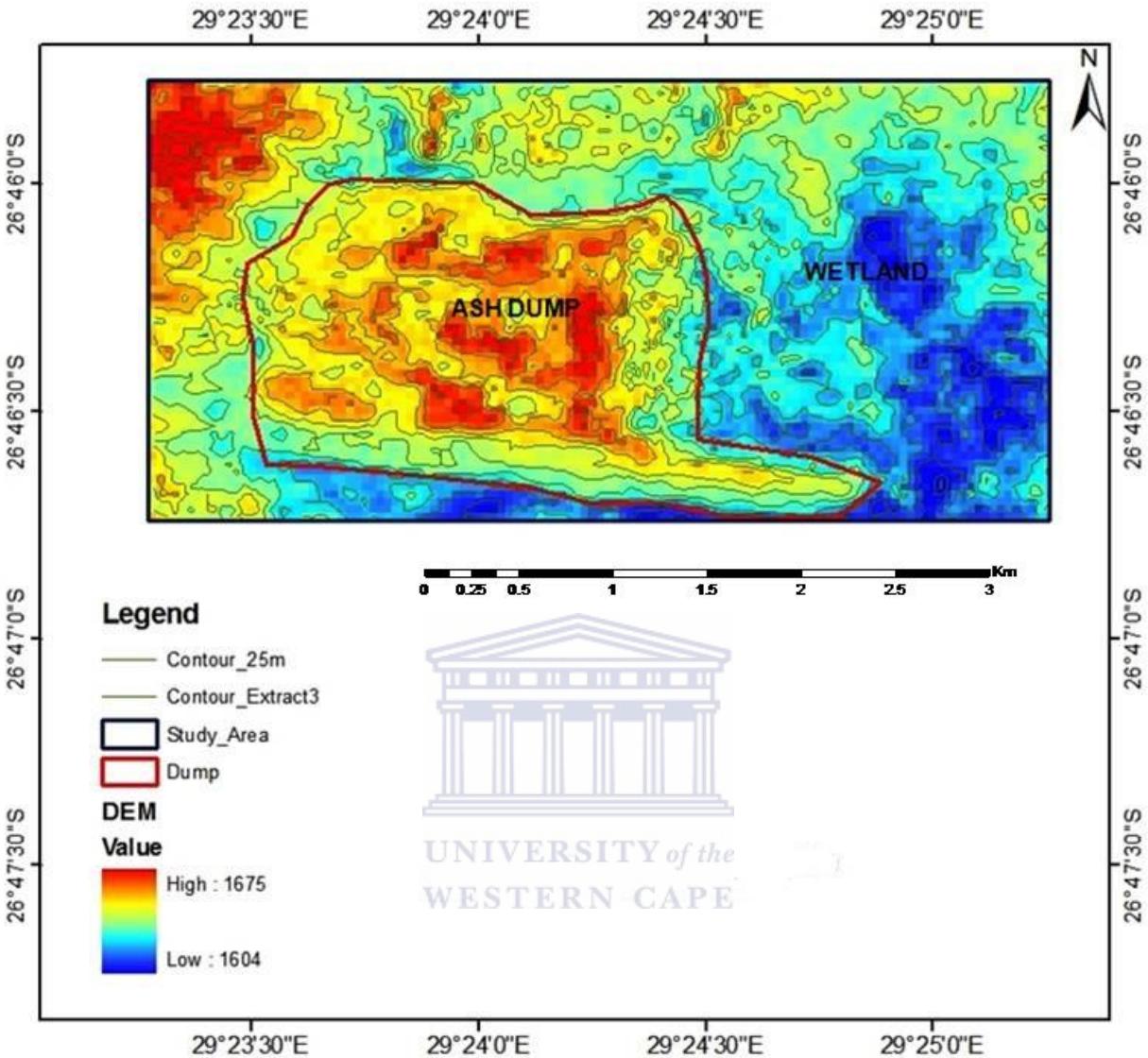


Figure 2.2. The topographical map of the study area, (developed from ARCGIS 9.3 software).

### 2.3 The geology and hydrogeology of the study area

Knowledge of the geology of the ash dump is also critical in the investigation of the effects of waste dump has on its underlying aquifer system. The geology and hydrogeology of the aquifer underlying the ash dump site will play a vital role in

managing the impact of waste disposal on the environment of the site regarding groundwater contaminant transport.

The Tutuka ash dump site is underlain by the natural bedrock consisting of dolorite, shale and sandstone. A clayey topsoil of between 0.2 and 1 meter thickness is found over most of the Tutuka ash dump site. Some of this topsoil was removed for soil cover of the final ash placement elevation. The underlying geology consists of sediments of the Permian Age Ecca Group of the Karoo Super group of formations, while quaternary deposits in the form of gravels containing cobbles and boulders occur along the rivers and streams in the area. The Ecca Group, which is often subdivided vertically into the Pietermaritzburg, Vryheid and Volkrust formations, overlies the Dwyka tillite conformably. By using this division, the area can be viewed as underlain by the Vryheid formation, which consists mainly of interbedded sand stones, siltstones, shales and coal. The sediments are mainly horizontally bedded, but slightly inclined in some areas, as witnessed by the gradual dip in elevation from 1 650 m in the north-west to 1 568 m in the south-east. The water dam north of the ash dump is consequently situated at a slightly higher elevation than the ash dump.

The Karoo formations below most of the ash disposal facilities in South Africa can be classified as a combination of intergranular and fractured aquifers. Intergranular aquifers comprise of unconsolidated to semi-consolidated material ranging from boulders through sand to clay size particles present in varying proportions (Nel et al., 2009). These include weathered shale, dolorite and sandstone formations, found throughout the central regions of South Africa.

Soil cover surrounding the ash appears relatively thin, particularly in the vicinity of the ash pile where soil has been removed for rehabilitation purposes. The type and distribution of site soils appears to be, in part, controlled by parent rock material. Soils overlying doleritic material are typically highly plastic, and dark brown to black in color, while those on Karoo sediments are typically lighter in color and moderate to highly reactive in character. Shrinkage cracks may be expected to develop in site soils irrespective of parent material during periods of prolonged dry weather.

#### **2.4 Ash handling procedure at Tutuka.**

There are two main ash disposal placement methods used in South Africa; dry or wet ash disposal mechanisms. Wet placement is any method that results in an excess of water that must be handled after the ash has been placed, that is, the fly ash is transported as slurry through pipes and disposed of in an impoundment called an ash pond. Dry ash placement involves any method that results in a solid material that does not drain water except during rainfall and irrigation.

The Tutuka Power Station started power generation around 1985, and is one of the most recent power stations constructed by Eskom. At Tutuka power station, fly ash is disposed using this dry ash dumping method. In this system, the ash is partially wetted at the power station by adding approximately 10-15% brine water before being transported by a conveyor belt to the ash dump. This moisture prevents the ash from blowing off the conveyor belt and a watering gun is also available in the area where the ash is being tipped to prevent it from drying out and creating a dust problem. The ash is then dumped onto the ash dump and levelled by a bulldozer after dumping. Brine irrigation will then be routinely done for dust suppression until rehabilitation of the site

occurs. The brine water used for irrigation is typically a sodium-chloride (NaCl) type water and can have a chloride concentration ranging from 23,000 mg/L up to 150,000 mg/L or greater.

The heaps of ash dumped at the site forms the unconsolidated ash sediments which overlay the parent dolomitic aquifer system that characterizes the study area. The ash dump currently covers approximately 190 ha, extends eastwards (Photo 2.1).





**Photo 2.1. The photographic setting of the Tutuka ash dump showing ash deposition, brine irrigation, and the areal extend of the ash dump. Stage 1 is the power station where coal is burned while stage 2 the by product of burned coal ash transported via conveyer belt onto the ash dump and deposited as shown in Stage 3. The deposited ash is then compacted in the form of stacks before irrigating the ash for dust suppression as shown in stage 4 and 5. Stage 6 provides an idea on the extent on the ash dump in the North - South direction.**

The ash dump is approximately 40m above ground level on the side where dumping takes place, and slopes gently towards the west. The deposition of ash over time results in the process of burial, which causes the ash to undergo hardening and as a result transforming into hard core ash. Ash dump rehabilitation is done by placing topsoil, which is removed from the natural soil at the foot of the progressing ash dump, and then placed on top of the dump. Van Niekerk and Staats (2010) estimated the recharge on the study area to range from 3% for normal geological formations and 20% for the unrehabilitated part of the ash dump, which forms the core of the study area. They also estimated an additional 2555 mm per year or 0.7MI/day of brine is irrigated onto certain parts of the ash stack.

The dangers of the ash disposal techniques on the environment include wind and/or water pollution of the ash and leaching of elements (e.g. salts, heavy metals) into the surrounding soils and groundwater. Surface fly ash particles are susceptible to wind erosion and this can be a major source of dust in the surrounding environment. Fly ash particulates when released into the atmosphere can cause irritation or inflammation to eyes, skin, throat and upper respiratory tract of humans (Haynes, 2009).

## **2.5 Summary**

To be able to use a particular methodology to characterize the transport properties of the ash dump, a thorough knowledge of the study area was presented. This chapter managed to look at all aspects which may act as controls in the assessment of potential solute transport within the ash dump and the of the potential impact on groundwater quality or its surrounding hydrologic systems. It also gave an overview of

all the natural hydrologic processes occurring in the ash dump setting. The ash disposal system and activities on and around the dumpsites already indicate that that ash dump are complicated entities. Based on the hydro-geological setting and dumping mechanism at the ash dump it can be noted that ash dam/dumpsites are porous mediums. However, the exact flow paths of the solute transport processes within the ash dump system are yet to be established.



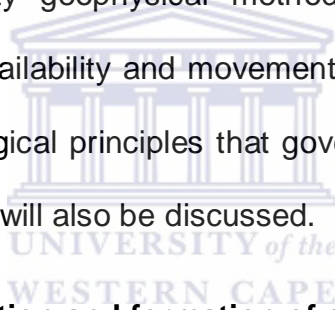


## CHAPTER 3

### REVIEW OF CONCEPTS AND THEORETICAL BACKGROUND

#### 3.0 Introduction

This chapter provides a brief review of important concepts, and recent scientific research on related topics. It first gives a general description of the characteristics of coal combustion by-products, It also provides a brief theoretical description of the principle of electrical resistivity geophysical methods, and the basics its use in monitoring and mapping the availability and movement of contaminants in unsaturated medium. The relevant hydrological principles that govern the unsaturated transport of moisture and salt contaminants will also be discussed.



#### 3.1 Thermal electricity generation and formation of coal ash

Despite projected shifts to cleaner fuel sources, in the near future, electric utilities will continue to rely heavily on fossil fuels, particularly coal as primary energy sources. From an environmental perspective, coal utilization presents a number of problems since coal combustion process generate significant amount of by products at each stage during electricity generation. Coal is often associated with the Industrial Revolution; coal remains an enormously important fuel and is the most common source of electricity world-wide. In the South Africa, for example, the burning of coal generates over half the electricity consumed by the nation. South Africa is the world's third largest coal

exporting country, exporting 25 % of its production internationally. South Africa uses 53 % of the balance of its coal production for electricity generation, 33 % for petrochemical industries (Sasol), 12 % for metallurgical industries (Iskor) and 2 % for domestic heating and cooking. Eskom is the 11th largest electricity generator in the world.

An overview of the stages in the coal combustion for electricity production is presented here. The schematic diagram for the whole combustion process is presented in Figure 3.1. Before combustion in a typical modern coal-burning power plant, coal is dried and ground to a fine powder in a pulverizer, as shown in Figure 3.1, to narrow the size distribution, so that 70% of the coal is less than 75 $\mu$ m in diameter (Dienhart et al., 1998). Pulverization increases the surface area available for combustion and thus improves combustion efficiency. The fineness to which the coal is pulverized depends on the coal rank and the corresponding reactivity of the coal (Beér, 2000). The pulverized coal is pneumatically transported and injected into the combustion chamber, where it is mixed with preheated excess air and ignited at temperatures reaching 1400°C (Babcock and Wilcox, 1978). Coal particles burn in a mode in which both external diffusion of oxygen to the particle surface and chemisorption of the oxygen at the particle surface and in the pores determine combustion progress. Diffusion controls the burning rate of large particles at high temperatures, and chemical kinetics controls the burning rate of small particles as the char burns out in the tail end of the flame (Beer, 2000).

During the combustion process, the hot combustion exhaust gases, combustion products, and radiant heat produce steam from water in heat exchangers (boiler tubes) surrounding the boiler. The superheated steam passes rapidly through a turbine and

expands with a decreasing temperature gradient. The expanding steam causes the turbine blades to rotate the turbine shaft and attached generator at extremely high velocities. The wire coils in the generator produce electric energy as they are rotated in a strong magnetic field. During this cycle, the steam is continuously condensed and returned to the boiler for reuse. At this point, the flue gases are still at elevated temperatures, between 370-537 °C, and would drastically decrease boiler efficiency if exhausted to the atmosphere at these temperatures (Babcock and Wilcox, 1978). Therefore, the heat content of these gases is recovered in one or both of two types of heat exchangers. One such heat exchanger is the air heater, in which some or all of the low-grade heat in the flue gas is used to preheat the air supplied for combustion. Another type of device, known as an economizer, is used to raise the incoming temperature of the feed water used for steam production in the boiler. Not only does this preheating improve efficiency with which steam is generated, it also serves the purpose of cooling the combustion products and exhaust gas to safer, easier to handle temperatures.

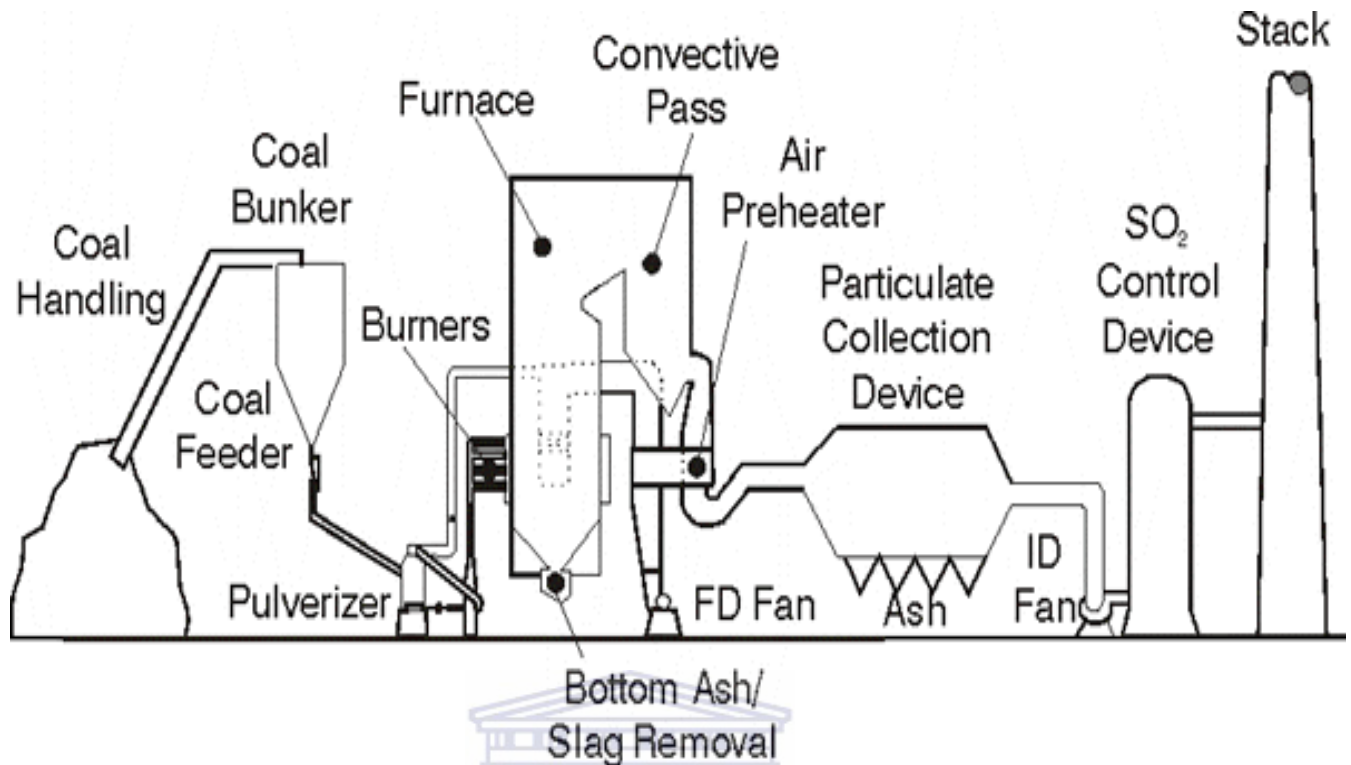


**Figure 3.1. Coal burning and production of fly ash in a dry-bottom utility boiler with electrostatic precipitator (U.S. Department of Transportation, 1998).**

UNIVERSITY of the

Although the combustion process is continually being optimized to increase the efficiency by which fuel is combusted for electricity production, there are still large amounts of process wastes and by products generated by electric utilities in the form of coal combustion products (CCPs) comprising of fly ash, bottom ash, boiler slag, and flue gas desulfurization (FGD) material. The CCPs originate primarily from the chemical compounds in a coal source that cannot be combusted during electricity production, but that are carried through the process by nature of the equipment and technology used. Coal is a complex mixture of organic and inorganic phases, combined with large quantities of physically and/or chemically bound water. The inorganic phase, which may amount to 15-20% of the total coal weight, is a complex mixture of quartz, pyrite, calcite, and silicates (Ledesma and Isaacs, 1990). Various metals are also present in trace

amounts. During combustion, the inorganic fraction of the coal is converted to ash, steam, and other non-combustible materials. Specifically, ash and slag are derived from the ash content of the source coal, and FGD material is generated upon removal of the sulphur present in the source coal.

The types of CCPs produced and their physical and chemical properties are determined primarily by the design and operation of the utility boiler furnace and the type of coal that is combusted (Joshi and Lohtia, 1997).

The amount of recycled ash is way less than the amount of ash produced during power generation. For instance, in South Africa, ESKOM produces about 20 million tons of coal ash annually, and only about 5% of the produced waste is reused and the rest is disposed at the ash stuck (Petrik et al, 2005). The major environmental concern in most instances is the potential availability of toxic elements which would leach through to the underlying aquifer system.

The major component of the coal combustion products produced by the bituminous coal is fly ash, which consists of a wide range of inorganic matter and contributes to 80% of total ash. It is defined as finely divided mineral residue resulting from the combustion of ground or powdered coal in electric generating plant which consists of inorganic matter present in the coal that has been fused during coal combustion. This material is solidified while suspended in the exhaust gases and is collected from the exhaust gases by electrostatic precipitators, and is further classified into Class C and Class F fly ash.

The high-calcium Class C fly ash that is normally produced from the burning of low-the coal (lignites or sub-bituminous coals) and has cementitious properties (Scheetz and Earl, 1998). On the other hand, the low-calcium Class F fly ash is commonly produced

from the burning of higher-rank coals (bituminous coals or anthracites) and is pozzolanic in nature (hardening when reacted with calcium hydroxide ( $\text{Ca}(\text{OH})_2$ ) and water). The principal difference between Class F and Class C fly ash is in the amount of calcium and the silica, alumina, and iron content in the ash. In Class F fly ash, total calcium typically ranges from 1 to 12%, mostly in the form of calcium hydroxide, calcium sulphate, and glassy components, in combination with silica and alumina. In contrast, Class C fly ash may have reported calcium oxide contents as high as 30–40%.

Since the particles solidify while suspended in the exhaust gases, fly ash particles are generally spherical in shape and is usually silt size (0.074 - 0.005 mm), (Ferguson et. al., 1999). The fine texture of fly ash results in water permeability and infiltration rates of ash deposits being characteristically low (Cope, 1962; Townsend and Hodgson, 1973; Bern, 1976). Cope (1962) noted that lateral hydraulic conductivity in fly ash deposits can be much greater than vertical conductivity. Bottom ash constitutes 20% of the total ash produced in a station and is usually heavy and coarse fraction ( $>100 \mu\text{m}$ ).

A mixture of both fly bottom ash and bottom ash is commonly referred to as pulverized ash. The physico-chemical properties of pulverized ash often vary with coal source and quality, combustion process, extent of weathering, particle size, and age of the ash. Hence pulverized coal ash is a heterogeneous material between and within the particles; it has varying particle size, moisture retention, and electrical conductivity (EC); low to intermediate bulk density (BD), nonmagnetic and magnetic components, high water-holding capacity (WHC) and low cation exchange capacity (CEC) than normal soil.

### 3.2 Physio-chemical properties of coal ash

The carbonaceous material in coal ash is composed of angular particles. Bhanarkar et al. (2008) recognized factors such as differences in the coal types, boiler types, combustion conditions and pollution control equipment may influence the size distribution of the particulate matter. The particle size distribution of most bituminous coal ash is generally similar to that of silt (less than a 0.075 mm in diameter) (Ahmaruzzaman, 2010). Although sub bituminous coal fly ashes are also silt-sized, they are generally slightly coarser than bituminous coal fly ashes (Digioia and William, 1972). Coal fly ash composed mostly of silt-sized spherical amorphous ferro-alumino silicate minerals and is usually characterized by low permeability, low bulk density, and high specific surface area (Petrik et al., 2007). Coal ash generally contains approximately 60 to 70 percent silt, and 30 to 40 percent sand size particles depending on the characteristics of the coal fuel used. As such, the soil classification for coal ash is normally that of silt loam characterized by a low permeability. The low permeability tends to reduce leaching of salts and metals to groundwater (Page *et al.*, 1979). The surface area is dependent on particle size. The large surface areas of pulverized coal ash are attributed to carbonaceous particles of highly porous character (Schure et al., 1985). The specific gravity of fly ash usually ranges from 2.1 to 3.0, while its specific surface area may vary from 170 to 1000 m<sup>2</sup>/kg (Mattigod et al., 1990a).

Rudolph et al., (1993) suggested that fly ash behave as a non-plastic light grey sandy silt to silt clay loam, fly ash has lower particle density compare to common rock forming minerals (GHT, 1998). The textural colour of fly ash can vary from tan to grey to black, depending on the amount of unburned carbon (Ahmaruzzaman, 2009). Laboratory

studies conducted by Rudolf et al., (1993) revealed that compacted dry bulk density of pulverised coal ash ranges between 1430 and 1570 kg/m<sup>3</sup> and that the hydraulic conductivity ranges between 0.01 and 2.1 m/day.

Pulverized ash contains leachable constituents such as heavy metals and salts which may constitute an environmental risk if they remain mobile and bio-available (Akinyemi, 2011). Minor or trace metals are then concentrated in fly ash as they are released in volatile form during combustion. These elements are likely formed in the surface layer of fly ash particles rather than within the glassy particles if it melts (Steenari *et al.*, 1999). The presence of these metals in higher concentration makes the disposal of fly ash an acute problem which requires attention. These elements tend to leach out to the surrounding soils when in contact with water. In addition, the leaching of elements from ash disposal is supposed to be site-specific considering variability in the climatic and weather conditions. Leaching losses from ash disposal sites are likely to be site-specific but a sparse number of studies have revealed enriched concentrations of elements such as Calcium (Ca), iron, (Fe), Cadmium (Cd) and Lead (Pb) in surrounding groundwater (Haynes, 2009).

As such coal-based power generation industry is under pressure to improve its environmental performance in terms of handling and disposal of coal ash. Studies have shown that 90–99% of the pulverized coal ashes consist of silicon (Si), aluminum (Al), iron (Fe), calcium (Ca), magnesium (Mg), sodium (Na), and potassium (K), with predominance of Silicon, Aluminium, Iron, Calcium, and minor content of Magnesium and Pottasium compounds. The sulphur content of the parent coal determines the pH of fly ash which could range between 4.5 and 12 (Adriano *et al.*, 1980). South Africa coal

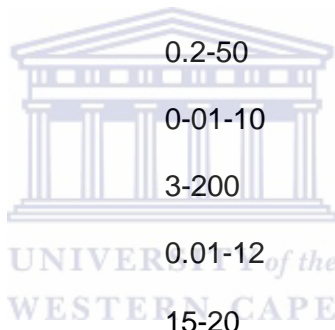


ash often originates from sub bituminous coal and tends to be lower in sulphur but higher in calcium.

Besides, major/micro- nutrients (like phosphorus (P), Boron, (B), Copper (Cu), Zinc (Zn), and Manganese (Mn)) coal deposits is also characterized by trace elements (like Cadmium (Cd), Arsenic (As), Selenium (Se), lead (Pb), nickel (Ni), Chromium (Cr), Cobalt (Co), etc.) (Fatoba, 2006). Aluminium, calcium and iron occur in concentrations typical of soils. Sodium is present in concentrations generally exceeding those found in soil. Fossil fuel wastes are also enriched with sulphur when compared with soil (Adriano et al., 1980, Mattigod et al., 1990a). The trace metals are often concentrated in fly ash as they are released in volatile form during combustion. The presence of these metals in higher concentration makes the disposal of fly ash an acute problem which requires attention. These elements tend to leach out to the surrounding soils when in contact with water. In addition, the leaching of elements from ash disposal is supposed to be site-specific considering variability in the climatic and weather conditions. Leaching losses from ash disposal sites are likely to be site-specific but a sparse number of studies have revealed enriched concentrations of elements such as calcium, (Ca), iron (Fe), Cadmium (Cd), and lead (Pb), in surrounding groundwater (Haynes, 2009). Hence a proper disposal plan or ash utilization scheme is required to reduce its negative environmental effects. The average concentration of trace elements in fly ash as reported by El-Mogazi et al., (1998) are outlined in Table 3.1.

**Table 3.1 : Typical concentrations of trace elements in pulverized coal ash**

Element	Chemical symbol	Amount (mg/kg)
Arsenic	As	3-312
Boron	B	10-500
Cadmium	Cd	0.1-100
Copper	Cu	10-2000
Chromium	Cr	30-900
Lead	Pb	3-500
Nickel	Ni	10-3000
Zinc	Zn	10-1000
Selenium	Se	0.2-50
Barium	Ba	0-01-10
Rubidium	Rb	3-200
Mercury	Hg	0.01-12
Cesium	Cs	15-20



Source: Page *et al.* (1979); El-Mogazi *et al.* (1988); Bilski *et al.* (1995); Asokan *et al.* (2005), Akinyemi (2011).

In addition to the trace elements, the pulverised coal ash also contains various oxides of different quantities and chemical properties. For instance, the average percentage content of these oxides for pulverized coal ash for most ash dumps in South Africa is presented in Table 3.2 (after Adriano *et al.*, 1980 and Akinyemi, 2011).

**Table 3.2: Nominal chemical composition of pulverized coal ash from Tutuka ash dump**

Element	Chemical symbol	%composition for South African coal ash
Silicon dioxide	SiO <sub>2</sub>	44.0
Aluminium oxide	Al <sub>2</sub> O <sub>3</sub>	33.2
Titanium oxide	TiO <sub>2</sub>	1.8
Iron oxide	Fe <sub>2</sub> O <sub>3</sub>	2.9
Chromium oxides	Cr <sub>2</sub> O <sub>3</sub>	Trace
Calcium oxide	CaO	9.5
Magnesium oxide	MgO	2.2
Sulphur trioxide	SO <sub>3</sub>	0.8
Phosphorous penta-oxide	P <sub>2</sub> O <sub>5</sub>	1.5

Source: Akinyemi (2011)

From Table 3.2, it is evident that the coal fly ash has a higher calcium oxide content and lower loss of ignition than fly ash from bituminous coals. Lignite and sub-bituminous coal fly ash may have a higher concentration of sulphate compounds than bituminous coal fly ash. It is partly these trace elements and minerals that are transformed during combustion and that are used as the criteria to differentiate the classes of fly ash. Minor or trace metals are then concentrated in fly ash as they are released in volatile form during combustion. These elements are likely formed in the surface layer of fly ash particles rather than within the glassy particles if it melts (Steenari et al., 1999).

The mineralogical composition of coal ash depends on the geological factors related to the formation and deposition of coal. The dominant mineral phases are quartz, kaolinite, illite, and siderite (Hulett et al., 1980; Spears, 2000). The less predominant minerals in the unreacted coals include calcite, pyrite and hematite. Quartz and mullite are the major crystalline constituents of low-calcium ash, whereas high-calcium fly ash consists of quartz (Norton et al., 1986; Vassileva et al., 1997; Vassileva et al., 2005; Kutchko and Kim, 2006). The potential for leaching is also influenced by the crystallinity of the fly ash, as this would dictate whether the metals are incorporated within the glassy phase or within crystalline compounds, which will hydrate. The metals in the glassy phase are expected to leach at much lower rate than that from the crystalline phase. The degree of crystallinity is a function of boiler design and remains relatively constant for a given source, leachable materials remain relatively constant for a given ash source. Some part of these metals leached from the fly ash will be adsorbed on the clay minerals of the soil.

The concerns of metallic elements and salt contaminants present in the ash dump have always been crucial during hazard assessment of both surface water and groundwater system of the surrounding area. For instance, in October 2009, Appalachian Voices released an analysis of monitoring data from coal waste ponds at 13 coal plants in North Carolina, United States of America. The study revealed that all of them are contaminating groundwater with toxic pollutants, in some cases with over 350 times the allowable levels according to state standards. The contaminants included the toxic trace metals arsenic, cadmium, chromium, and lead, which can cause cancer and neurological disorders. Analysis of heavy metals in groundwater near a coal ash

disposal site in Orissa, India showed that Zn, Cu and Pb were found in high concentration in tube well water located in the vicinity of an ash pond while Cu, Mn, Pb and Zn were the major contaminants in groundwater (Praharaj et al., 2002).

Thus, it is necessary to have an efficient ash handling system in place, in coal-fired power station where large quantities of coal ash are created. This dry ash disposal system is widely applied in most thermal power stations in South Africa, and the most common concentration of chemicals in the coal ash are sodium and sulphate (Hodgson, 1999). In this dumping protocol, as the upper layers go through alternate wetting and drying cycles due to brine irrigation, rainfall and evaporation, sufficient water and air to exchange allows the establishment of a pozzolanic layer of up to a metre or more on the top and along the sides of these dumps. A pozzolan is defined as a siliceous or siliceous and aluminous material that by itself exhibits little or no cementitious properties but in the presence of moisture, chemically reacts with calcium hydroxide (lime) at standard temperature and pressure to form compounds exhibiting cementitious properties. The pozzolanic reactivity of the fly ash is dependent on a number of ash properties which include the particle density and surface characteristics of the glass phase particles (Lohtia and Joshi, 1995). Thus, the pozzolanic action results the formation of cementitious material by the reaction of free lime (CaO) with the pozzolans (Aluminium oxide ( $\text{Al}_2\text{O}_3$ ), Silicon dioxide ( $\text{SiO}_2$ ), and iron oxide ( $\text{Fe}_2\text{O}_3$ )) in the presence of water is known as hydration. The hydrated calcium gel or calcium aluminate gel (cementitious material) can bind inert material together.

### 3.3 Leaching in dry ash dumps

The primary soil and groundwater contaminants related to waste disposal sites are salts, heavy metals and process chemicals (Marr-Laing and Severson-Baker, 1999). Of these, salts are often the most difficult to deal with due to the fact that they are highly mobile and do not biodegrade over time. The content of trace elements in coal fly ash is also relevant to any environmental aspect during beneficiation or usage and disposal, for instance, the ministry of Environment in Israel, considers the use of fly ash as landfill potentially harmful, and forbids its use as landfill (Foner et al., 1999), maybe in response to the greater leaching test results of Nathan et al. (1999). The major trace element that might pose a problem in dry coal ash dumps is hexavalent chromium (Foner et al., 1999). The major environmental concern with fly coal disposal is the possible leaching of heavy metals and toxic element to the groundwater underneath the disposal site. Therefore, leaching characteristics is one of the major environmental concerns of coal ash. The leaching behaviour is influenced by several factors therefore results can be expected to vary for ash samples from different sources (Yan and Neretnieks, 1995).

The composition of ash can influence the constituent released during leaching. Wan et al. (2006) reported that the leaching behaviour of heavy metals such as zinc, lead, cadmium and copper in MSWI fly ash have a dependency relationship with the components of calcium, such as apthitalite, calcite, anhydrite and calcium aluminate or calcium alumina-silicate. The main components of coal ash are anhydrous phases such as alumina-silicates and salts such as sulphates, oxides and chlorides formed at high temperatures in coal-fired power generating stations (Mattigod et al., 1990; Gitari et al.,

2006). Some of these phases (alkali metal oxides, sulphates, and chlorides) are highly unstable at room temperature and pressure and in presence of water. When the ash contacts water these phases will dissolve completely, thus more stable and less soluble mineral phases will thereafter precipitate. Hence, the concentration of some constituent species in the leachate will be controlled by the solubility of the precipitating secondary mineral phases and concentration of other species will be controlled by their availability to the leachate solutions and by their diffusive flux into solution from the leaching of the primary phases with time (Eary et al., 1990; Prasad et al., 1996; Spears and Lee, 2004). The water used for the ash rehabilitation process is usually a sodium-chloride (NaCl) type water with a chloride concentration ranging from 23,000 mg/L up to 150,000 mg/L or greater (Hitchon et al., 1998). Typical environmental impacts associated with excess salt in soil and surface or groundwater include degradation of soil chemical properties and impaired vegetative growth, degradation of soil physical properties caused by excess sodium, and degraded water quality.

In order to come up with mitigation procedures for the environmental impact of dry ash dumps, a proper understanding of the processes involved in predicting leachate flow as well as the path of the contaminant plumes in the ash dump need to be established. Models are often developed for predicting the salt transport for ash dumps. Hunsen et al., (2002) suggested that these models should exhibit some of the following hydro-dynamical features:

- Hydrodynamic behaviour, reflecting variations in degree of saturation corresponding to different disposal methods.

- Hydrodynamics Fluid behaviour within a deposit is an important consideration when modelling ash deposits.
- Subsequent fate and transport of contaminants once the leachate flow rate and concentrations have been determined, i.e., the fate of the contaminants in the environment needs to be determined.

Studies carried out by suggested that the potential for immediate groundwater contamination by downward percolation of pore water through ash dumps is high, especially when the underlying soil is highly permeable.

Nevertheless Jones, (1995) also suggested that the dry ash dumping method is often characterised by a reduced salt leaching as compared to wet ash dumping since the compaction of the ash and the formation of a pozzolanic crust also help to limit leaching as a wetting front must first penetrate through a mass of dry ash before the underlying groundwater can be contaminated. Continuous rehabilitation of dry ash dumps is becoming common practice and involves covering the ash with a layer of soil and establishing suitable vegetation (Carlson and Adriano, 1993) further limiting leaching. In this case, groundwater pollution can occur through the gradual seepage of the ash pore water through the deposit or, alternatively, in the event of a substantial rainfall event, resulting in a subsequent flush out of any accumulated salts in the ash dump where the flow behaviour would be characterised by liquid trickling over the surface of the solid particles of the remaining void volume.

While much has been written on the composition, trace metal content, leachability, physical and chemical properties of fine-grained or coarse ashes (i.e. fly or bottom ash), there is little information on the hydraulic parameter properties (porosity, moisture



content, hydraulic conductivity, etc.) of ash particles (Menghistu, 2010). The hydraulic conductivity and moisture retention properties of fly ash is a major impacting factor if it is to be applied in an open cast situation. The hydraulic properties (hydraulic conductivity, porosity and/or initial and boundary parameters) of an ash dump must be known/estimated to properly evaluate the environmental impact of ash on the porous dump site. The hydraulic conductivity and moisture retention characteristics of the fly/coarse ash will depend, among other things, on the degree of change that the ash has undergone in the ash dump, through pozzolanic crystallization (Hodgson and Krantz, 1998), the way the ash is placed and the engineering of the ash dump. Mudd (2002) also estimated that the unsaturated hydraulic conductivity ( $K_{uns}$ ) values range from 0.167- 0.886 m/day, compared to the estimated saturated hydraulic conductivity ( $K_{sat}$ ) value of approximately 0.3 m/d. October et al, (2009), did column experiments using the Tutuka ash and obtained hydraulic conductivity values of between 1m/day to 2.6m/day depending on the degree of water saturation of the ash medium. From the hydraulic conductivity literature review one can argue that leachate/ drainage of waste from an ash dump to the underlying aquifer (clay specifically) is not a serious concern for groundwater quality, specifically if the ash forms a pozzolanic crystallization as it then acts as a barrier. Seepage to the surface could be a point of concern for surface water especially if it joins some streams.

Once the flow rate through the unsaturated ash dump medium has been established, the fate of the contaminants in the environment can be easily determined. The extent to which a salt contaminant moves through the ash dump environment is dictated by processes which both encourage and retard transport. In addition, factors which relate

to the unsaturated hydraulic properties of the ash environment and the and the characteristics of the salt contaminant itself also need to be considered. The hydro-physical mechanisms which influence the movement of contaminants through the unsaturated zone of the ash dump depends on factors, such as the geo-hydrological properties of the underlying aquifer, leachate composition and the characteristics of the ash in deposit. However prior to modelling of any plume migration in such an environment, it is necessary to obtain a simplified visual representation of the leachate flow system surrounding the ash dump. The establishment of this system is usually based on the hydro-physical framework of the ash dump and the resulting effect on environmental performance.

### **3.4 Non-invasive characterization**

The term non-invasive is an adjective, characterized by the not invading, and relates to the principle of not involving the penetration of making use of any tool which has to physically penetrate a particular medium. Non –invasive characterization has often been useful in the determination of subsurface hydraulic properties and is a key step towards the solution of real-life problems in hydrology, hydrogeology, soil science and geo-technical applications. In contaminant transport non- invasive characterization has often proved to be an efficient tool as compared to traditional characterization methods which are inherently invasive (drilling and sampling) and in most cases do not allow for the space and time resolution needed for the monitoring of hydrological and environmental processes. Of particular importance are the abilities of the non-invasive methods to describe two aspects of the vadose zone transport mechanisms:

- Static aspects, which do not change over time, principally related to physical and chemical properties of the geological medium;
- Dynamic aspects, which do change over time in response to changes in fluid saturations, contaminant transport and water chemistry.

Unsaturated zone hydrology is often characterized by a complex, non-linear behavior, controlled by gravity and capillary forces and is often characterized by large spatial variations in the moisture content of the medium. In addition, the hydrological characterization of the vadose zone is technically challenging, particularly when the investigation is invasive, based on drilling, and consequently can cause major disturbance to the natural in-situ conditions, particularly moisture content. This fact has led to the increasing use of non-invasive, hydrologic and geophysical methods characterize vadose zone transport (e.g. in Slater et al. 1997; Binley et al. 2001, 2002a; Alumbaugh et al. 2002; Cassiani et al 2004).

The use of these techniques in different configurations in the shallow and deep vadose zones can provide high-resolution images of hydro-geological structures and, in some cases, a detailed assessment of dynamic processes in the subsurface environment. Both natural infiltration processes and specifically designed tracer tests can be monitored over periods of time that can last from a few hours to several years. The data from non-invasive techniques can subsequently be used to provide physical-mathematical models for water flow in the unsaturated zone. The construction of the conceptualization of non-invasive characterization of contaminant transport mechanisms used in this study is presented in Figure 3.2.

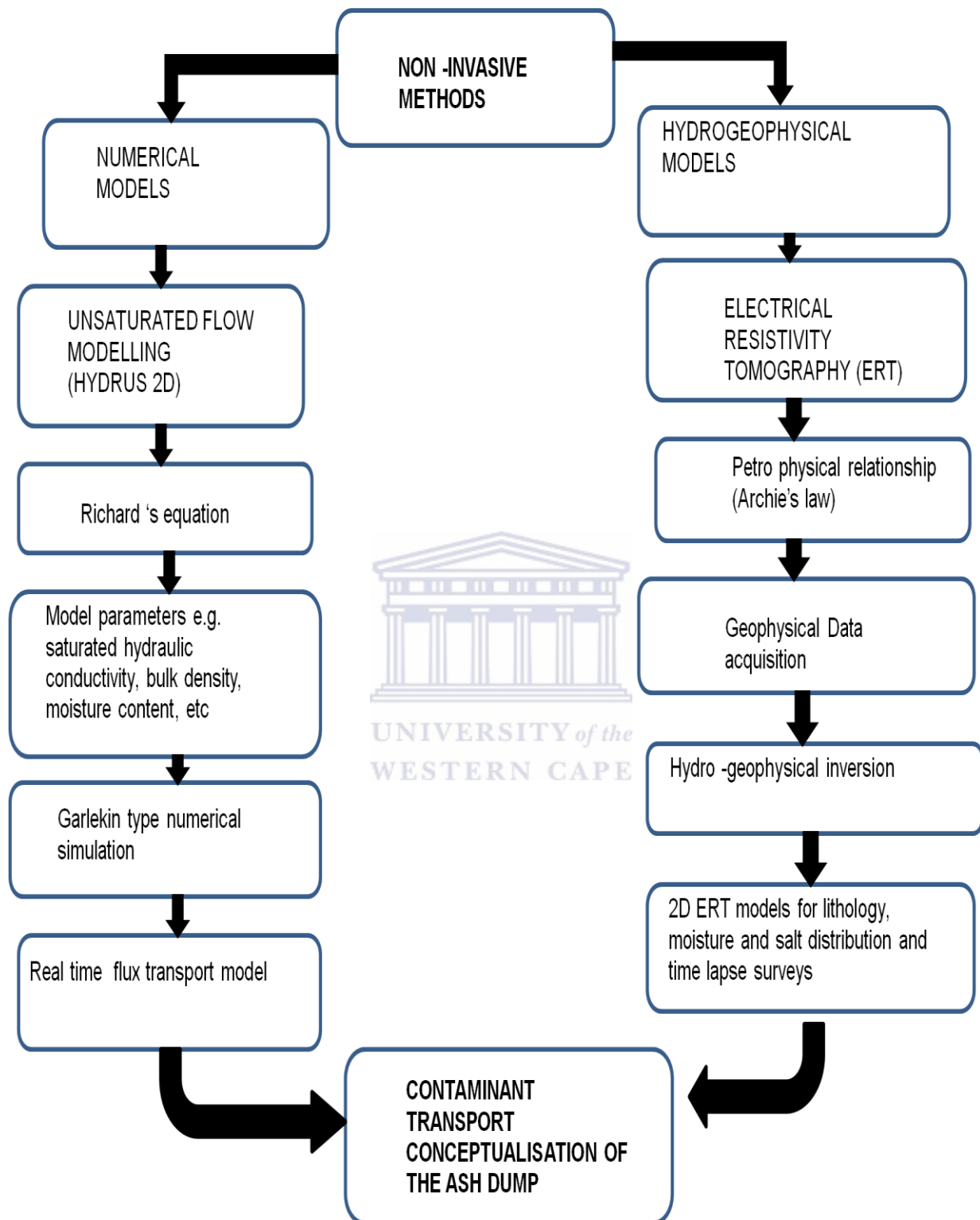


**Figure 3.2.** The conceptual framework for the application of non-invasive techniques that was adopted in characterizing contaminant transport for the current study.

A hydrological model approach coupled with a geophysical modeling technique shall be applied in the current research. The geophysical technique used for the research is the electrical resistivity method, whose properties are heavily varies according to moisture content and degree of salinity for the medium being investigated. Hydrologic modelling will be based on the unsaturated transport modelling using a numerically developed computer program HYDRUS2D which applies the Garlekin type numerical simulation to produce real time flux transport models for which characterize the unsaturated zone transport processes of the medium.

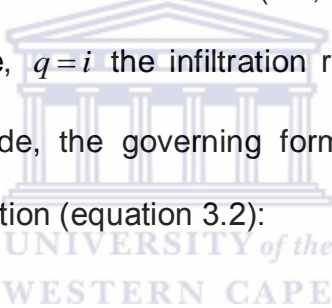
### **3.5 Theory of water flux movement in the unsaturated zone**

Since the transport of contaminants is closely linked with the water flux in soils and rocks making up the vadose zone, any quantitative analysis of contaminant transport must first evaluate water fluxes into and through the vadose zone. In the case of dry ash dumps these fluxes enter the vadose zone in the form of precipitation and /or brine irrigation on the top surface of the dump, and may progressively ingress through the vadose zone to the groundwater table. If the water table is close enough to the soil surface, the process of capillary rise may move water from the groundwater table through the capillary fringe toward the root zone and the soil surface. The process of water entry into soil medium is controlled by several factors, including the time from the onset of precipitation (or irrigation), the initial water content, the hydraulic properties of the surface soil, and the hydraulic properties of layers deeper within the profile (Hillel 1980).

The relationships that govern the flow of water in unsaturated medium for the model are quasi-linear equations of the parabolic type. Because of the close link between water flow and solute transport, a brief focus on the physics and mathematical description of water flow in the vadose zone is presented. In order to derive the mathematical equations describing unsaturated flow, an isothermal uniform Darcian flow of water in a variably saturated rigid porous medium is assumed;

$$q = -K \frac{\partial H}{\partial z} = -K \frac{\partial}{\partial z} (h - z) \dots\dots\dots 3.1$$

where  $q$  is the flux,  $H$  the total hydraulic head,  $h$  the soil water pressure head,  $z$  the vertical distance from the soil surface downward (i.e., the depth), and  $K$  the hydraulic conductivity. At the soil surface,  $q = i$  the infiltration rate in an unsaturated soil,  $h$  is negative. In 2-dimensional mode, the governing form for unsaturated zone flow is described by the Richard's equation (equation 3.2):



$$\frac{\partial \theta(h)}{\partial t} = \frac{\partial}{\partial x_i} \left[ K(h) \left( K_{ij}^A \frac{\partial h}{\partial x_j} + K_{iz}^A \right) \right] - S \dots\dots\dots 3.2$$

Where  $\theta(h)$  [ $L^3L^{-3}$ ] is the volumetric moisture content,  $x_i$  are spatial coordinates [L]  $t$  is the time [T],  $h$  is the pressure head [L] ,  $K(h)$  is the unsaturated hydraulic conductivity function [ $LT^{-1}$ ], often given as the product of the relative hydraulic conductivity,  $K_r$ , and the saturated hydraulic conductivity,  $K_s$ ;

$$K(h, x, y, z) = K_s(x, y, z) K_r(h, x, y, z) \dots\dots\dots 3.3$$

$K_{ij}^A$  are components of a dimensionless anisotropy tensor whose purpose is the account for the anisotropic nature of the medium.  $S$  is a sink term representing capillary water uptake and is usually given as;

$$S = C(h) \frac{\partial h}{\partial t} \dots\dots\dots 3.4$$

with

$$C(h) = \frac{dV}{dc} \dots\dots\dots 3.5$$

$C(h)$  is the soil moisture capacity , popularly known as the field capacity of the soil medium. It is defined as the amount of soil moisture or water content held in soil after excess water has drained away and the rate of downward movement has materially decreased. The unsaturated soil hydraulic parameters,  $\theta(h)$  and  $K(h)$  are highly non-linear functions of the pressure head. In this analysis, the following constitutive relationships for effective saturation proposed by van Genuchten (1980) are used;

$$S_e = \left[ \frac{1}{(1 + |\alpha h|^n)} \right]^m \dots\dots\dots 3.6$$

where  $\alpha$  and  $n$  are unsaturated soil parameters with  $m = (1 - (1/n))$  and  $S_e$  is the effective saturation defined as

$$S_e = \frac{\theta - \theta_r}{\theta_s - \theta_r} \dots\dots\dots 3.7$$

where  $\theta_s$  and  $\theta_r$  are the saturated moisture content and the residual moisture content of the medium respectively. The unsaturated hydraulic conductivity,  $K(h)$ , functions is given by;

$$K = K_s S_e \left[ 1 - \left( 1 - S_e^{\frac{1}{m}} \right)^m \right]^2 \dots\dots\dots 3.8$$

where  $K_s$  is the saturated hydraulic conductivity Brooks and Corey (1964).

The highly nonlinear Richards equation can be solved analytically only for a very limited number of cases involving homogeneous soils, simplified initial and boundary conditions, and relatively simple constitutive relationships describing the unsaturated soil hydraulic properties. In most practical cases, numerical models have been successfully applied to provide a satisfactory solution to the Richard's equation for unsaturated medium.

The impacts of ash dumps on unsaturated flow will depend on a number of factors, including the degree of contrast in hydraulic properties between the ash dumpsite and the surrounding spoil or geologic strata, the moisture content, and the geometry of dumpsite emplacement (Hillel, 1998). As discussed earlier, research on unsaturated flow suggests that at times of low infiltration, water in the unsaturated zone may flow preferentially through fine-grained ash dump layers rather than through the coarser-grained ash materials. Thus, large uncertainties remain regarding flow in the unsaturated zone in complex settings, especially those with great contrasts in hydraulic conductivity.

When the ash dump is situated close to the water table, a thick capillary fringe could form within the materials. Studies of groundwater flow through mine tailings with similar particle size distributions and hydraulic conductivities as fly ash, noted a thick capillary fringe, ranging from tens of centimetres up to six metres in thickness (Blowes and Gillham, 1988; Al and Blowes, 1996a). Under such conditions, the addition of only a



small amount of water, such as a minor precipitation event, can lead to a pronounced rise in the water table and increased potential for contaminant transport to surface water bodies.

### **3.6 Numerical solution for the water flow equation in the unsaturated zone**

Numerical methods have been widely used to solve unsaturated transport models, as allow users to design complicated geometries which represent the complex natural hydrologic conditions, control parameters in terms of space and time, prescribe more realistic initial and boundary condition and permit implementation of non-linear constitutive relationships. The numerical methods usually subdivides the time and spatial coordinates into smaller pieces such as finite differences and finite elements as well as allowing for reformulating the continuous form of governing partial differential equations. A review of the history of various techniques used in the vadose zone flow and transport model as given in Šimůnek 2011 is presented in Figure 3.3.

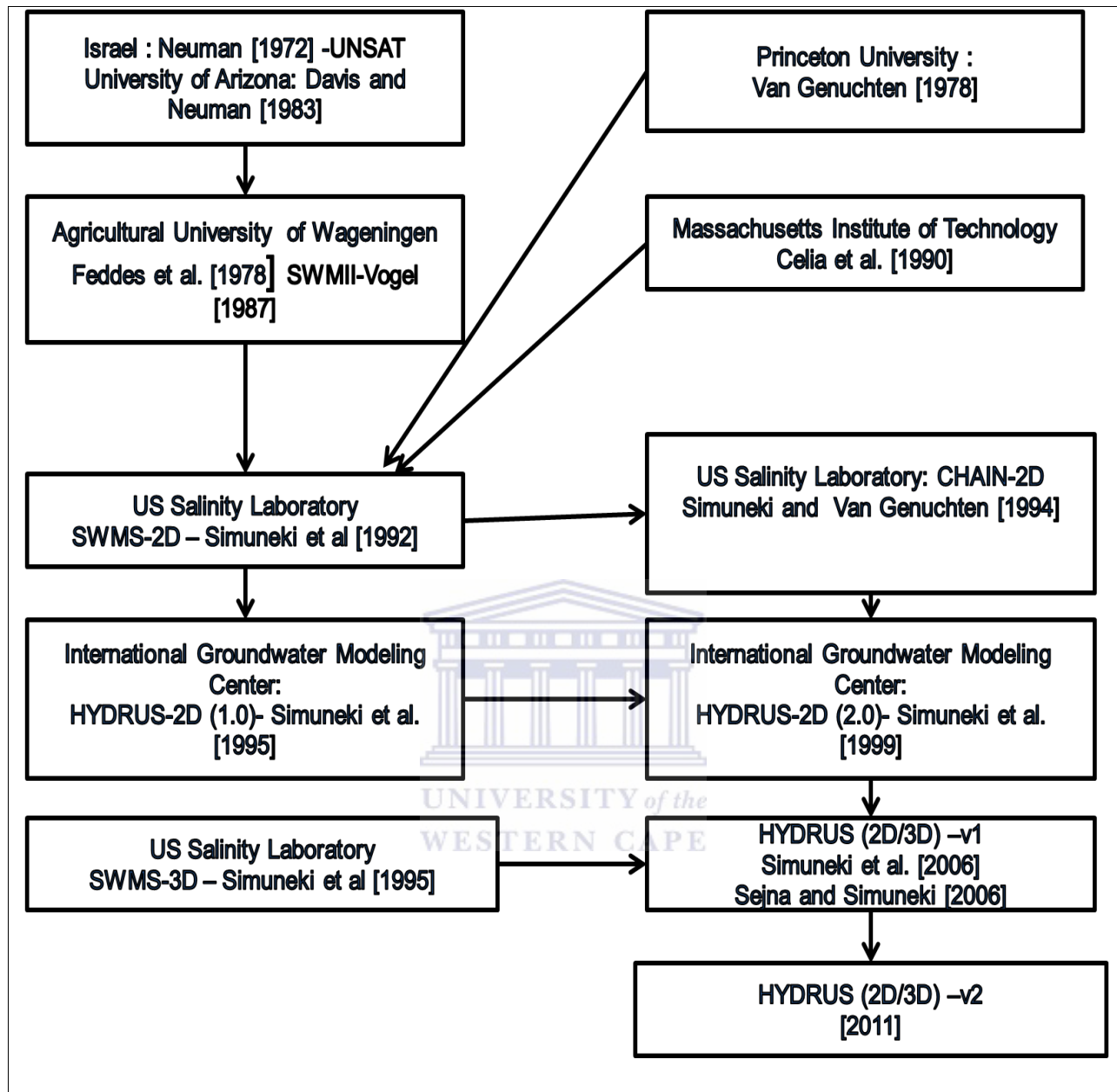


**Figure 3.3. History of development of HYDRUS-2D and related software packages. (Šimunek 2011).**

The dynamics of unsaturated zone moisture and solute transport is often cast in the form of mathematical expressions that describe the hydrological relations within the system. The governing equations define a mathematical model in the form of a set of partial differential equations, together with auxiliary conditions. The auxiliary conditions

must describe the system's geometry, the system parameters, the boundary conditions and the initial conditions. Operations with such a mathematical model are called simulation. In most cases numerical simulation models are applied for unsaturated zone transport. A fair description of the flow in the unsaturated zone is crucial for predicting the movement of pollutants through a particular medium. The formulation and solution of unsaturated flow problems often requires the use of indirect methods of analysis, based on approximations or numerical techniques. In this research, a numerical model, Hydrus2D will be used in the modelling of unsaturated flow. The model uses the Galerkin finite element method is used to obtain a solution of the Richard's equation subject to imposed initial and boundary conditions. This method is covered in detail in Newman, 1975 and in Zienkiewicz, 1977. A brief outline of the steps involved in the numerical simulation of unsaturated flow will be presented. In order to produce a 2-D finite element solution to the Richard's equation, the flow region is divided into a network of triangular elements which are considered to be the nodal points and the pressure head function,  $h(x, y, z, t)$  is approximated using an arbitrary function  $h'(x, y, z, t)$  as;

$$h'(x, y, z) = \sum_{n=1}^N \Phi_n(x, y, z) h_n(t) \dots\dots\dots 3.9$$

where  $\phi_n(x, y, z)$  are linear basis functions and N are is the total number of nodal points. The Galerkin method postulates that the differential operator associated with the Richard's equation is orthogonal to each of the N basis functions such that;

$$\int_{\Omega} \left\{ \frac{\partial \theta}{\partial t} - \frac{\partial}{\partial x_i} \left[ K \left( K_{ij}^A \frac{\partial h}{\partial x_j} + K_{iz}^A \right) \right] + S \right\} \Phi_n d\Omega = 0 \dots\dots\dots 3.10$$

Applying Green's first identity to the above equation and replacing h by  $hN$  yields;

$$\sum_e \int_{\Omega_e} \left( \frac{\partial \theta}{\partial t} \Phi_n + K K_{ij}^A \frac{\partial h'}{\partial x_j} \frac{\partial \Phi_n}{\partial x_i} \right) d\Omega = \sum_e \int_{\Gamma_e} K \left( K_{ij}^A \frac{\partial h}{\partial x_j} + K_{iz}^A \right) n_i \Phi_n d\Gamma + \sum_e \int_{\Omega_e} \left( -K K_{iz}^A \frac{\partial \Phi_n}{\partial x_i} - S \Phi_n \right) d\Omega \dots\dots\dots 3.11$$

where  $\Omega_e$  represents the domain occupied by an element e and  $\Gamma_e$  is a boundary segment of the element. The natural flux type (Neumann 1973) and the gradient type boundary conditions can be immediately incorporated into the numerical scheme by specifying the line integral of the Equation 3.11 and the equation will become simplified into a system of time depended ordinary differential equations with non-linear coefficients. In linear form the equations are given by;

$$[F] \frac{d}{dt} \{\theta\} + [A\{h\}] = \{Q\} - \{B\} - \{D\} \dots\dots\dots 3.12$$



where

$$A_{nm} = \sum_e K_l K_{ij}^A \int_{\Omega_e} \Phi_l \frac{\partial \Phi_n}{\partial x_i} \frac{\partial \Phi_m}{\partial x_j} d\Omega = \sum_e \frac{\kappa}{4A_e} \bar{K} \left[ K_{xx}^A b_n b_n + K_{xz}^A (c_m b_n + b_m c_n) + K_{zz}^A c_m c_n \right] \dots\dots\dots 3.13$$

$$B_n = \sum_e K_l K_{iz}^A \int_{\Omega_e} \Phi_l \frac{\partial \Phi_n}{\partial x_i} d\Omega = \sum_e \frac{\kappa}{2} (K_{xz}^A b_n + K_{zz}^A c_n) \dots\dots\dots 3.14$$

$$F_{nm} = \delta_{nm} \sum_e \int_{\Omega_e} \Phi_n d\Omega = \delta_{nm} \sum_e \frac{\kappa}{3} A_e \dots\dots\dots 3.15$$

$$Q_n = -\sum_e \sigma_{ln} \int_{\Gamma_e} \Phi_l \Phi_n d\Gamma = -\sum_e \sigma_{ln} L_n \dots \dots \dots 3.16$$

$$D_n = \sum_e S_l \int_{\Omega_e} \Phi_l \Phi_n = \sum_e \frac{K}{12} A_e (3\bar{S} + S_n) \dots \dots \dots 3.17$$

The over lined variables represents the average values over an infinite element e, and the subscripts i and j are space directional indices (i, j=1, 2 for 2d surveys). For a two dimensional problem;

$$l = 1, 2, \dots, N \quad n = 1, 2, \dots, N \quad m = 1, 2, \dots, N$$

$$b_i = z_j - z_k$$

$$b_j = z_k - z_i$$

$$b_k = z_i - z_j$$

and

$$c_i = x_k - x_j$$

$$c_j = x_i - x_k$$

$$c_k = x_j - x_i$$

$$A_e = \frac{c_k b_j - c_j b_k}{2}$$

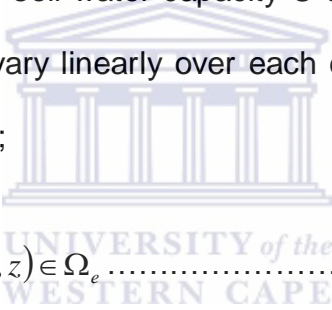
$$\bar{K} = \frac{K_i + K_j + K_k}{3} \quad \bar{S} = \frac{S_i + S_j + S_k}{3} \quad \dots \dots \dots 3.18$$

Since moisture and solute flow is described by the flux boundary the equation involving the  $Q_n$  (Equation 2.16), the system of equations described above hold for two dimensional Cartesian domain which was applied for this research study. The subscripts l, j and k in the flow equation represent the three corners of a triangular element e.  $A_e$  is the area of the two dimensional element, and  $\bar{K}$  and  $\bar{S}$  are the average hydraulic conductivity and the root water extraction values over an element e and  $L_n$  is the length of the boundary segment connected to the node n.  $\sigma_n$  represents the flux [ $LT^{-1}$ ] across the boundary in the vicinity of the boundary node n. The boundary flux is assumed to be uniform over each boundary segment.

The numerical procedure leading to equation 4 incorporates the assumption that the time derivatives of the nodal values of water are weighted according to;

$$\frac{d\theta_n}{dt} = \frac{\sum_e \int_{\Omega_e} \frac{\partial \theta}{\partial t} d\Omega}{\sum_e \int_{\Omega_e} \Phi_n d\Omega} \dots\dots\dots 3.19$$

The assumption is made so as to improve the rate of convergence in the iteration solution process, (Newman 1973). Another assumption which is made is that the anisotropy tensor  $\mathbf{K}^A$  is constant over each element. By contrast, the water content  $\theta$ , the hydraulic conductivity  $K$ , the soil water capacity  $C$  and the root extraction rate  $S$  at any given point is assumed to vary linearly over each element  $e$ . The water content is expanded over each element as;



$$\theta(x, z) = \sum_{n=1}^3 \theta(x_n, z_n) \Phi_n(x, z) \text{ for } (x, z) \in \Omega_e \dots\dots\dots 3.20$$

where  $n$  represents the corners of the element  $e$ .

The integration of equation 2.12 is archived by discretizing the time domain into a sequence of finite intervals and replacing the timer derivatives by finite derivatives. An implicit finite difference scheme is for the unsaturated flow conditions would present the final set of algebraic equations to be solved as;

$$[F] \frac{\{\theta\}_{j+1} - \{\theta\}_j}{\Delta t_j} + [A]_{j+1} \{h\}_{j+1} = \{Q\}_j - \{B\}_{j+1} - \{D\}_j \dots\dots\dots 3.21$$

Where  $j + 1$  denotes the current time level at which the solution is being considered,  $j$  represents the previous time level, such that  $\Delta t_j = t_{j+1} - t_j$ .

Because of the non-linear nature of Equation 3.21, an iterative process is used to obtain solutions of the Global matrix equation through deriving a system of linearized algebraic equations which are then solved using either the Gauss elimination method by making use of the banded and symmetric feature of the matrices in Equation 3.7. The iterative process continues until a satisfactory degree of convergence is observed, i.e. until at all nodes in the unsaturated region, the absolute change in water content between two successive iterations becomes less than some value determined by an imposed water content tolerance (Šimůnek and van Genuchten, 1994).

### **3.6.1 Hydrus2d numerical package**

HYDRUS2D was developed by U.S. Salinity Laboratory, U.S. Department of Agriculture, (Simunek and van Genuchten, 1999). Adequate description of solute and contaminant transport in the vadose zone heavily relies on accurate estimates of the soil water retention and hydraulic conductivity properties at the application scale of the model. The minimum requirement to run the HYDRUS software with the GUI includes an x86 CPU (Intel or AMD) at 1 GHz or faster, 512 MB RAM, a graphics card with a resolution of 1024 × 768 pixels, and 10 GB total hard disk capacity with about 500 MB reserved for installation. The model has a mesh generator for unstructured finite element grids, MESHGEN\_2D, which has the capability of simulating flow on irregular boundaries. Some of the applications of HYDRUS2D include irrigation management, seasonal simulation of water flow and plant response, deep percolation, seepage in highway design, lake basin recharge, groundwater aquifer and stream interaction, and

environmental impacts of drawdown of shallow water tables. HYDRUS model is used in field and laboratory works, to simulate water flow, soil hydraulic properties, solute transport in both saturated and unsaturated medium.

Input preparation for HYDRUS2D includes soil hydraulic parameters, initial and boundary conditions, and mesh generation. The code allows users to select three types of models to describe the soil hydraulic properties: van Genuchten, Brooks and Corey, and modified van Genuchten type equations. The Hydrus code is coupled with Rosetta V1.0 which is a Windows based program that can estimate unsaturated hydraulic properties from surrogate soil data such as soil texture data, bulk density using pedotransfer functions (PTFs) that translate basic soil data into hydraulic properties. Rosetta was used to estimate the water retention parameters according to van Genuchten (1980), the saturated hydraulic conductivity and unsaturated hydraulic conductivity parameters according to van Genuchten (1980) and Mualem (1976).

### **3.6.1.1 Software process & model implementation for HYDRUS2D**

This software acts in three stages of pre-processing, calculation, and post-processing.

Inputs in pre-processing:

- The main processing menu: At this part, considered simulation should be selected.
- **Geometric Data:** This section allows the user to choose between simple geometries having a structured finite element mesh (i.e., 2D-Simple (Parametric) or more general geometries having an unstructured finite element mesh (i.e., 2D-General). Two-dimensional geometries can be specified in the Horizontal or Vertical Plane, or can be radially symmetrical around the vertical axis.



- **Time Data:** This includes the specification of information associated with the Time Discretization, Time Units, and implementation of Boundary Conditions. The times which are specified include the initial and final time of calculation, and the minimum time increment for the model.
- **Information about Results Print:** This section allows the user to specify the nature of the presentation of the output from the computational module of HYDRUS. The user decides whether certain information concerning mean pressure heads and concentrations, mean water and solute fluxes, cumulative water and solute fluxes, and time and iteration information is printed at each time step (T-Level Information), after n time steps (Every n time steps), at a certain defined time interval (Interval Output), or if the information is sent to the screen during the calculations (Screen Output).
- **Numerical Solution Conditions:** In this section, one specifies the maximum number of iterations during one time step, and the water content and pressure head precision tolerances. It thus enables the specification of information related to the iterative process that is used to solve the Richards equation. Since the Richards equation is non-linear in nature, an iterative process must be used to obtain solutions of the global matrix equation at each new time step. For each iteration, a system of linearized algebraic equations is first derived and then solved using either Gaussian elimination or the conjugate gradient method. After solving the matrix equation, the coefficients are re-evaluated using this solution, and the new equations are again solved. The iterative process continues until a satisfactory degree of convergence is obtained, i.e., until for all nodes in the

saturated (unsaturated) region the absolute change in pressure head (water content) between two successive iterations becomes less than some small value determined by the imposed absolute Pressure Head (or Water Content) Tolerance.

- **Soil Hydraulic Properties:** This allows the user to select the Hydraulic Model to be used for the soil hydraulic properties, and specify whether or not Hysteresis is to be considered during the calculations. HYDRUS model solves Richards's equation using linear finite elements pattern, for simulation of water movement in soil.
- **Water flow parameters:** It allows the specification of the hydrologic parameters of the soil hydraulic model under consideration. The unsaturated soil hydraulic properties in the HYDRUS code are described with a set of closed-form equations resembling those of van Genuchten (1980) who used the statistical pore-size distribution model of Mualem (1976) to obtain a predictive equation for the unsaturated hydraulic conductivity function.

**Calculation Steps are as follows:**

1. Solving governing equation (Richards, 1931) using finite element method (Equation 1 for one-dimensional mode and equation 2 for two-dimensional mode)
2. Calculation of absorption & moisture values in successive iteration based on specified time steps.
- 3- Comparison of absorption & moisture values between

two successful iteration as compared with solving accuracy (tolerance) given to the model

3. Provided that,  $\Delta h$  or  $\Delta \theta$  is larger than the given accuracy, the continuation of calculations goes to the next iteration and if  $\Delta h$  or  $\Delta \theta$  is smaller than the given accuracy, calculations is done at the next time step.

This software starts calculations by performing a model with an initial time step, and then compares the obtained values in iteration to the given accuracy, eventually, arrange and modified values according to maximum & minimum time steps specified in software.

The output data of the model includes: simulation time, number of iterations in each time step, total cumulative of the number of iterations, flow variations in upstream border, total cumulative input flow in upstream, total cumulative water absorption by root, total cumulative output flow in downstream, Matrix potential in upstream, downstream and by root. Several boundary conditions can be described with HYDRUS2D including prescribed and variable pressure head, prescribed and variable flux, no flux, free drainage, seepage and atmospheric conditions. A combination of polylines, arcs, circles, and splines define the specifications of the flow region. Domain geometry as well as initial conditions can also be imported from files (Simunek and van Genuchten, 1999).

### **3.7 Theory of Electrical resistivity methods and their application in the monitoring of potential groundwater contamination.**

In order to overcome the limitations sited above, geophysical methods are often used as non-contact methods in monitoring the movement of fluids in subsurface structures. Several geophysical methods, including the electrical resistivity methods, ground penetrating radar, electromagnetic profiling methods and the self-potential methods have been widely used to investigate and map contaminant plumes and leachate flow. The electrical resistivity method is one of the several geophysical methods which have been used as a non-invasive and non-destructive tool for monitoring and investigating leaching in ash dumps and landfills. The electrical resistivity geophysical methods are most appropriate for non-intrusive data collection for a medium under investigation due to the fact that most soil materials and properties are strongly correlated and can be quantified through the geo-electrical properties. In fact, the flux of electrical charges through materials permits conductor materials like moisture or electrolytes to be distinguished the host medium. This analogy between the flow of electric current and hydraulic and transport properties in the unsaturated zone has motivated many to pursue research towards the use of electrical resistivity measurements to predict of hydraulic conductivity and hydro-physical properties of a medium.

The resistivity method is based on the fact that different subsurface materials are less or more resistive to electrical current flow. Schlumberger in 1912 cited by Meyer de Stadelhofen (1991) introduced the idea of using electrical resistivity measurements to study subsurface rock bodies. This method was first adopted in geology by oil companies searching for petroleum reservoirs and delineating geological formations.

A direct current (DC) or slowly varying AC current is injected into the earth by means of pairs of grounded current electrodes. The voltage drops between pairs of grounded potential electrodes are then measured at selected positions. These voltage drops are dependent on the resistivities of the materials through which the electrical currents are flowing. By assuming that the earth is homogeneous and isotropic, measurements of the injected electrical current and measured voltage drops, as well as the distances between the different electrodes, may be used to calculate an apparent resistivity for the earth at a specific position and (pseudo-)depth. The apparent resistivity is an averaged resistivity of the specific resistivities of the subsurface materials through which electrical current flow takes place. To obtain a model of the resistivity distribution within the subsurface, the calculated apparent resistivity values need to be inverted. During inversion the subsurface is divided into discrete units with distinct resistivities. By means of a mathematical process, the resistivities of the units are adjusted in such a way that the difference between the modelled apparent resistivities and the recorded apparent resistivities are reduced in an iterative process. The modelled resistivity distribution may now be interpreted in terms of the local subsurface conditions by incorporating known information on the site conditions. Electrical resistivity methods were developed in the early 1900s and have been widely used since 1970s, due primarily to the availability of computers to process and analyze the data. These techniques are used extensively in the search for suitable groundwater and to monitor types of groundwater pollution.

The direct-current (DC) electrical resistivity method has proved very popular with groundwater studies due to the simplicity of the technique and the ruggedness of the instrumentation. Before the vertical electrical soundings were used a failure rate of over

82% was recorded for boreholes. With the geophysics and a combination of geological and photo geological inspection this was dramatically reduced to less than 20% failure. Van Overmeeren (1989) showed the use of electrical measurements in mapping boundary conditions in an aquifer system in Yemen. Beeson and Jones (1988), Olayinka and Barker (1990), Hazell et al. (1988 and 1992), Barker et al. (1992) and Carruthers and Smith (1992) all have demonstrated the use of electrical techniques for siting wells and boreholes in crystalline basement aquifers throughout sub-Saharan Africa. Other similar examples are given by Wurmstich et al. (1994), Yang (1998), and Yang et al. (1994). Botha and Vorster (1993) demonstrated a useful development of electrical techniques by considering the conductance of the DC section as a guide to overall aquifer potential for mapping groundwater resources in the Kalahari Basin. This type of approach may find applicability in many mafic-basin groundwater studies. Sauck and Zabik (1992) have demonstrated a development of the sounding technique by conducting azimuthal surveys. This method was successfully used to assess the directional variation in hydraulic conductivity of glacial sediments in Switzerland. A similar approach has been tested by Marin et al. (1998). The purpose of electrical resistivity surveys is to determine the resistivity distribution of the sounding soil volume. Artificially generated electric currents are supplied to the soil and the resulting potential differences are measured. Potential difference patterns provide information on the form of subsurface heterogeneities and of their electrical properties (Kearey et al., 2002). The greater the electrical contrast between the soil matrix and heterogeneity, the easier is the detection. Electrical resistivity of the soil can be considered as a proxy for the variability of soil physical properties (Banton et al., 1997).

Electrical resistivity geophysical methods are based on the resistivity contrasts of subsurface materials. The electrical resistance,  $R$  of a material is related to its physical dimension, cross-sectional area,  $A$  and length,  $l$  through the resistivity,  $\rho$  or its inverse, the electrical conductivity,  $\sigma$  by:

$$\rho = \frac{1}{\sigma} = \frac{RA}{L} \dots\dots\dots 3.22$$

When performing electrical resistivity measurements, low frequency alternating current is employed as source signals in the determination of subsurface resistivity distributions. Thus, the magnetic properties of the materials can be ignored (Telford et al., 1990) so that Maxwell's equations of electromagnetism are reduced to:

$$\nabla \cdot E = \frac{1}{\epsilon_0} q \dots\dots\dots 3.23$$

$$\nabla \times E = 0 \dots\dots\dots 3.24$$



where  $E$  is the electric field in  $V/m$ ,  $q$  is the charge density in  $C/m^3$  and  $\epsilon_0$  is the permittivity of free space ( $\epsilon_0 = 8.85 \times 10^{-12} F/m$ ). These equations are applicable to continuous flow of direct current; however, they can be used the effects of alternating currents at low frequencies such that the displacement currents and the induction resistances are negligible. Usually, a complete homogeneous and isotropic earth medium of uniform resistivity is assumed for analysis. In this medium, the current density  $J$  is related to the electric field through Ohm's law:

$$J = \sigma E \dots\dots\dots 3.25$$

The electric field vector  $E$  can be represented as the gradient of the electric scalar potential,

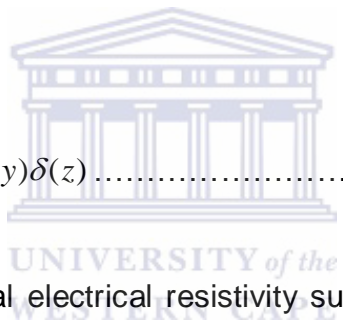
$$E = -\nabla\Phi \dots\dots\dots 3.26$$

By combining the equations 3.23 and 3.26, the fundamental Poisson equation for electrostatic field is obtained as;

$$\nabla^2\Phi(x, y, z) = -\frac{1}{\epsilon_0}q(x, y, z) \dots\dots\dots 3.27$$

The equation of continuity for a point in 3D space and time  $t$  is defined by the Dirac Delta function which is given as:

$$\nabla \cdot J(x, y, z) = \frac{\partial}{\partial t}q(x, y, z)\delta(x)\delta(y)\delta(z) \dots\dots\dots 3.28$$



The current sources in a typical electrical resistivity survey are usually point sources. Thus the current and current density over a volume element  $\Delta V$ , around a current source located at  $(x_s, y_s, z_s)$  are given by the relation suggested in Dey and Morrison, (1979) as;

$$\nabla \cdot J = \left(\frac{I}{\Delta V}\right)\delta(x - x_s)\delta(y - y_s)\delta(z - z_s) \dots\dots\dots 3.29$$

where  $\delta$  is the Dirac Delta function. Hence the potential distribution in the ground due to a point current source is given as;

$$-\nabla \cdot [\sigma(x, y, z)\nabla\Phi(x, y, z)] = \left(\frac{I}{\Delta V}\right)\delta(x - x_s)\delta(y - y_s)\delta(z - z_s) \dots\dots\dots 3.30$$



The above relation is a partial differential equation which is self adjoint, strongly connected and non-separable elliptic equation of the second order, and it gives the subsurface potential distribution in an isotropic non-uniform 3D medium due to a point current source. Numerous techniques have been developed to solve this problem, i.e., to determine the potential distribution that would be observed over a given subsurface structure. The potential  $\Phi(x, y, z)$  and the normal component of the current density  $\sigma \frac{\partial \Phi}{\partial n}$  are continuous across the boundary between two media of different resistivities but the current lines are always refracted in accordance with the boundary conditions. Electrical resistivity methods employ an artificial source of current which is injected into the subsurface through point electrodes and the resulting potential difference is measured at other electrodes positions in the neighbourhood of the current flow. For a semi-infinite conducting layer of uniform resistivity bounded by the ground surface, an applied current will be radially distributed over a hemispherical shell of an underground region of resistivity  $\rho$ .

At a distance  $r$  from the point source the surface area of the shell is  $2\pi r^2$  so that the potential for the homogeneous half space is;

$$\Phi(r) = \frac{\rho I}{2\pi r} \dots\dots\dots 3.31$$

In practice, two current electrodes are usually used and the potential distribution is symmetrical about the vertical placed at the mid-point between the two current electrodes. The potential at an arbitrary point from a given pair of current electrodes is given as:

$$\Phi(r) = \frac{\rho I}{2\pi} \left( \frac{1}{r_{c1}} - \frac{1}{r_{c2}} \right) \dots\dots\dots 3.32$$

where  $r_{c1}$  and  $r_{c2}$  are the respective distances from the source and sink electrodes to the arbitrary point. Theoretically the current electrodes can also be used to measure the potential distribution of the subsurface. However, since the influence of resistances between the surface and current electrodes is not precisely known (Cheng et al., 1990), two potential electrodes,  $P_1$  and  $P_2$  are dedicated for the detection of the response signal such that the potential difference between them becomes;

$$\Delta\Phi = \frac{I\rho}{2\pi} \left[ \frac{1}{C_1P_1} - \frac{1}{C_1P_2} - \frac{1}{C_2P_1} + \frac{1}{C_2P_2} \right] \dots\dots\dots 3.33$$

The above relation (Equation 3.33) describes the potential that would be observed over a homogeneous configuration. However in reality the subsurface is typically heterogeneous so that the resistivity observed is apparent, i.e. the resistivity of a homogeneous subsurface medium that would give the same resistivity value for the same electrode configuration (Figure 3.4).

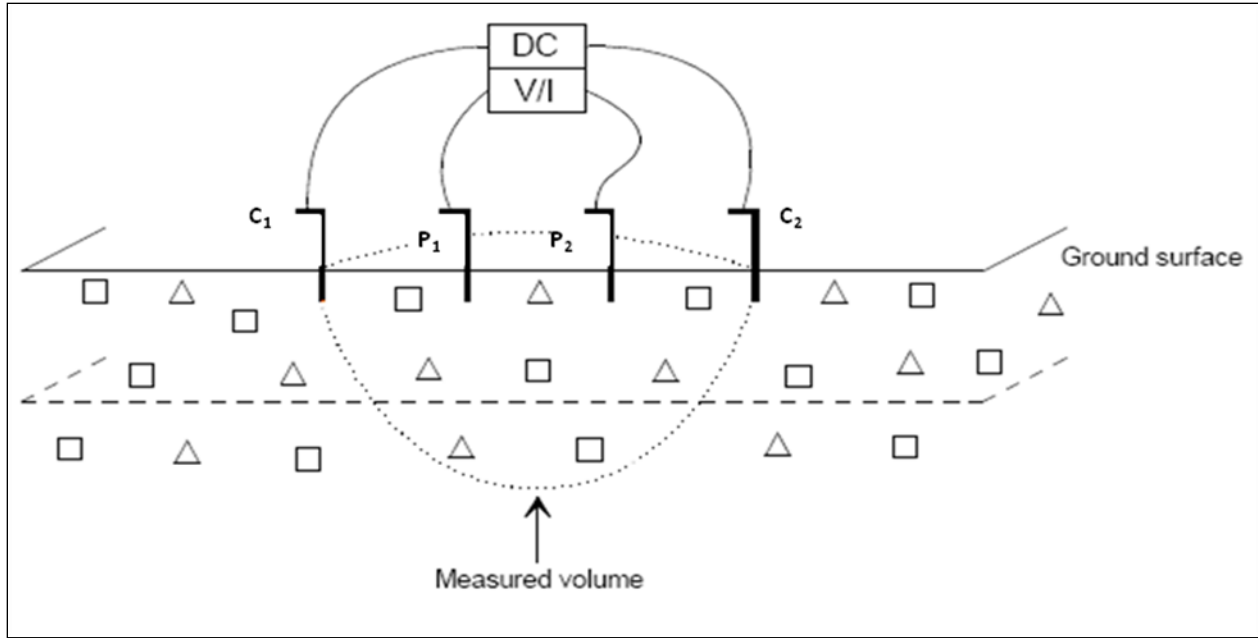
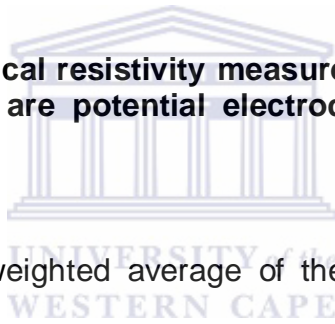


**Figure 3.4. Principle of electrical resistivity measurements C<sub>1</sub> and C<sub>2</sub> are current electrodes whilst P<sub>1</sub> and P<sub>2</sub> are potential electrodes, (redrawn from Aaltonen, 2001).**



The apparent resistivity is a weighted average of the resistivities of the subsurface volume under the four electrodes (Figure, 3.4) the apparent resistivity depends on the configuration of electrodes and is determined by the injected current  $I$ , and the voltage  $\Delta\Phi$  as;

$$\rho_a = G \frac{\Delta\Phi}{I} \dots\dots\dots 3.34$$

Where  $G$  is the geometric factor which depends on the electrode spacing as

$$G = \frac{2\pi}{\frac{1}{C_1P_1} - \frac{1}{C_1P_2} - \frac{1}{C_2P_1} + \frac{1}{C_2P_2}} \dots\dots\dots 3.35$$

The volume, hence the depth of investigation is determined by the distance between the distance between the outer electrodes in the electrode array used. Barker (1989) has estimated the depth of investigation for a Wenner configuration to be  $0.17 \times L$  and for a Schlumberger configuration to be  $0.19 \times L$ , where  $L$  is the total electrode array length.

### 3.7.1 Electrical properties of earth materials

Electric current flows in earth materials at shallow depths through two main methods. They are electronic conduction and electrolytic conduction. In electronic conduction, the current flow is via free electrons, such as in metals. In electrolytic conduction, the current flow is via the movement of ions in groundwater. In environmental and engineering surveys, electrolytic conduction is probably the more common mechanism. The apparent resistivity varies from fractions of  $\Omega\text{m}$  to several tens of thousands of  $\Omega\text{m}$  and is mainly dependent on:

- degree of water saturation
- amount of dissolved solids
- content of organic matter
- grain size
- grain shape of the soil matrix

The resistivity of common rocks, soil materials and chemicals (Keller and Frischknecht 1966, Telford et al. 1990) is shown in Figure 3.5.

The resistivity of these rocks is greatly dependent on the degree of fracturing, and the percentage of the fractures filled with water. Thus a given rock type can have a large range of resistivity, from about 1000 to 10 million  $\Omega\text{m}$ , depending on whether it is wet or

dry. This characteristic is useful in the detection of fracture zones and other weathering features, such as in engineering and groundwater surveys. Unconsolidated sediments generally have even lower resistivity values than sedimentary rocks, with values ranging from about 10 to less than 1000  $\Omega\text{m}$ . The resistivity value is dependent on the porosity (assuming all the pores are saturated) as well as the clay content. Clayey soil normally has a lower resistivity value than sandy soil. The resistivity values of several industrial contaminants are given in Figure 3.5.

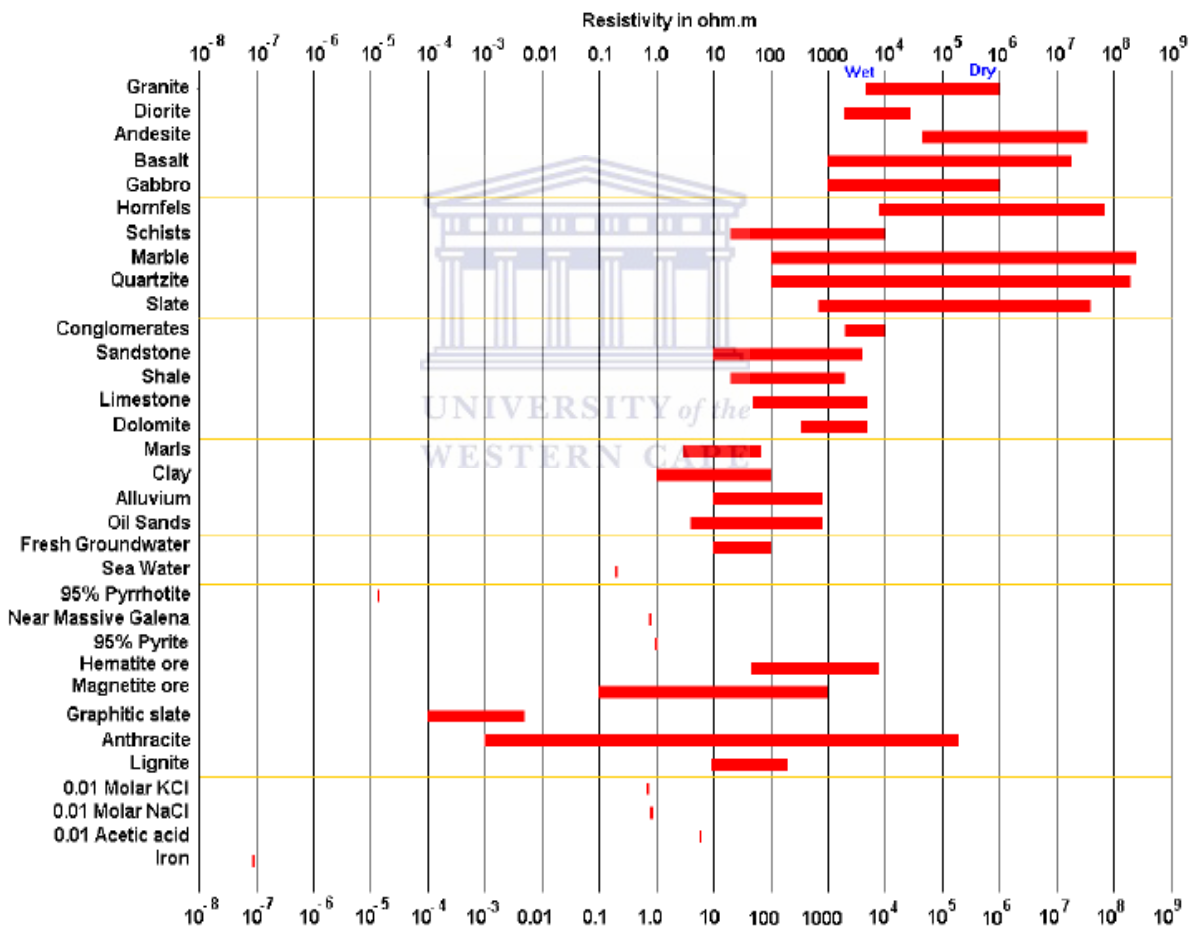
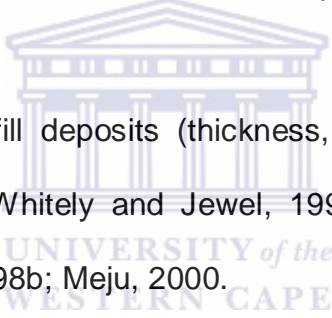


Figure 3.5. Resistivities of rocks, soils and minerals (after Loke 2001).

Metals, such as iron, have extremely low resistivity values. Chemicals that are strong electrolytes, such as potassium chloride and sodium chloride, can greatly reduce the resistivity of a medium to less than 1  $\Omega\text{m}$  even at fairly low concentrations.

The use of resistivity methods in contamination investigations is based on the fact that the resistivity variations in a medium are dependent upon the amount of moisture and salinity of the medium, as well as the properties of the porous matrix. This creates the potential to detect leachate flow, as part of the change in resistivity is due to the change in concentration of dissolved ions (contamination). Resistivity measurements have often been used for a variety of purposes in environmental applications. Some of these works include:

- 
- Characterization of landfill deposits (thickness, internal structure, cover): e.g. Carpenter et al. 1990; Whitely and Jewel, 1992; Kobrand and Linhart 1994; Bernstone and Dahlin 1998b; Meju, 2000.
  - Detection of the presence of the contaminants in the vadose zone and as well as delineating patterns of movements: e.g. Kelly and Acse , 1977; EPA 1978, Masac et al., 1987; Buselli et al., 1992.
  - Location and extent of capped Landfills: e.g. Cardarelli and Bernabini, 1997; Bernstone and Dahlin 1998b.
  - Hydrogeological, lithological and structural characterisation of the investigation site: e.g. Masac et. al., 1987; Petersen et al 1987; Barker et al., 1990.
  - Groundwater flow, including relationships between the groundwater-surface water interactions: e.g. Kelly and Asce, 1977; Nobes, 1996 Lile et al., 1997.
  - Composition of groundwater: e.g. Masac et al., 1987; Nobes, 1996.

The resistivity measurements are usually carried out in the following ways:

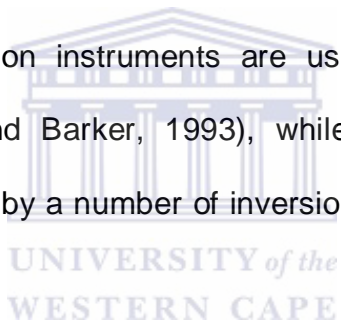
- Vertical electrical sounding (VES): Vertical measurements at a single location but with increasing electrode spacing and hence increasing the measured volume.
- Electrical Resistivity Tomography (ERT): This technique provides a two-dimensional depth section or modeled pseudo section across a survey area or feature as opposed to a map which is produced by an earth resistance survey. The technique can be used to estimate the dimensions and nature of sub-surface targets such as the soil/bedrock interface, strata thickness, depth to and width of walls and ditches.

### **3.7.2 Electrical resistivity tomography**

The use of electrical resistivity surveys for investigating subsurface layered media has its origin in 1912 due to the work of Conrad Schlumberger, who conducted the geo-electrical resistivity experiment in the fields of Normandy, and the idea was further developed by Frank Wenner in 1915, (Kunetz, 1966). Ever since, the geo-electrical resistivity survey has greatly improved, and has become an important and useful tool in geological studies, mineral prospecting and mining, as well as in environmental and engineering applications, (e.g. in Griffiths et al, 1999, Dahlin and Loke, 1998, Olayinka, 1999, Amidu and Olayinka, 2006, and Aizebeokhai et al, 2010). The classical methods of electrical resistivity surveys have undergone significant changes in the three decades. The traditional horizontal layering technique for interpreting geo-electrical resistivity data are rapidly being replaced by 2D and 3D models of interpretations, especially in complex and heterogeneous

subsurface media. The 2D and 3D interpretations are often referred to as electrical resistivity tomograms. In principle, electrical resistivity tomography is a geophysical technique for imaging sub-surface structures from electrical measurements made at the surface, or by electrodes in one or more boreholes.

Over the last decade the Electrical Resistivity Tomography (ERT) has been extensively used in geophysical investigations (Dahlin, 2001). Compared to conventional measuring modes ERT prospecting can be successfully used in areas with complex geology, since it provides information in both lateral and vertical directions and defines in a qualitative manner the shape and depth of the subsurface targets. Resistivity acquisition instruments are used in order to carry out field measurements (Griffiths and Barker, 1993), while the interpretation of field or synthetic data is carried out by a number of inversion programs available (Loke and Barker, 1996a).



Changes of resistivity because of the migration of contaminants and/or water in the vadose zone have been observed commonly and form the basis of electrical monitoring techniques in environmental geophysics (e.g., Greenhouse and Harris, 1983; Kean et al., 1987; Asch and Morrison, 1989; Bevy and Morrison, 1991). In recent years, electrical resistivity tomography has been used at different landfills and disposal sites for various applications, like mapping land fill cover (e.g. Leroux, 2007), detecting and mapping pollution plumes (e.g. Rosqvist et. al., 2003), and for studies of moisture and leachate migration processes, (e.g. Marcoux et al, 2007 and Rosqvist at al., 2005). Resistivity measurements are often used to map fluid migration at ash disposal sites, since the resistivity of any porous earth material is a function of the amount of fluid



which fills the pores, the conductivity of the fluid and the clay content in the material forming the dump, (Kean et. al., 1988). Two dimensional electrical resistivity prospecting methods have also proved to be efficient in the monitoring of subsurface fluid migration within a particular medium e.g. in Barker and Moore (1998). The same methods have also been applied to map salt tracer movements in the subsurface (e.g. White, 1988; Bevc and Morrison, 1991; Kemna et al., 2002), and to delineate pollution with contaminants (Osiensky and Donaldson, 1995; Benson et al., 1997; Atekwana et al., 2000; de la Vega et al., 2003). Bauer (2005) used electrical resistivity methods to determine the salinity distribution below Thata and Tshwene Islands, Botswana, by making use of the different direct current resistivity of saline and fresh groundwater. Electrical resistivity methods have also been successfully used to monitor moisture movement in infiltration surveys, e.g. Barker and Moore (1998) reported successful results when they did a time lapse infiltration survey and used resistivity methods to map the flow of water from the ground surface downwards through the unsaturated zone and into the water table in the Birmingham area of England, after 10 hours of irrigation. In an electrical resistivity tomography, the spatial variations of subsurface resistivity are measured through a four electrode electrical circuit. By putting two electrodes into the ground and inducing an electric current through the ground, a potential field is created. Measurement of the potential difference between two voltage electrodes permits the determination of the subsurface resistivity, known as apparent resistivity. Increasingly deeper measurements are achieved by using a bigger separation between the current electrodes. Inverse methods are then applied to the apparent resistivity measurements in order to determine an image of the subsurface.

### 3.7.3 Geophysical inversion of electrical resistivity data

Many geophysicists have shown that it is possible to reconstruct an accurate resistivity image of the subsurface using a large number of measured data and employing 2-D and 3-D imaging or inversion schemes. Software applications for inversion of two-dimensional apparent resistivity to solve for true resistivity can be classified as either smooth inversion (DeGroot-Hedlin and Constable, 1990) or block inversion (methods, each of which has some disadvantages. Smooth inversion has a tendency to smear both resistivity and depth to interfaces even in the case of well-defined structures with sharp resistivity contrasts. On the other hand block inversion requires a starting model close to the truth, which is rarely known precisely and is difficult to construct especially in complex cases. In the 2-D inversion algorithm, an optimally smooth geo-electrical model of the earth is calculated. This involves the inversion of the data until the roughness term  $dR$  is minimized under the constrain that the sum of squared errors  $S$  is also minimized or becomes equal to  $X_d$ , which is the acceptable average error in view of data uncertainties. The values of  $dR$  and  $S$  are given by the equations:

$$dR = (C_x dx)^T C_x dx + (C_z dx)^T C_x dx \dots\dots\dots 3.36$$

and

$$S = (W_d dy)^T (W_d dy) \dots\dots\dots 3.37$$

where  $C_x, C_z$  are model smoothness matrices in the x and z axes respectively  $dy$  is the vector of differences between the observed data  $d_{obs}$  and the modeled data  $d_{calc}$  (calculated using the forward modeling technique),  $W_d$  is the data weighting matrix and T denotes the transpose. In the standard Bayesian formulation  $W_d$  is the inverse square

root of the a priori data covariance matrix, which is usually assumed (independent data errors) to be a diagonal matrix containing inverse data errors,  $\sigma_i$ , ( $i=1, \dots, n$ ) when using  $n$  data (e.g., Tarantola, 1984), in which case Equation 3.27 becomes:

$$S = \sum_{i=1}^n \frac{dy_i^2}{\sigma^2} \dots\dots\dots 3.38$$

Minimization is achieved by the use of the Lagrangian multiplier technique, which yields the non-linear smoothness constrained inversion algorithm (Sasaki, 1992). The inversion is iterative and the resistivity  $x_{k+1}$  at the  $k+1^{\text{th}}$  iteration is given by:

$$x_{k+1} = x_k + dx_k \dots\dots\dots 3.39$$

$$= x_k + \left[ (W_d J_k)^T (W_d J_k) + \mu_k (C_x^T C_x + C_z^T C_z) \right]^{-1} \times (W_d J_k)^T W_d dy_k$$

where  $J_k$  and  $\mu_k$  is the Jacobian matrix estimate and the Lagrangian multiplier respectively for the  $k^{\text{th}}$  iteration.

In the above formulation it is common that logarithmic model resistivities and apparent resistivities positive and to accelerate the convergence of the iterative algorithm (Park and Van, 1991). Inversion's theoretical formulation requires that the main stopping criterion in the above iterative formulation is to reach a target misfit value (to avoid fitting data to noise). However, in practice this has limited value since there is no objective way to get an accurate estimate of this misfit value, given that field data noise as estimated by instruments is only approximate and certainly unable to describe many other important sources of noise (i.e. modelling, linearization errors etc.). Thus we have adopted the observation of a slow convergence rate as a single stopping criterion, which is commonly used by many researchers (Loke and Barker, 1996a).

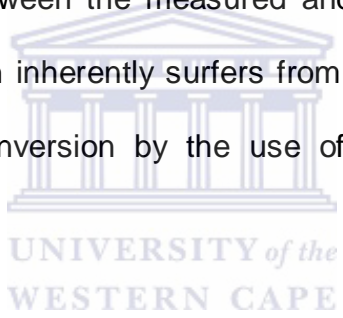
In this case, the iterative procedure described when no significant improvement (i.e. 5%) of the RMS error is observed, where the RMS is given by:

$$\sqrt{\frac{\sum_{i=1}^n dy^2 / \sigma_i^2}{\sum_{i=1}^n 1 / \sigma_i^2}} = \sqrt{S / \sum_{i=1}^n 1 / \sigma^2} \dots\dots\dots 3.40$$

where S is as described earlier on. The equation 3.40 shows that minimization of S in the case of independent to minimization of S in the case independent data errors for typical Bayesian formulation. In the case of constant or not available data errors Equation 3.40 becomes the usual:

$$RMS = \sqrt{\sum_{i=1}^n dy^2 / n} \dots\dots\dots 3.41$$

The quality of the inversion output is guided by an acceptable value of the minimum absolute error (RMS error) between the measured and predicted apparent resistivity. However, geophysical inversion inherently suffers from non-uniqueness, which can be reduced by constraining the inversion by the use of additional information or any additional models.



### 3.8 Development of conceptual models

The conventional definition of a conceptual model is that of a qualitative and often pictorial description of the all the hydrological aspects of a particular system, including a delineation of the hydro-geologic units, the system boundaries, inputs/outputs, and a description of the soils and sediments and their properties. The conceptual model also presents the flow, transport processes and estimates of the magnitudes of all the relevant parameters (Rushton, 2003). Conceptual models can initially start with a sketch and later develop into a detailed three dimensional diagram. The structural and/or hydro-geological framework in the form of cross sections are most probably the first

attempts of conceptualizing aquifer systems and as more information are contributed the complexity of the conceptual model increases. Using the definition of a conceptual model given above, a mathematical model can be thought of as a quantitative representation of the conceptual model. Typical components of a conceptual model are the physical environment, hydraulic properties and transport properties. Researchers have built many conceptual models of the natural processes in play at potential waste disposal sites, and have implemented these models in computer codes that are used to predict the fate of the waste (e.g., Wu and Pruess, 2000; Dolmar, 2001). Likewise, several researchers have studied water and solute movement in dry coal ash dumps through field studies and modelling investigations and have proposed different conceptualization of the ash dump hydrology for the Tutuka ash dump site. Such findings are summarized in October (2009) and Mengitsu, (2010).

Because the mathematical model is quantitative, it can be used to interpret site observations and to make quantitative predictions about the future conditions of the site. As a part of this process, the conceptual model, and consequently the mathematical model also, may be modified to account for new observations. To properly evaluate the potential impact of the disposal of coal combustion by-products on groundwater quality, the physical and chemical properties of these by-products, transport processes in groundwater, and the solution techniques of mathematical models must be understood all need to be incorporated in the conceptual model characterizing the ash dump thereby ensuring that the site is conceptualized thoroughly so that all the physical features are incorporated in the conceptual model.

### **3.9 Summary**

This chapter managed to present a detailed review of all the necessary concepts which are necessary to understand the setting of the Tutuka ash dump which was used as the study site including the presentation of a detailed review of the formation, and constituents of the coal ash. A mathematical analysis and physical review on the development of the study tools which will be used for the study was also presented. The concepts reviewed and discussed in the chapter will also be instrumental in developing and implementing proper methodologies for the research goals.



## CHAPTER 4

### GEOELECTRICAL CHARACTERISATION OF THE ASH MEDIUM

#### 4.0 Introduction

Hydrology research has developed a number of sophisticated tools to try and account for model uncertainty, particularly with respect to the limited knowledge of the subsurface in terms of its hydraulic property distribution (Aaltonen, 2001). In particular, stochastic modelling techniques have had a tremendous development in both surface (e.g., Bras and Rodriguez-Iturbe, 1993) and subsurface hydrology (e.g., Rubin, 2003). However, in most cases, the models require even more data than traditional deterministic models, as an estimate of the underlying spatial statistical structure of the governing parameters is needed. Heavy reliance is often put on densely monitored sites with several monitoring boreholes drilled over the study area. Overmore, this approach has often been discredited in that it can result in the creation of unwanted preferential pathways that may act as possible conduits for contaminant transport in the medium under investigation. As a consequence, during the 1990s there was a rapid growth in the use of geophysics to try and provide spatially dense, quantitative information about hydrological properties and processes.

This need, along with the growing availability of fast field acquisition instruments and powerful computational tools, has led to the current developments in hydro-geophysics in particular, in the structural characterization of the subsurface medium for evaluating fluid-dynamics and detecting the presence and movement of potential contaminants. Geophysics has long been used to support delineation of lithological boundaries

predominantly in the structural (geometrical) characterization of aquifers by highlighting contrasts in physical properties that distinguish geological formations (e.g., Giustiniani *et al.*, 2008). In addition to that geophysics has been used to exploit the physical nature of measurements at the same time translating the measurements into quantitative estimates of the soil/rock properties.

In view of the needs above, the current developments in hydro-geophysics are aimed at providing quantitative information on the hydrological and hydraulic characteristics of the soil and subsoil, as well as quantitative data on the presence and motion of fluids and solutes in and through the medium of interest. Amongst a variety of non-invasive geophysical method measuring changes in the subsurface physical properties in relation to changes in transport properties of the medium, the electrical resistivity tomography has often been the most popular tool in contaminant transport.

Electrical resistivity of a particular medium matrix can be considered as a proxy for the spatial and temporal variability of many other soil physical properties (i.e. structure, water content, or fluid composition). Since changes in moisture and salt concentrations usually provide contrasts in electrical properties in the host media, electrical resistivity methods can be used as a tool in monitoring the progression of the water/salt plumes as well as to detect any preferential hydraulic paths within the ash medium. Because the method is non-destructive and very sensitive, it offers a very attractive tool for describing the subsurface properties without digging.

Several studies have used electrical resistivity techniques to investigate changes of resistivity because of contaminant migration through the unsaturated zone (e.g., Greenhouse *et al.*, 1983; Macfarlane *et al.*, 1983, Bevy *et al.*, 1991, Muhktar *et al.*,



2000, Abdullahi et al., 2011). Rodgers et al., (1980), reported successful monitoring of groundwater contamination at a fly ash disposal site. In particular, 2D Electrical resistivity tomography (ERT) has been frequently used to monitor water infiltration into the soil or at waste disposal sites (e.g. Mukhtar et al., (2000)).

Electrical resistivity tomography (ERT) has often been used to monitor salt leachate flow in on the coal ash dump on the basis of decreasing resistivity during leachate flow (Guerin, 2004; Moreau, 2003). Recently, the ERT method has been proved to be efficient to monitor moisture distribution during leachate flow at waste disposal sites, (Moreau et al. 2003; Rosqvist et al. 2003; Guerin et al. 2004). Nevertheless, no general relationship between electrical resistivity and moisture content has been reported for the coal ash medium, although Kean et al., (1980), showed that electrical resistivity techniques can be used to monitor the salt leachate flow and estimate the variations in moisture content within the coal ash dump. An understanding of the variation of electrical resistivity with moisture content of the ash medium is used to evaluate the suitability of the electrical methods in monitoring moisture and leachate flow in the ash medium.

**4.1.1 Archie’s law and the physical interpretation of the cementation factor**

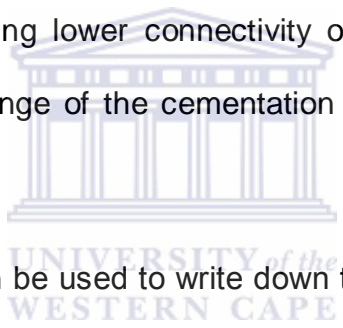
Archie (1942) suggested that the resistivity of any medium matrix  $\rho$  is related to the resistivity of pore water  $\rho_w$  an empirical ratio which he termed the formation factor of the medium through Equation 4.1.

$$F = \frac{\rho}{\rho_w} \dots\dots\dots 4.1$$

The formation factor is a property of a medium and varies between zero and infinity. From the results of his experiment, Archie (1942) also proposed that the formation factor was also related to the porosity of the medium through an inverse power law (equation 4.2).

$$F = \Phi^{-m} \dots\dots\dots 4.2$$

The index factor of the relationship  $m$  was termed the cementation exponent, suggesting that it was related to the degree of cementation of the medium matrix. In words,  $m$  is related to the sensitivity of the medium to changes in porosity, with a high cementation exponent suggesting lower connectivity of the medium matrix (Ellis and Singer, 2007). In reality, the range of the cementation exponent is usually small, with  $1 \leq m \leq 5$  (Glover, 2010)..



Thus equations 4.1 and 4.2 can be used to write down the general form of Archie's law as shown in equation 4.3 as

$$\rho = \rho_w \Phi^{-m} \dots\dots\dots 4.3$$

It can also be shown that the formation factor  $F$  can also be used to define the electrical tortuosity ( $\tau$ ), a factor depended on the porosity of the medium as;

$$\tau = F\Phi \dots\dots\dots 4.4$$

Thus by combining equations 3.4 and 3.5 , the formation factor can be expressed in terms of the porosity and the cementation exponent as (equation 4.5):

$$F = \Phi \Phi^{1-m} \dots\dots\dots 4.5$$

Physically, the formation factor represents the conductivity of the medium matrix normalised to the conductivity of the saturating fluid. However, the formation factor has been described in terms of electrical resistivity since electrical resistance is easily determined from electrical surveys. However in order to obtain the physical understanding of the cementation exponent, it is often useful to consider electrical conductivity. Thus the conductivity formation factor relationship can be written in terms of an inverse of the resistivity formation factor as shown in Equation 4.6.

$$G = \frac{\sigma}{\sigma_w} = \frac{1}{F} \dots\dots\dots 4.6$$

G often increases from 0 to 1 and increases with increase in the porosity of the medium. This factor often referred to as the dilution factor, where the conductivity of the pore fluid  $\sigma_w$  is diluted by the mineral grains of the solid matrix of the medium. It thus gives a measure of the availability of fluid pathways for electrical transport and therefore it gives a measure of the interconnectedness of the pore and fracture network of the medium, i.e. the connectedness of the porous medium was defined in Glober (2002), as;

$$G = \Phi^m \dots\dots\dots 4.7$$

Thus the conductivity of a medium can be expressed in the form of Archie 's law and is described as;

$$\sigma = \sigma_w \Phi^m \dots\dots\dots 4.8$$

Equation 4.8 represents the electrical connectedness of the of the medium matrix. The connectivity of the total pore network  $\chi$  of the medium is usually defined as the inverse of electrical tortuosity, i.e.;

$$\chi = \frac{1}{\tau} \dots\dots\dots 4.9$$

Thus in terms of porosity, the pore network  $\chi$  can be written as;

$$\chi = \Phi^{m-1} \dots\dots\dots 4.10$$

Thus the conductivity formation factor G, can thus be written as;

$$G = \Phi^m = \Phi \Phi^{m-1} = \Phi \chi \dots\dots\dots 4.11$$

and hence the connectedness of a medium matrix is largely due to the pore volume available for fluid conduction as represented by the 3 dimensional arrangement of the porosity of the medium matrix. Differentiating Equation 4.11 with respect to the pore connectivity  $\chi$  and  $\Phi$  porosity a differential relation for the cementation exponent is obtained as;

$$m = \frac{d}{d\chi} \left( \frac{dG}{d\Phi} \right) = \frac{d^2G}{d\chi d\Phi} \dots\dots\dots 4.12$$

Equation 4.12 thus suggests that the cementation exponent is the sensitivity to changing connectivity of the conductivity formation factor i.e. how the presence of non-conducting grains of the medium varies as a function of porosity and the connectivity of

the matrix, as suggested in Globber (2010). Recent studies have successfully used empirical experiments in the laboratory to determine the cementation factor for the medium through the application of percolation principles in the particular porous medium. As such similar application can also be applied to the ash medium, since that the physical meaning and the importance of determining this parameter has been explored.

#### **4.2 Determination of the cementation factor for coal ash matrix**

The suitability of application of the electrical resistivity method is more acceptable in medium whose resistivity characteristics obey Archie's laws. Before application of the Electrical resistivity geophysical methods in a medium whose resistivity-moisture characteristics is unknown, it is therefore necessary to establish if the cementation characteristics of the medium fall within the specified range for the electrical resistivity behaviour to be obeying Archie's law. The main procedure for establishing whether the electrical behaviour of a material is suitable for electrical resistivity methods is through establishing if its cementation factor falls within specified ranges for Archie's law to hold. This involves the empirical determination of the cementation exponent for the medium matrix, (e.g. in Fukue et al., 1999, Michot et al., 2003, Börner and Schön 1991, McCarter, 1984). In this study the analogy between electric current flow and water/or moisture content and electrical resistivity was used to establish a value of the cementation parameter for the ash medium and to assess the suitability of applying electrical resistivity methods characterising the fluid migration in the medium.

Electrical resistivity is a function of the textural and structural characteristics and is particularly sensitive to the water content of the geological formation, (Arora and

Shakeel, 2010). Water and salt infiltration can be determined by studies of variations in electrical resistivity measurements as change in moisture content affects the resistivity in a nonlinear way. Electrical resistivity of a medium is usually dependent on the degree of water saturation, amount of dissolved solids, content of the organic matter, grain shape of the medium matrix, and the mineral content of the soil or material forming the medium matrix. The degree of water saturation has the greatest effect on the resistivity, for a homogeneous medium comparable to the ash medium.

Archie's law allows correlating electrical resistivity and saturation and porosity for rocks and soils. Grellier (2005) managed to reduce the Archie's law for a soil medium, to:

$$\rho = \alpha \rho_w \theta_w^{-m} \dots\dots\dots 4.13$$



where  $\theta_w$  and is the gravimetric moisture content of the soil medium (Equation 4.14) and  $\alpha$  is a parameter that includes the bulk density of the medium.

The moisture content of the ash samples was measured using the standard laboratory procedure of roasting them at 105 °C for 24 hours so as get the dry mass,  $M$ . A known volume of brine water was added to a known the ash sample and the new mass of the sample and the brine water was also recorded. The wet moisture content of the sample was then calculated, using the standard formulae suggested in Bowles, (1992) as in Equation 4.14.

$$\theta_w = \frac{M}{M_t} \dots\dots\dots (4.14)$$

where  $M$  is the dry mass of the sample and  $M_t$  is the total mass of the wet sample.

After the determination of the sample moisture content, the electrical conductivity of the sample was determined using the YSI model 35 soil conductance meter (Photo 4.1).

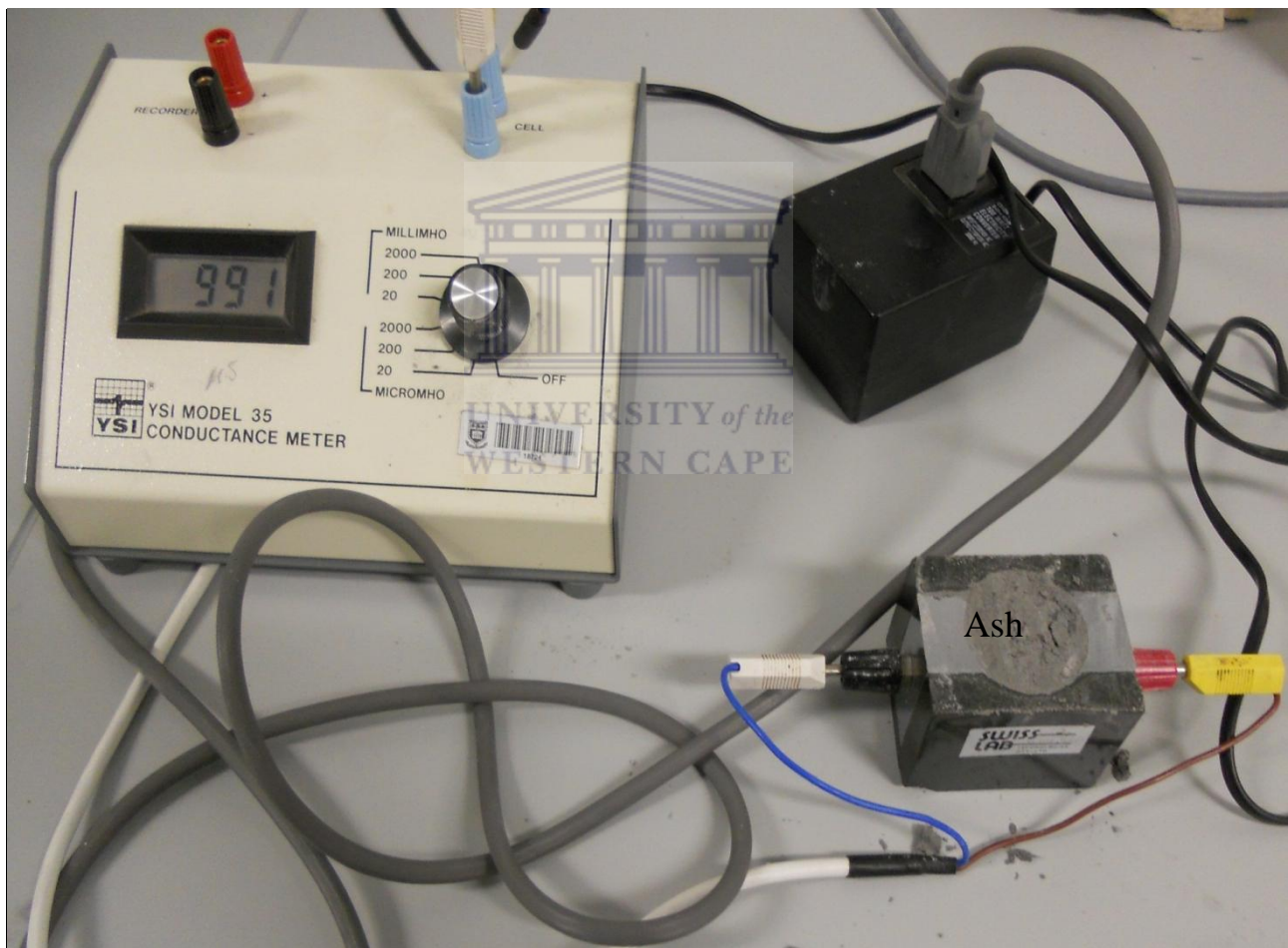


**Photo 4.1. The experimental set up for determining the variation of electrical resistivity (conductivity) with salt and moisture content.**

The experimental procedures were repeated for different values of moisture content, with water (electrical conductivity 5 $\mu$ S/cm) and industrial brine used for ash irrigation (electrical conductivity 1950mS/cm). The measured electrical conductivity values were converted to electrical resistivity and plots of variation of resistivity with moisture content for both still water and brine water were done (Figure 4.1 (a) and (b)). An excel generated line of best fit was fitted to the plot and the corresponding trend equation was used to infer empirical values for the cementation exponent of the medium.

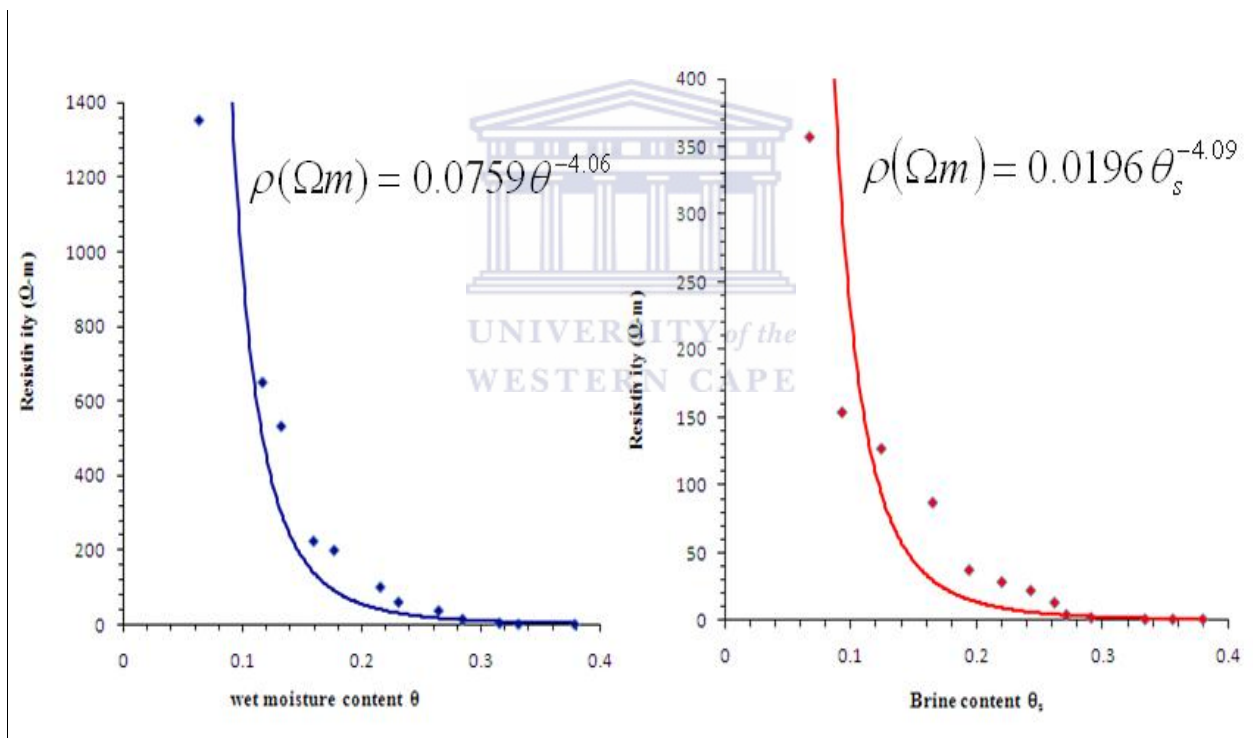


**Figure 4.1. Experimental variation of electrical resistivity with water / salt content.**

The results suggest an inverse relation between electrical resistivity with both moisture and brine saturation and are both in agreement with Archie's law. High moisture content was associated with low electrical resistivity and vice versa. A power law relation was



used to obtain the best estimate in of resistivity variation with moisture content. The empirical relationship between moisture content and electrical resistivity suggested by the trend equation fitted on the plot which describes an inverse power law with a power exponent of  $m \approx 4.06$  (Equation 4.15).

$$\rho_w(\Omega m) = 0.0759\theta^{-4.061} \dots\dots\dots 4.15$$

The trend equation for the variation of electrical resistivity with brine content also followed a similar inverse power with a power exponent of  $m \approx 4.09$  (Equation 4.16).

$$\rho_s(\Omega m) = 0.0196\theta^{-4.096} \dots\dots\dots 4.16$$



The relationship between moisture/salt content and electric resistivity for the ash medium was a negative non-linear relation. From equations 4.15 and 4.16, it is deduced that the cementation factor of the ash matrix, (equivalent to the power exponent for the relations) is approximated as  $m \approx 4.1$ . Such high cementation factor is often associated with a medium whose pore spaces are less well connected as, suggested in Tiab and Donaldson (1994). This value of the cementation factor is in agreement with the ash medium high which is associated with a decrease in the pore network connectivity of the medium (Glover, 2010) and increase in cementation properties through pozzolanic action responsible for partial cementation in the ash medium. The experiments also suggested that the cementation factor for the ash medium this is within the range of application of Archie’s law (between 1 and 5). Therefore, since the ash medium matrix

is in agreement with Archie's conditions, the apparent formation factor is equivalent to intrinsic formation factor, and electrical resistivity geophysical methods can be reliably used to characterise the transport properties of the medium.

In conclusion, the experimental results offered information on the use of resistivity method as a suitable tool for monitoring the moisture and salt flow in the ash dump. The resistivity response on changes in ash moisture content is the key mechanism that permits the use of non-invasive ERT techniques to monitor the vadose zone in time-lapse mode, i.e. via repeated measurements over time.

#### **4.3 Time lapse infiltration survey using electrical resistivity tomography**

Electrical resistivity measurements provide a powerful tool for detailed studies of vertical water movement in the unsaturated soil zone and therefore should help to assess the boundary conditions for infiltration modelling (Benderitter and Schott, 1999). Recent research in monitoring solute plumes during tracer tests, and attempts to estimate a quantitative assessment of the transport characteristics (breakthrough curves), gives a better understanding of transport processes, and provides a promising tool to calibrate solute transport modelling (Binley et al., 1996; Kemna et al., 2002; Slater et al., 2000, 2002). In this study, time-lapse ERT survey was used to monitor the rate of brine ingress through the unsaturated zone of the ash dump in a field experiment. The electrical resistivity method consists of injecting an electrical current ( $I$ ) through two metallic electrodes and measuring the potential difference ( $\Delta V$ ) between two other

electrodes. The apparent resistivity ( $\rho_a$ ) is given by the following relationship (Dahlin, 2001).

$$\rho_a = K \frac{\Delta V}{I} \dots\dots\dots 4.17$$

with K a geometrical factor which only depends on electrode position. The  $\rho_a$  is the ratio of the potential obtained in situ with a specific array and a specific injected current by the potential which will be obtained with the same array and current for a homogeneous and isotropic medium of 1  $\Omega\text{m}$  resistivity. The apparent resistivity measurements provide information about resistivity for a medium whose volume is proportional to the electrode spacing (Figure 4.2).

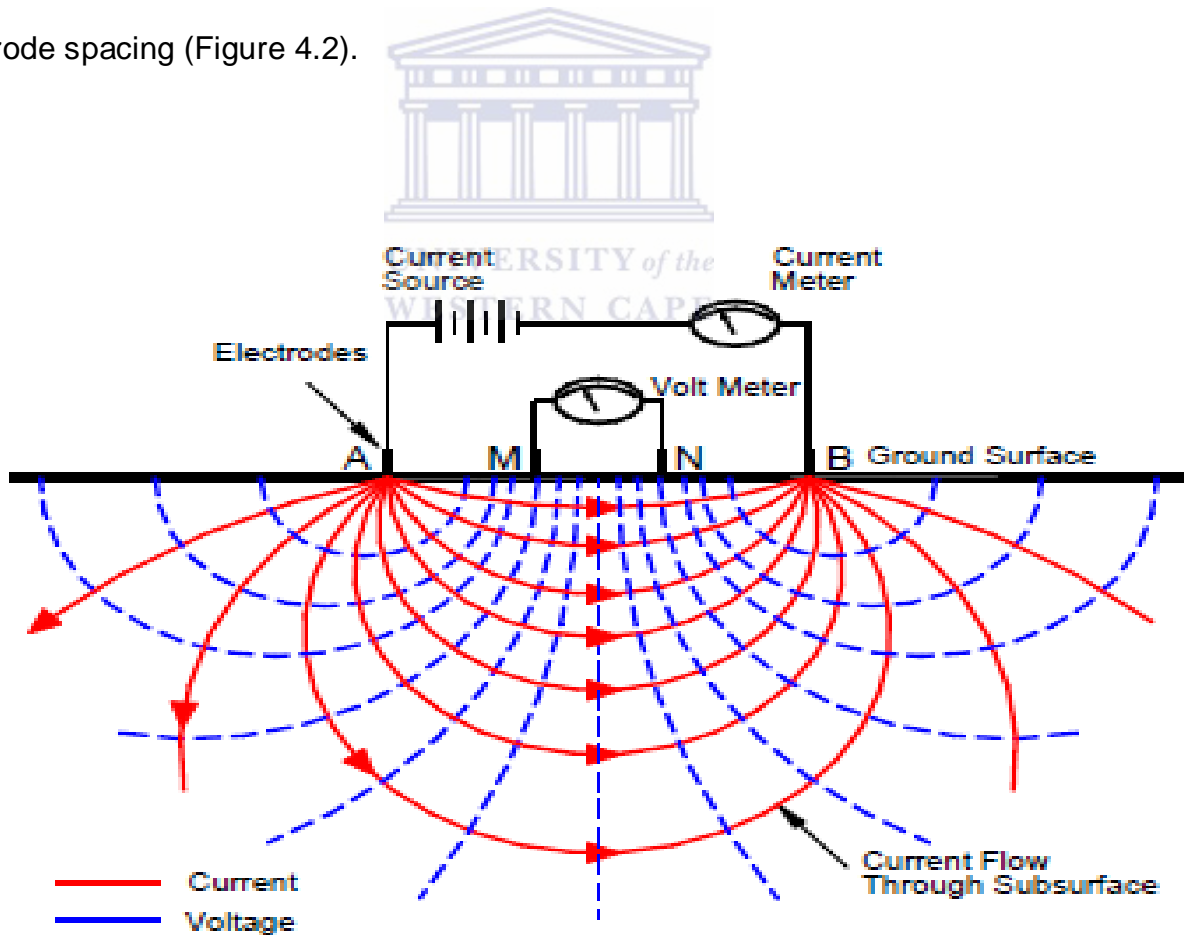
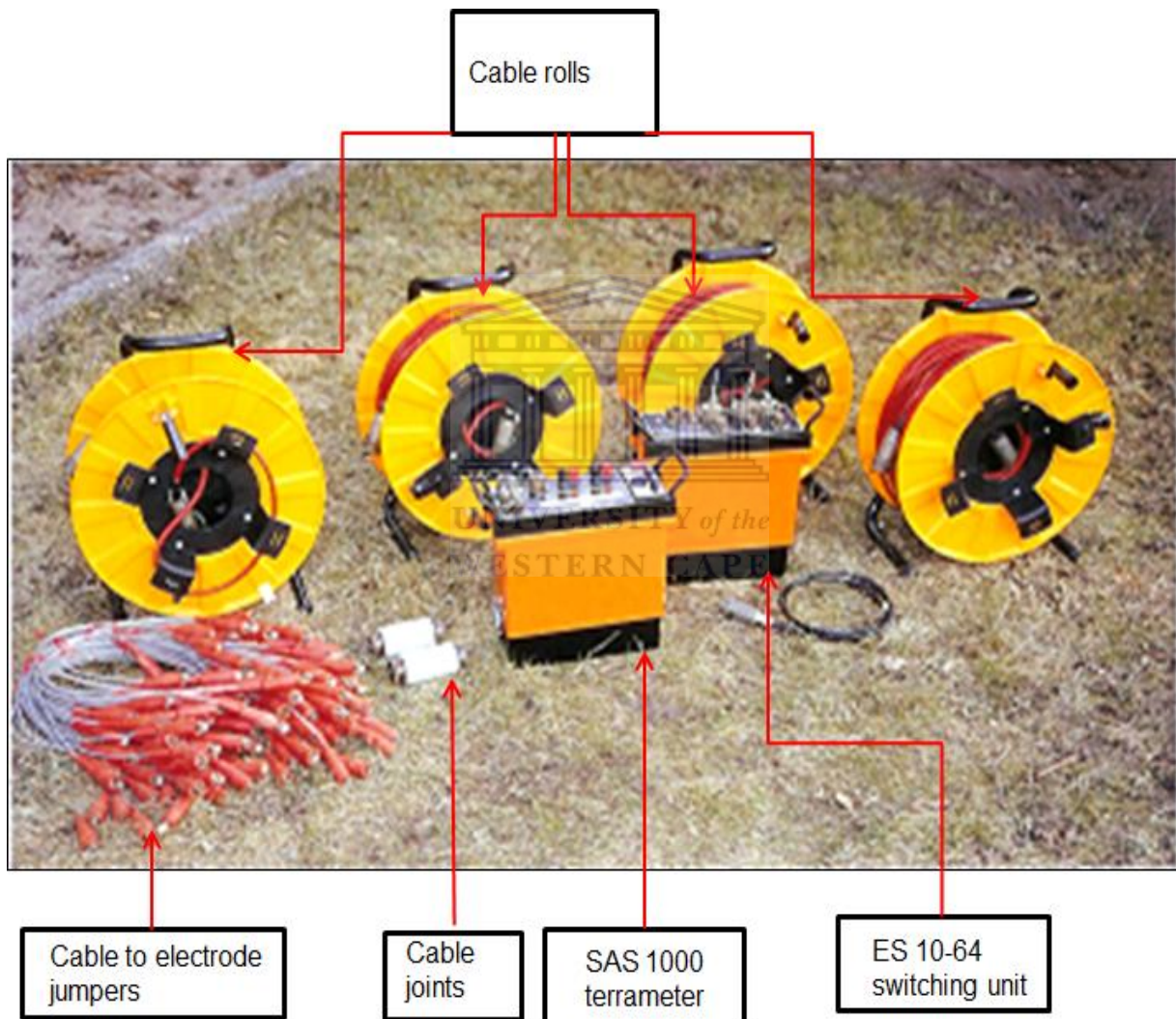


Figure 4.2. Basic concept of electrical resistivity subsurface measurement (Adopted from Marescot, 2008).

The resistivity data acquisition system used for this survey was the ABEM Lund Imaging System (Dahlin, 1996) which uses an Abem SAS 4000 terrameter and ES 10-64 switching unit, with 60 standard stainless steel electrodes and four multi-core cables with 20 electrode connection points for each cable (Photo 4.2).



**Photo 4.2. The SAS 1000 LUND imaging system and the ES 464 switching unit used for the electrical resistivity tomography survey.**

Wenner long and short electrode geometry protocols was used for the survey. In this protocol, the inner electrodes have a spacing equivalent to half the standard Wenner electrode separation,  $a$ , thereby ensuring a dense measuring network on the central region of the profile. In order to get high spatial resolution data an electrode spacing of 1 m for the long protocol and 0.5m for the short protocol. A low alternating current of 100mA, with a frequency of 50 Hz was injected into the ash medium. The multicore cable was connected to a switching unit cascaded to a laptop computer. The automatic acquisition systems used in modern surveys made it possible to collect dense data sets. The sequence in which measurements are made, the type of electrode array that was being used for taking the measurements and the value of the input current were entered on the switching unit of the switching unit.

The survey was conducted during the period 15 - 18 March 2010. An initial preliminary electrical resistivity tomography was done on either site so as to ascertain the initial resistivity distribution before the start of the infiltration test. The electrodes were left undisturbed and the same cable sequence was maintained during the whole survey. The stainless steel electrodes were hammered approximately 30-40 cm into the ash. After the initial electrical resistivity profiles, the injection pit was dug into the ash at selected positions and 3m<sup>3</sup> of brine was allowed to infiltrate into the ash dump through the infiltration pit (Photo 4.3).

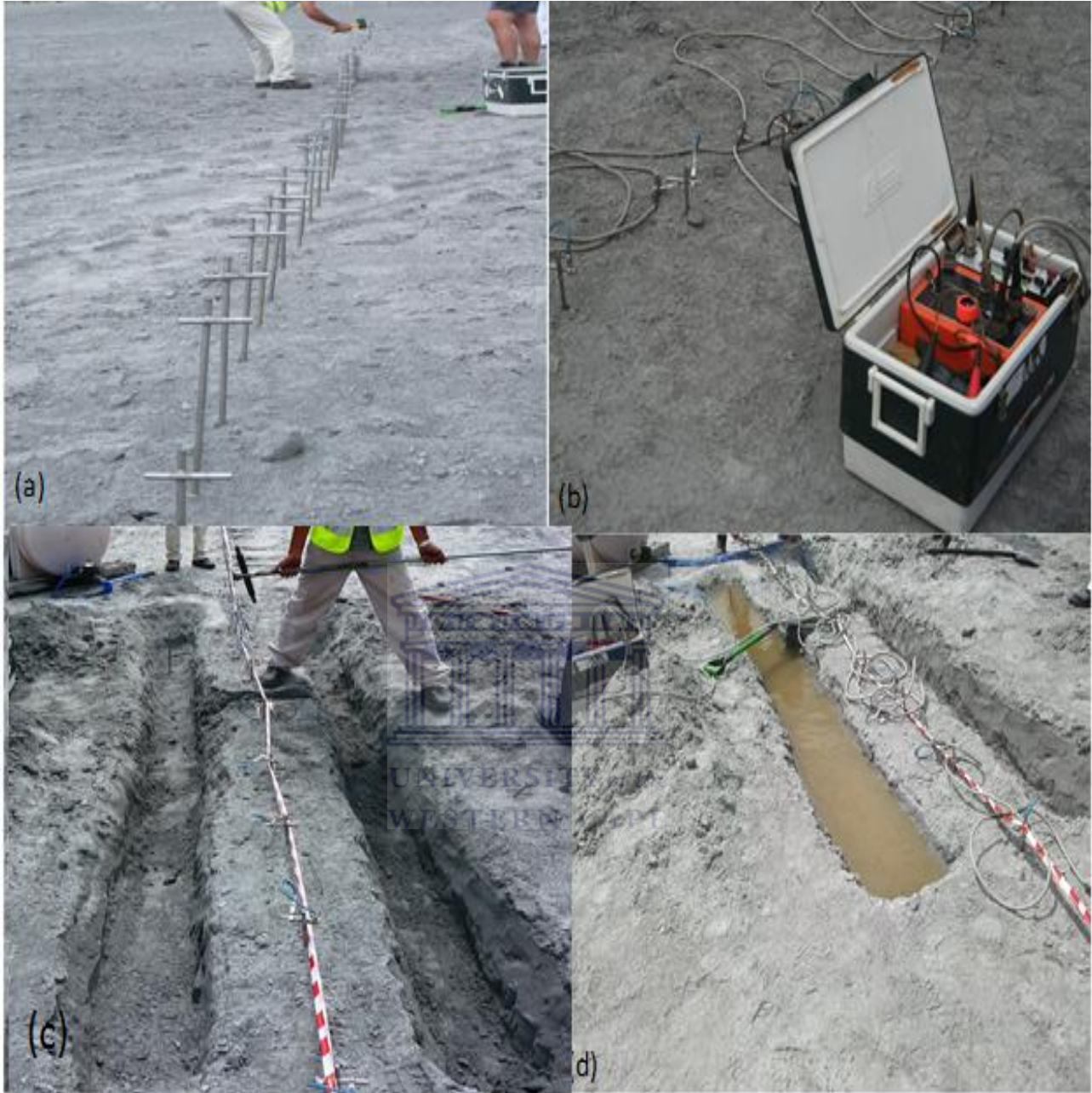


**Photo 4.3. A description of the methodology infiltration procedure; (a) the initial hammering in of the steel electrodes, in preparation for the initial preliminary survey using (b) the ABEM Lund Imaging System and cables before (c) the infiltration pit was dug and (d)  $2\text{m}^3$  of brine water allowed to infiltrate and monitored.**

Routine measurements were done at different time intervals during the first day. After the resistivity measurements were done, an additional  $2\text{m}^3$  of brine water was then added into the trench so as to observe the general effect of the volume of infiltrating brine on the rate of progression of the moisture plume through the unsaturated zone. The array geometry was then changed to the Wenner array which has high vertical resolution and a low sensitivity to noise ratio. In order to investigate the variations in homogeneity within the ash dump, as well as to investigate the existence of any lateral heterogeneities that could affect the movement of moisture within the ash dump. A second infiltration survey was set up at a different site of the ash dump using the same measuring and data acquisition procedures. The same measuring protocol and electrode spacing was maintained for the two surveys so as to ensure consistency in the observed results.

The apparent resistivity values were inverted using the time-lapse approach based on cross models implemented in the RES2DINV inversion software (Loke, 2006). The basic of a cross model is the use of an inverted model from a base dataset as the reference model for later datasets. Changes in subsurface resistivity are computed by using the apparent resistivity changes to ensure that changes of inverted resistivity values are only due to changes in apparent resistivity values (Loke, 1999). The inversion routine used is based on the smoothness constrained least squares technique (Loke et al., 1996a). The program automatically creates a 2D model by dividing the subsurface into rectangular blocks and then chooses optimum inversion parameters for the data which include the damping factor, vertical to horizontal flatness filter ratio, convergence limit and number of iterations. The resistivity of the model blocks is

adjusted iteratively until the calculated apparent resistivity values of the model agree with the actual measurements. Since time-lapse measurements are performed, changes in ERT images with time could easily be assessed by subtraction of pixel-by-pixel values from some background image. The model obtained from the first data set was used as a reference model for all the later data sets. The least-squares smoothness constrain option was used to ensure that the differences in the model resistivity varied in a smooth manner. The data from time-lapse surveys conducted at different times was therefore inverted independently and the changes in the subsurface resistivity values was then determined by comparing the model resistivity values obtained from the inversions of an initial data set and the later time data and presented as the percentage change in the model resistivity. The inversion of the data sets was carried using a joint inversion technique where the model obtained from the initial technique was used to constrain the inversion of the later resistivity model (Loke, 1999). To minimize possible distortions in the time series models, a joint inversion technique was applied that uses the model from the initial data set to constrain the inversion of the later time data sets.

The distribution of the infiltrating brine in the subsurface of the ash dump was not very clear from a direct comparison of the inversion models alone, but was more easily determined by plotting the percentage change in the subsurface resistivity of the inversion models for the data sets taken at different times. The resistivity scale the models was relatively small (0-120  $\Omega\text{m}$ ) compared to the normal resistivity values used in groundwater investigations (usually 0- over 1000 $\Omega\text{m}$ ), which had been suggested by the laboratory results, indicating low resistivity scales associated with the ash medium.



In order to accommodate the range of resistivities present, a logarithmic colour scale has been used for visualization of the resistivity maps.

#### **4.2.1 Time lapse results for Site 2**

The first set of results for Site 1 were obtained just 1.5 hours after the beginning of the infiltration survey, and showed that the plume had progressed to depths below 0.9 m (Figure 4.3). Forward plume migration seems to take place shortly after the brine injection into the ash but the downward movement of the plume after the first 20 hours seems to have progressed slightly.



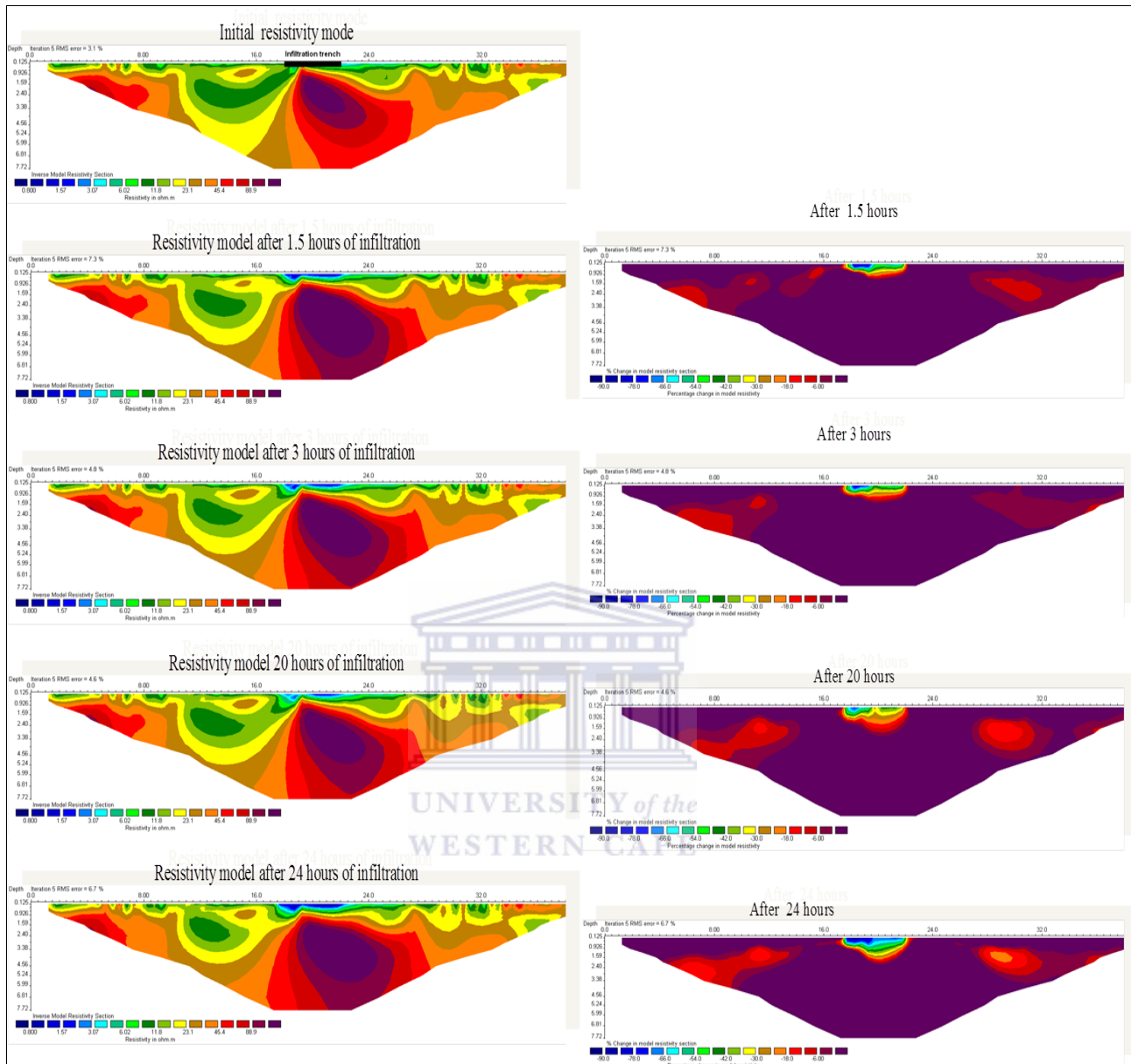


**Figure 4.3. Time lapse results for a time lapse Survey at Site 1.**

The models on the left represent the inverse model pseudo sections taken at specific times as the plume was progressing in the ash dump. The models on the right represent the percentage change in resistivity of that particular resistivity model with respect to the initial resistivity model. As soon as the brine was injected into the ash medium, the trends of conductive brine are observed by low resistivity values around the injection pit.

A clear picture is observed from the percentage change models. It was also noted that the resistivities of the material immediately below the pit also appear reduced as compared to the background resistivities.

The percentage change models show areas of slight change (anomalies) on the flanks of the model. These spurious changes can be regarded as the result of noise or minute measuring fluctuations in the later time surveys. By increasing the time-constrain weight (an option whereby the relative importance of keeping the later time models as similar as possible to the reference model), these changes would be reduced, but it will give an increasing in the RMS misfit between the calculated and measured data. The default value of 3 for the time-constrain weight were however used to minimize the RMS data error.

Although plume migration started shortly after the brine injection into the ash, the overall plume spreading was less pronounced. The respective depths of the wetting front were plotted against the time of survey time in order to obtain an estimate of the infiltration rates (Figure 4.4).

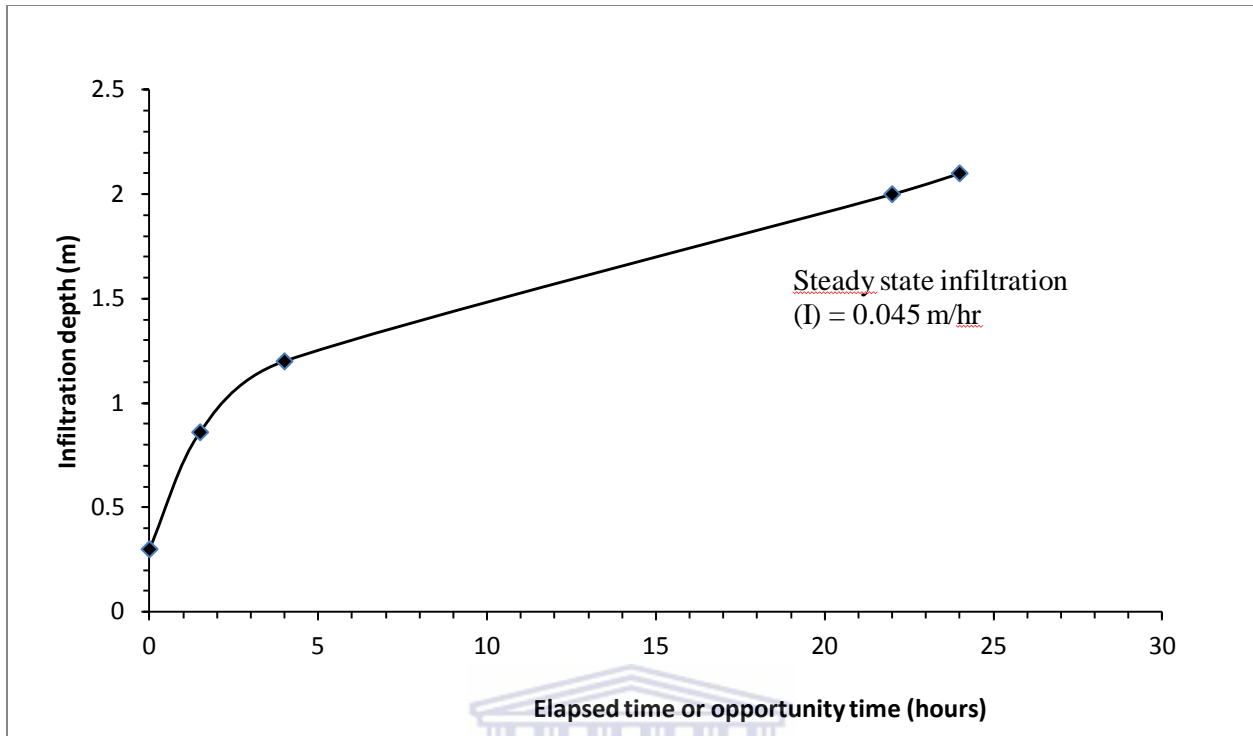


**Figure 4.4. Variation of depth of infiltration with elapsed time.**

Using an anisotropic model (Amoozegar, 1992), the best estimate of vertical infiltration (I) rate obtained based solely on the centre-of-mass motion was  $1.13 \text{ m/day}$ . In order to observe the effects of the volume of brine on the rate of progression of the moisture plume, an additional  $2\text{m}^3$  of brine water was poured into the infiltration trench. The rate of progression of this plume increased abruptly soon after the addition of the extra brine, such that it had progressed to depths of well below the 6 meters within a time space when the last set of readings were made after 42 hours from the start of the survey (Figure 4.5).

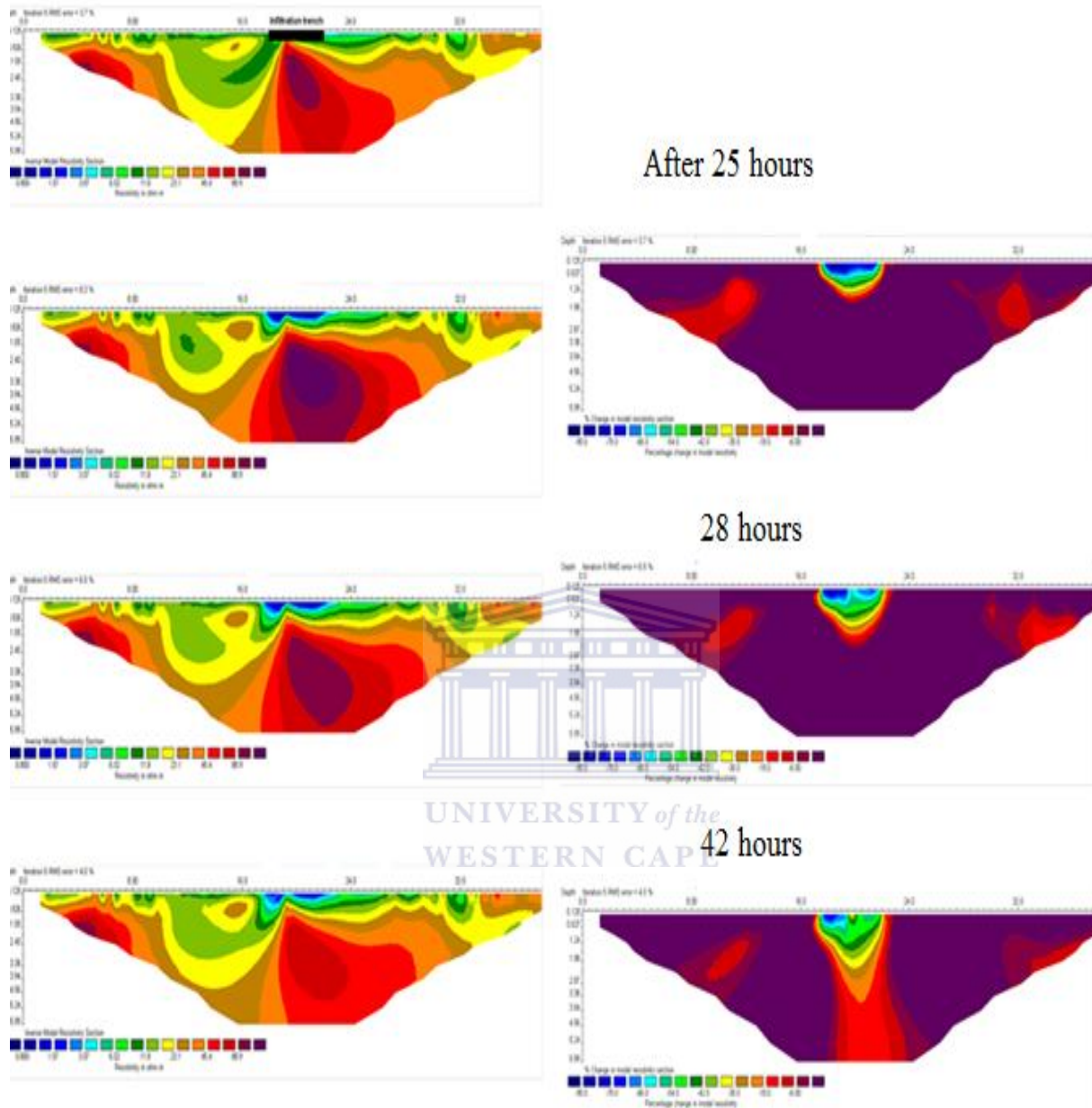


**Figure 4.5. Results of the time lapse infiltration survey results for site 1 after adding more brine.**

The infiltration rate increased abruptly soon after the addition of the extra of brine, although there is some observed distortion on the percentage change in resistivity model 42 hours, which is attributed to the fact that most current was being trapped

within the progressing plume. Using the same approach used previously, the steady state infiltration rate was 3.85 m/day.

Electrical resistivity measurements thus provided a powerful tool for detailed studies of vertical water movement in the unsaturated zone of the ash dump and hence could help to assess the rates and conditions for infiltration modelling. Although there are other sources of energy, the flow of a fluid in the unsaturated zone of the ash medium is thus based on the gravitational potential energy of the fluid, the energy of fluid pressure and the kinetic energy of the fluid.

The sudden increase in infiltration rates suggests that the field capacity of the ash dump had been exceeded and brine water was infiltrating at a faster rate. The field capacity is defined as the maximum amount of water that a soil or rock can hold, as by capillary action, before the water is drawn away by gravity. However, the infiltration showed a vertical infiltration indicating that gravity forces are the main drivers of the moisture movement in the ash dump. This can occur after heavy rainfall events or due to over continuous irrigation at one position of the dump.

#### **4.2.2 Time lapse results for Site 2**

An additional infiltration survey was done at a separate site of the ash dump with an aim of determining the lateral variation in the rate and manner of the infiltration and movement of brine through the ash dump. The survey was done using the cross survey technique with one profile along the East-west and the other in the North South direction. The two sets of measurements were recorded after two hours and six hours for each axis. Results of the time lapse survey from the North to South (X) direction of

Site 2 are presented in Figure 4.6(a). Figure 4.6(b) gives respective percentage changes in resistivity between a profile measured after a particular time lapse and the initial resistivity model. This percentage change in resistivity displays the extent and distribution of the infiltrating fluid at the time of measurement.



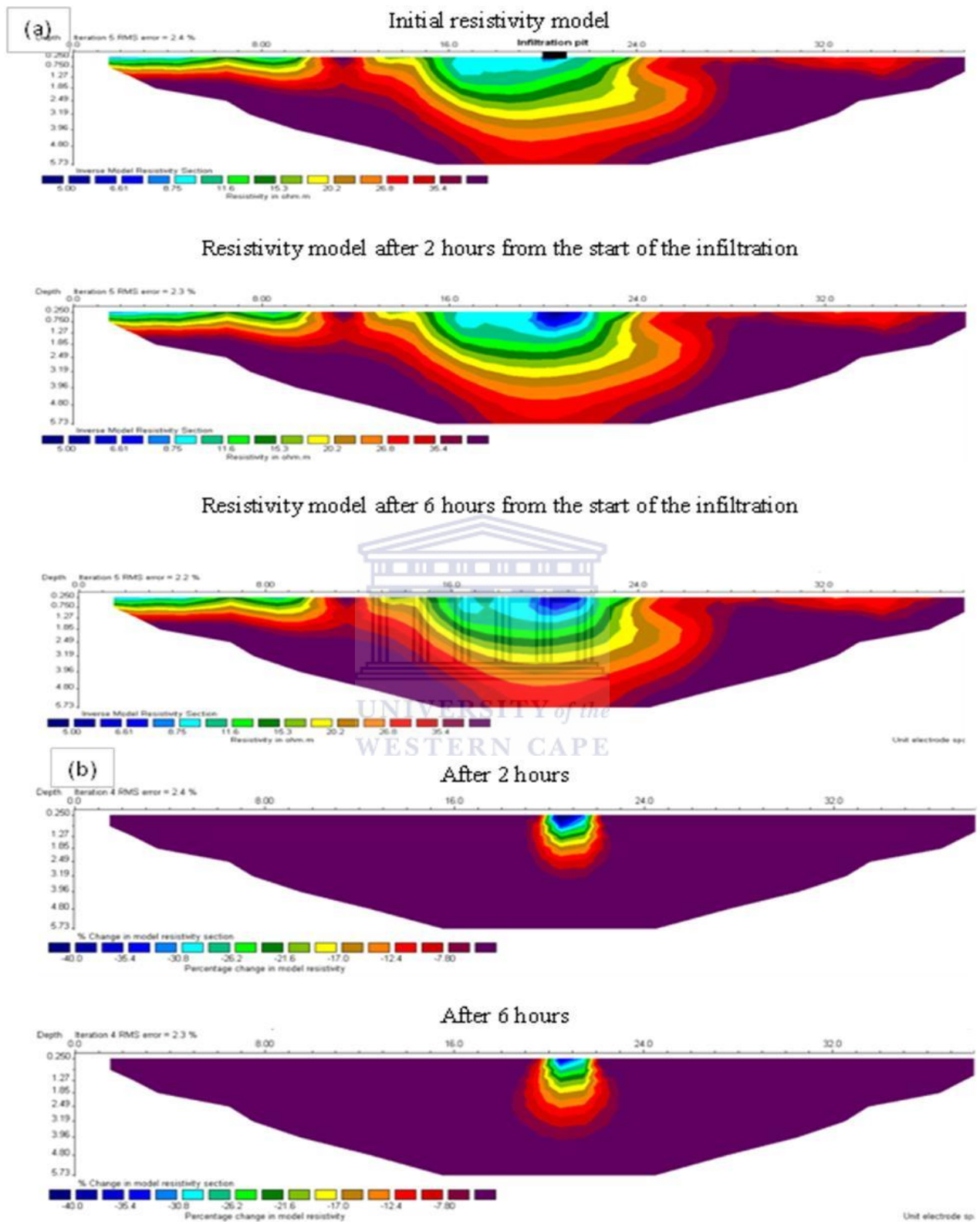
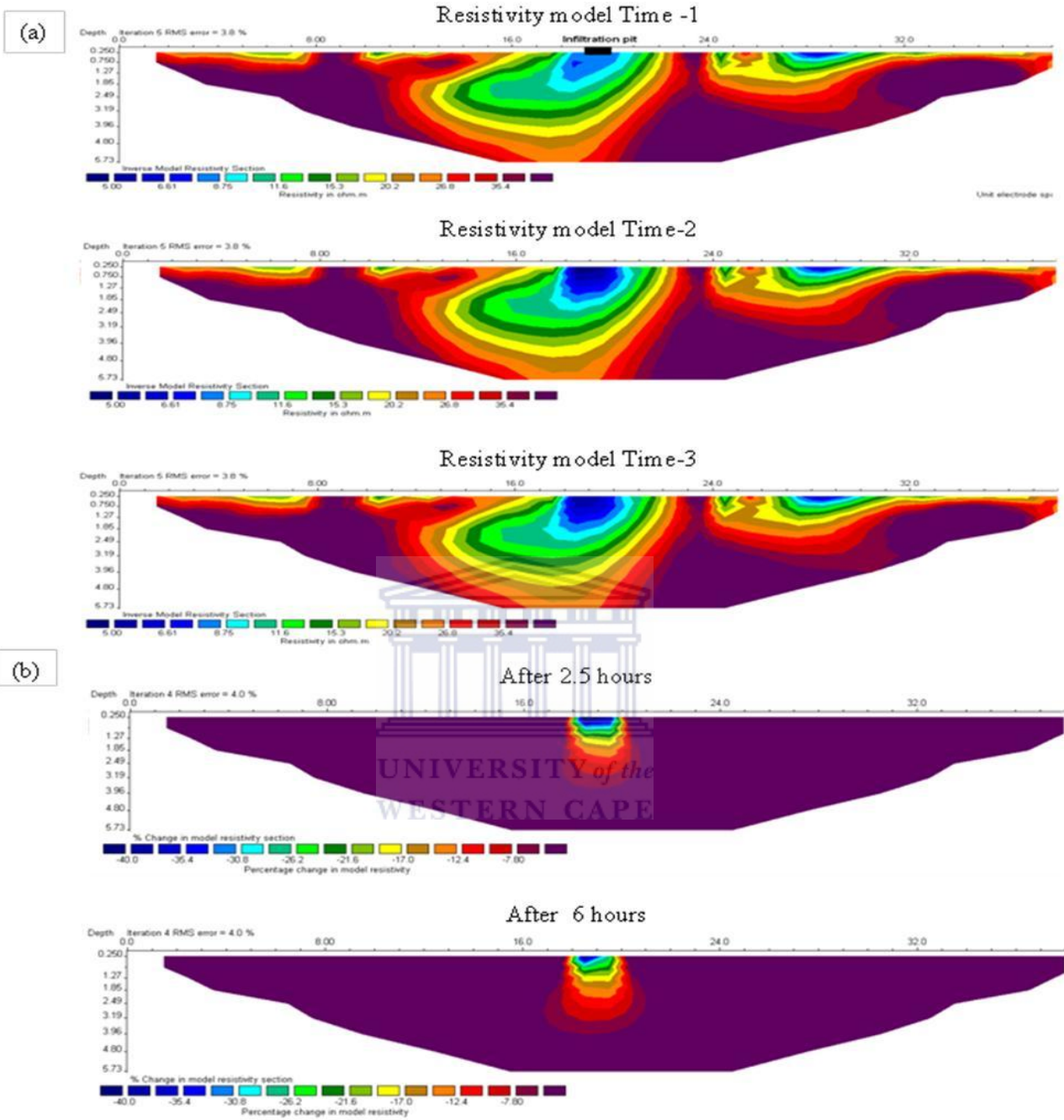


Figure 4.6. (a) Inverse model resistivity results for the X (North-South direction) of Site 2 and (b) Results of the percentage change in resistivity for the time lapse infiltration survey along the North-South direction (X-axis) of Site 2.





**Figure 4.7. Resistivity model results for the time lapse infiltration survey along the East-West direction (Y-axis) (b) Model results of the percentage changes in resistivity for the time lapse infiltration survey along the East –West (Y) direction of Site 2.**

After two hours, the plume had progressed to depth of over 3 m and was also spreading in a radial pattern, even though the vertical progression was more pronounced. The

zone which had the highest resistivity change, (shown as blue contours ) had progressed to depths of just over 1m, and also spreading radially suggesting that most of the infiltration fluid was still trapped within the top section region. Four hours later, the plume had progressed considerably into the ash dump, to depths below 4.8 m, as shown by the second set of the results. The radial spread of the moisture plume at deeper depths along the Y axis is not as pronounced as in the X axis. This could be due to the relative position of the infiltration trench with respect to the profile line. The general movement of moisture and hence the potential movement of salt leachates in the unsaturated zone of the ash dump seem to be controlled by the effects of gravity rather than the lateral inhomogeneities of the ash dump.

#### **4.2.3 Conceptual understanding of the infiltration process in the ash dump.**

The knowledge of the infiltration behaviour of the ash dump is critical in assessing the recharge properties of the dump itself. Both natural charge (through rainfall) and artificial recharge (through brine irrigation) plays a critical role in assessing potential movement of contaminants in the ash dump since it acts as a solute medium through which the salts and any trace elements may be leached.

The changes in electrical resistivity in the ash medium were subject to vary in space and time, because of the movement of solute fluxes within the medium itself. This was evidenced by the continuous spatially and temporal variations in the time-lapse infiltration surveys. The results from both sites suggested that the unsaturated zone of the ash dump homogeneous medium which makes the infiltrating fluid progress vertically downwards under effect of gravity forces and there is no evidence for the

existence of preferential pathways within the ash dump. The volume of the infiltrating liquid also determines the rate of infiltration as was observed from the results for Site 1. Since the increase in infiltrating brine caused an increase in rate of infiltration, there is need to strictly control the irrigation schedule and guard against over irrigation, as it may saturate the ash and cause the flushing away of any soluble salt leachates that may be contained in the unsaturated zone into the groundwater system.

The time lapse infiltration experiments suggested that moisture content of the compaction of the medium, usually represented as the bulk density of the medium, is a critical component in the determination of the ash dump transport parameters of the ash dump. Figure 6.1 gives a conceptual model that was developed for the parameters affecting the infiltration rates through the ash dump.

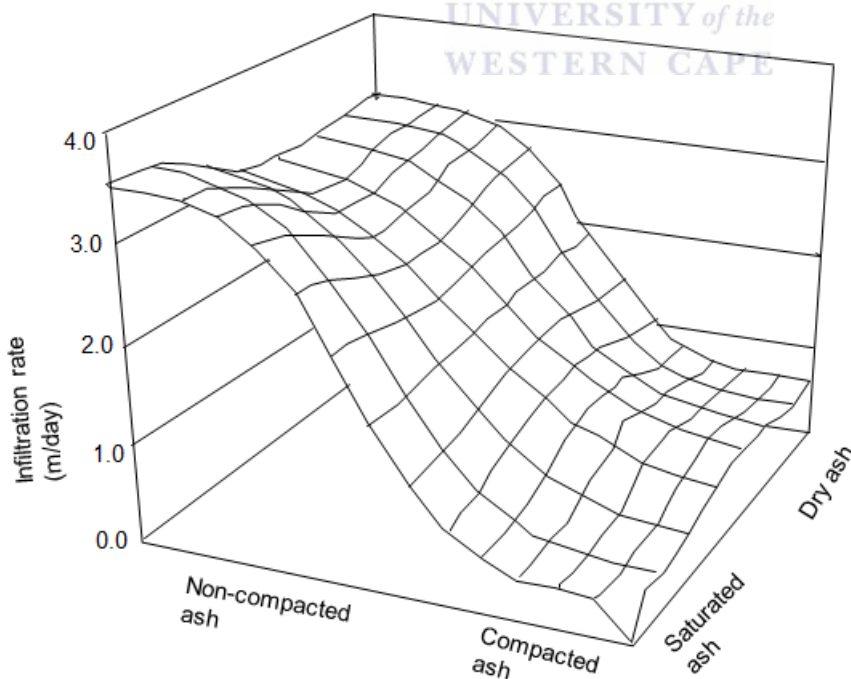


**Figure 4.8. An infiltration conceptual model for the ash dump.**

The conceptual model suggests that the infiltration is controlled by the physical parameters of the ash medium consisting of an unsaturated zone which is characterized by relatively higher infiltration rates. The non compacted ash is characterised by high infiltration rates due to the presence of unfilled pore spaces which would act as water conduits through the ash medium.

The non compacted zone of the saturated zone of the ash dump is characterised by high infiltration rates, as suggested by the infiltration results obtained after adding a further 2m<sup>3</sup> of brine. The reason for such characteristically high infiltration is explained by high moisture content within pore spaces due to the ash dump exceeding its field capacity (the maximum water which the medium can hold before being drained away under gravity). The high infiltration rates for saturated ash also explains the exceeding of the field capacity of the ash dump which could probably lead to further leaching of any contaminants trapped in the ash dump. Henceforth care should be taken to ensure that the level of optimal compaction on the ash dump is reached. A well compacted, (well cemented) ash medium is characterised by lower infiltration rates in both the saturated and the unsaturated sections of the dump as inferred from the conceptual model (Figure 4.8), and observed in the time lapse infiltration experiments.

#### **4.3 Geophysical assessment and Long term monitoring of the ash dump**

In August 2008 and September 2010, the electrical resistivity surveys were carried out on the same line as where a geophysical profile was done in 2006. The main objective of the profile was to carry out a repeat survey on the same line in order to compare the bi-annual profiles and provide an attempt to detect any changes in salt and water

transport through the ash dump during this period. This profile transacted the ash dump from old ash placed more than 20 years ago on the western side of the dump with an ash depth of approximately 40 m.

Time dependent surveys are critical since they help to identifying any changes in the salt and water content in the ash dump over time thereby mapping zones in the underlying geology where potential contaminants will preferentially infiltrate the groundwater system. Mapping of salt distribution and water content in the ash dump is easily achieved since electrical resistivity varies depends mainly on variations in water content, dissolved ions and the composition of the matrix.

The profile was surveyed using a 10 meter electrode separation with the Wenner measuring protocol and the depth of investigation was between 60 and 80 meters. The Wenner measuring protocol as was applied in the “roll-along” surveying technique was used for the field measurements. The roll-along method (Figure 4.9.) is a profile technique used to extend horizontally the area covered by the survey, particularly for a system with a limited number of electrodes. After completing the sequence of measurements, the cable is moved past one end of the line by several unit electrode spacing. All the measurements which involve the electrodes on part of the cable which do not overlap the original end of the survey line are repeated.

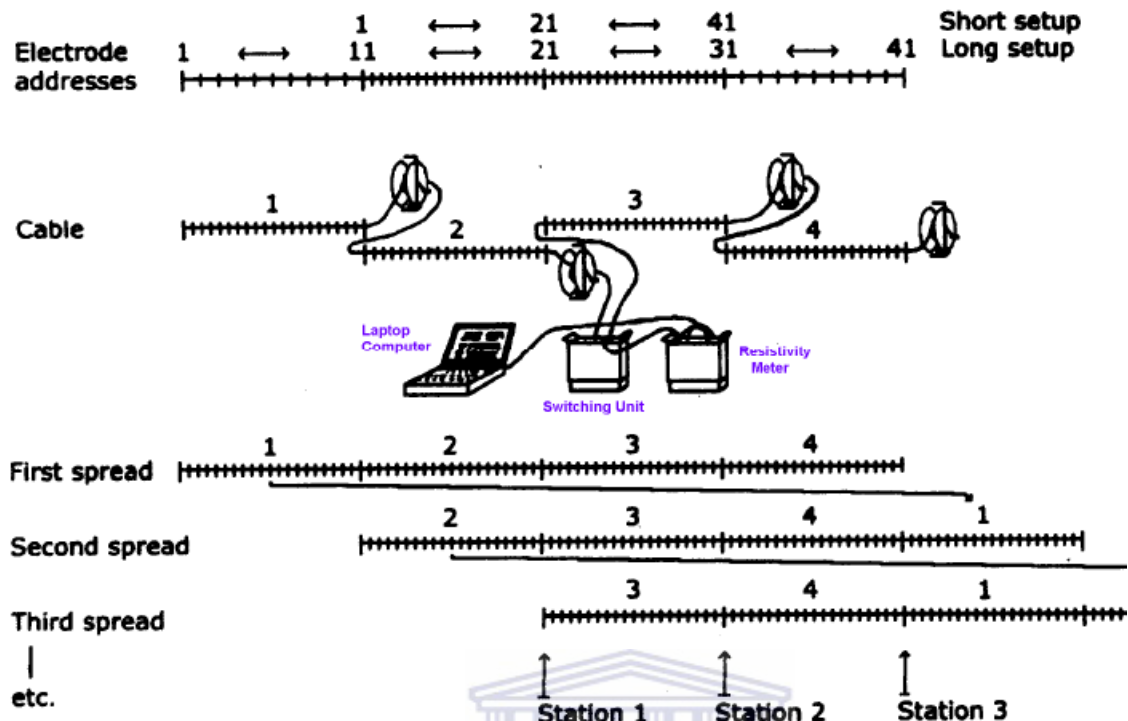


Figure 4.9. Illustration of a computer controlled field data acquisition system using the roll along technique (Adopted from Dahlin, 2001).

UNIVERSITY OF THE WESTERN CAPE

#### 4.3.1 Comparison between the 2006 and the 2008 Profiles

Figure 4.10 presents the electrical resistivity topographies as measured from the top terrace of the ash dump for the 2006 and 2008 profiles. The profiles were surveyed using a 10 meter electrode separation with the Schlumberger-long measuring protocol with an investigation depth of approximately 80 meters. The electrical resistivity method was applied to establish variations in ash characteristics, salt deposition and water level distribution in the subsurface.

Most of the general features that are observed in 2008 are similar to the 2006 profile and is highlighted again on this profile. The most noticeable difference between the

2006 and the 2008 profile being the additional ash dumped between station 1680 and 1920 to the east. The shallow (near surface), approximately 18 m thick, highly resistant-layer (red-purple contours in) is associated with dry disposed ashes.

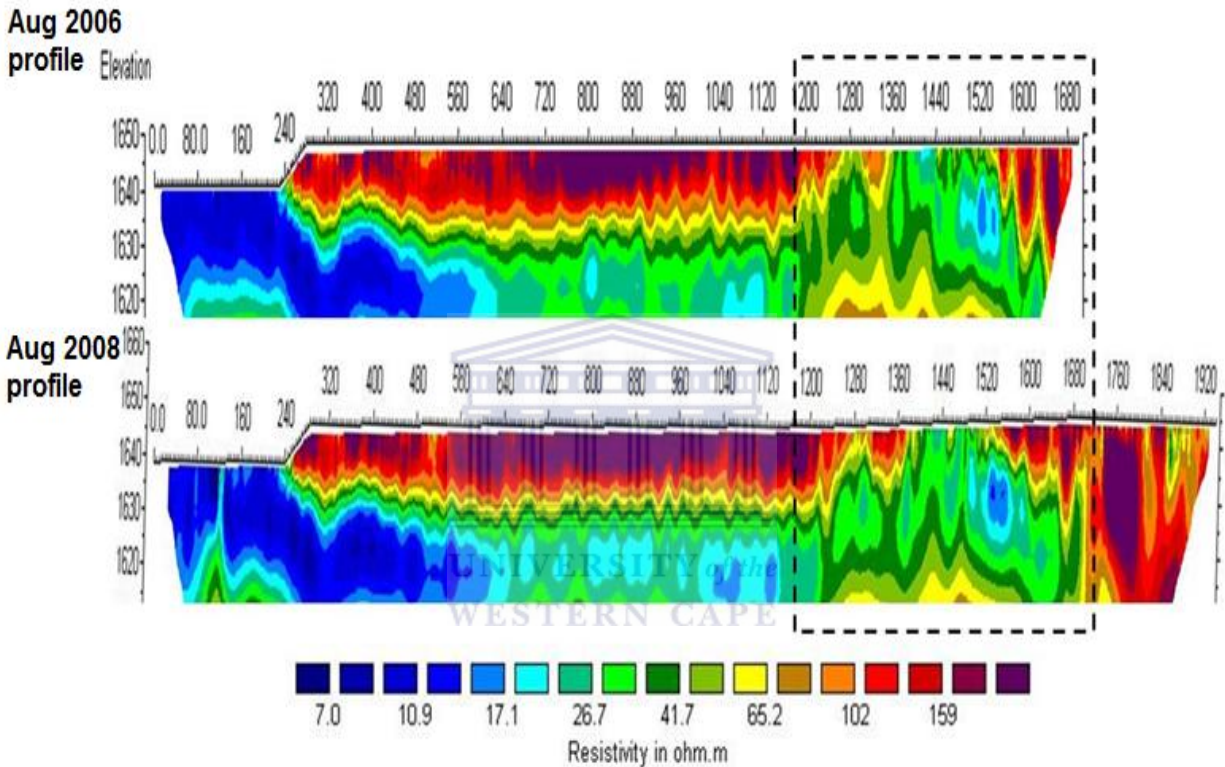


**Figure 4.10. Comparison of the August 2006 and August 2008 electrical resistivity data sets.**

In general, it is observed that the resistivity of the rehabilitated part of the ash dump (from 240m to nearly 1200m mark of the profile) is characterized by high resistivity values (65-159  $\Omega$ m) than the surrounding medium, indicating a low degree of water saturation in the rehabilitated section of the ash dump. The ERT resistivity profiles produced can be interpreted by considering specific sections of the profiles. Both profiles show a top layer of dry ash of about 15 m thickness that is covering the first part

of the ash dump and is characterised by very relatively higher resistances. This near surface high resistive layer (red-brown contours) on the resistivity section is associated with dry ashes and extends from the 240 m mark, where the ash dump starts, until around the 1360 m mark for both profiles.

This section mainly covers the rehabilitated part of the ash dump, suggesting that the rehabilitation process was responsible for the formation of a solid cap which would prevent any further recharge and resulting contaminant transport through the ash medium. This highly resistant layer which disappears at a distance of 1280 m from the origin of the profile reappears at approximately 1550 m and attains its maximum thickness in the far eastern side of the resistivity section. This layer behaviour can be ascribed to the ash having different composition in that part of the profile. The layer reappears again at approximately 1550 m and its maximum thickness is found on the far eastern side of both profiles, a direction to which the ash dump is extending.

Low resistivity values below 10  $\Omega$ m are observed extending into the shallow subsurface geology of the study area and are consistent for both profiles. This more conductive (less resistive) layer (blue-yellow contours) below the ash layer is associated with a weathered dolomite sill body of approximate 30 m thickness with apparent resistivity between 7 and 60  $\Omega$ m. This layer reaches minimum resistivity values on the western side of the profile where it is not covered the clays are more exposed to the surface and more weathering is imminent. Of interest is the “valley” shaped anomalies in this layer at stations 320 and 1100 meters which are observed for both profiles. These anomalies can probably be associated with paleo valleys in the bedrock and thus preferential groundwater flow paths in a clayey formation. The valley feature at 1100 m corresponds



proximately with old stream or drainage feature on the study site map (Chapter 2, Figure 2.1).

Despite most of the similarities observed for the profiles, there is a different resistivity signature between stations 1280 – 1550 m (the boxed section of Figure 4.10). The more conductive nature of the ash in this area can result from over irrigation using brine and its subsequent leaching through the unsaturated zone of the ash dump. In this highlighted zone, there is clear evidence from the resistivity signatures of the two profiles that there was fluid migration within the particular medium of concern as certain regions in the 2008 profile showed a much reduced resistivity values than the 2006 profile (Figure 4.11) suggesting the presence of more salts in 2008.

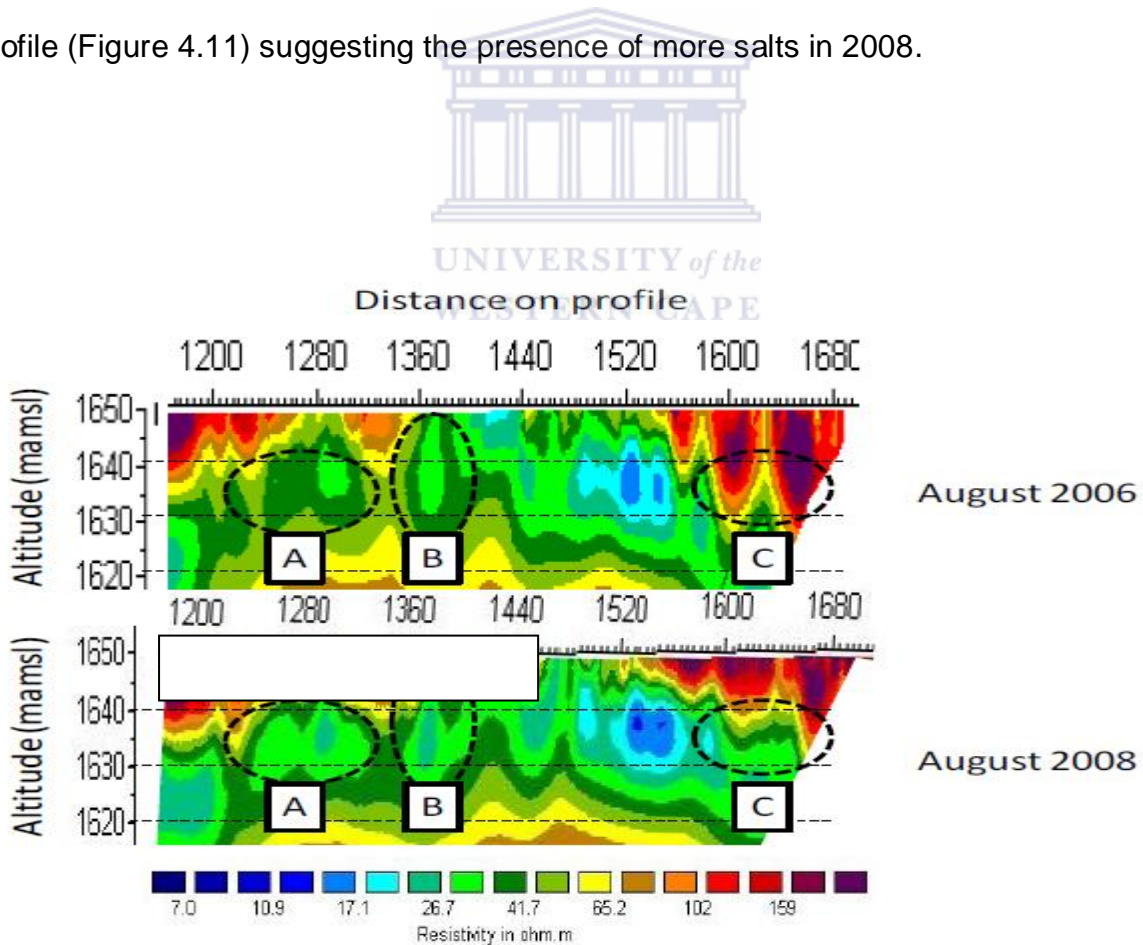


**Figure 4.11. Zoomed in section of August 2006 and August 2008 electrical resistivity cross sections highlighting 3 areas where moisture and salt content increased over time.**

The three zones marked in the zoomed in section shows evidence of a remarkable time lapse changes in the salt and moisture transport wit zones over the period of two years. Although area A has a similar shape for the 2006 and 2008 profiles, the 2008 profile shows colors with a lower resistivity, indicating more salt and/or water in this zone has migrated through to this region. This phenomenon is also partly observed in area B and the suggestion of a downward movement of the wet zone in to the deeper subsurface areas is very imminent, there by exposing the underlying aquifer to potential salt contamination at this region. However, a higher resistivity zone is forming in the top layer indicating loss of moisture in the surface zones, most probably due to evaporation and sedimentation of the ash. In region C, a much more saturated/ highly saline zone is observed at a depths below 15 meters from the top of the ash dump. This could be a result of irrigation practices and/or high rainfall events that predominated in this area at this time step. The area above region C shows a marked increase in general resistivity indicating an unsaturated area forming above the more saturated or salt laden zone in this region.

#### **4.3.2 Comparison of the 2008 and the 2010 Profiles**

In September 2010, electrical resistivity tomography was conducted on the same profile line as for the 2006 and 2008 profiles. The main objective of this profile was to do a long term monitoring of any salt transport in the ash dump, thereby establishing its sustainability as a salt sink. The same measuring protocol and electrode spacing as the one used for the previous surveys was used. The results of the comparison between the 2008 and the 2010 profile lines are presented in Figure 4.12.

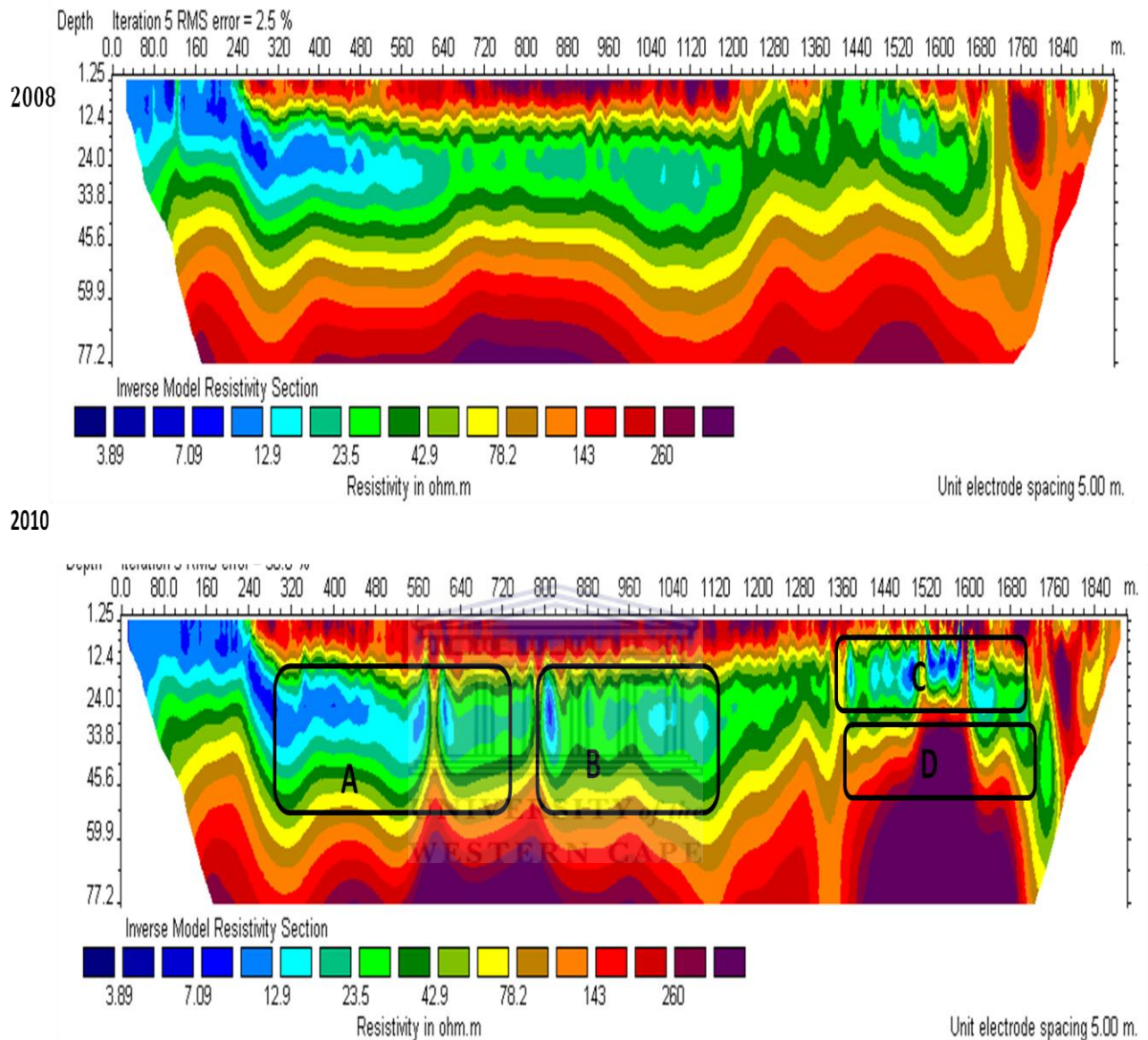


**Figure 4.12. Results of the 2008 and 2010 ERT profiles used to show evidence of potential salt movement within the ash dump.**

There are few traceable changes between the two profiles and in most cases they show same characteristics. This included the dry top near surface high resistive layer on the resistivity section is associated with dry ashes which covers the rehabilitated part of the ash dump. Likewise, a high resistivity region is also observed for the top layer of the ash

dump after the 1550 m mark. However, there are notable regions whose resistivity values are observed to be lower than the 2008 profiles which could be used to provide evidence of salt movements through to the underlying aquifer. Of particular concern are the regions marked A-D. To add to that the decrease in resistivities at deeper depths of this section demonstrate evidence that there have been salt/moisture plume movement. Region D is an anomalously high resistivity zone which is seated just below region C. This region is explained in terms of the fact that the salts trapped in region C would tend to introduce a drier region below the high saline zone. This will force the ash medium in region C to absorb moisture through capillary action, hence introduce a drier region below C. Region A and B show decreased resistivities in the vadose and fractured zone of the underlying aquifer system, which could also be interpreted as evidence of moisture transport into the underlying shallow aquifer system. In general there are notable features which suggest that there was plume movement through the ash dump.

Although it is not possible to determine the hydrogeological parameters (such as porosity, transmissivity) of a formation from geophysical data, lower electrical resistivities in a homogenous formation are normally associated with higher porosity and transmissivity. On the other hand, low resistivity values are normally associated with clayey formations and filled with groundwater. Geophysical pseudo sections therefore managed to present with the information that is very useful in conceptualizing the salt and moisture transport through the ash dump. It also managed to give an acceptable characterisation of the underlying aquifer system.

#### 4.6 Correlation of geophysical results with pre-existing borehole data.

The key objective of the study was to demonstrate the use of non-invasive methods in characterizing the ash dump and its environment. To do this, the lithographic results from previous studies were used to validate the geophysical survey results discussed in this study. Pre-existing borehole from test boreholes drilled on the ash dump and reported in Nel et al., (2007) were used to provide a correlation between the observed geophysical results and borehole information. The boreholes were located along the geophysical profile as shown in Figure 4.13.

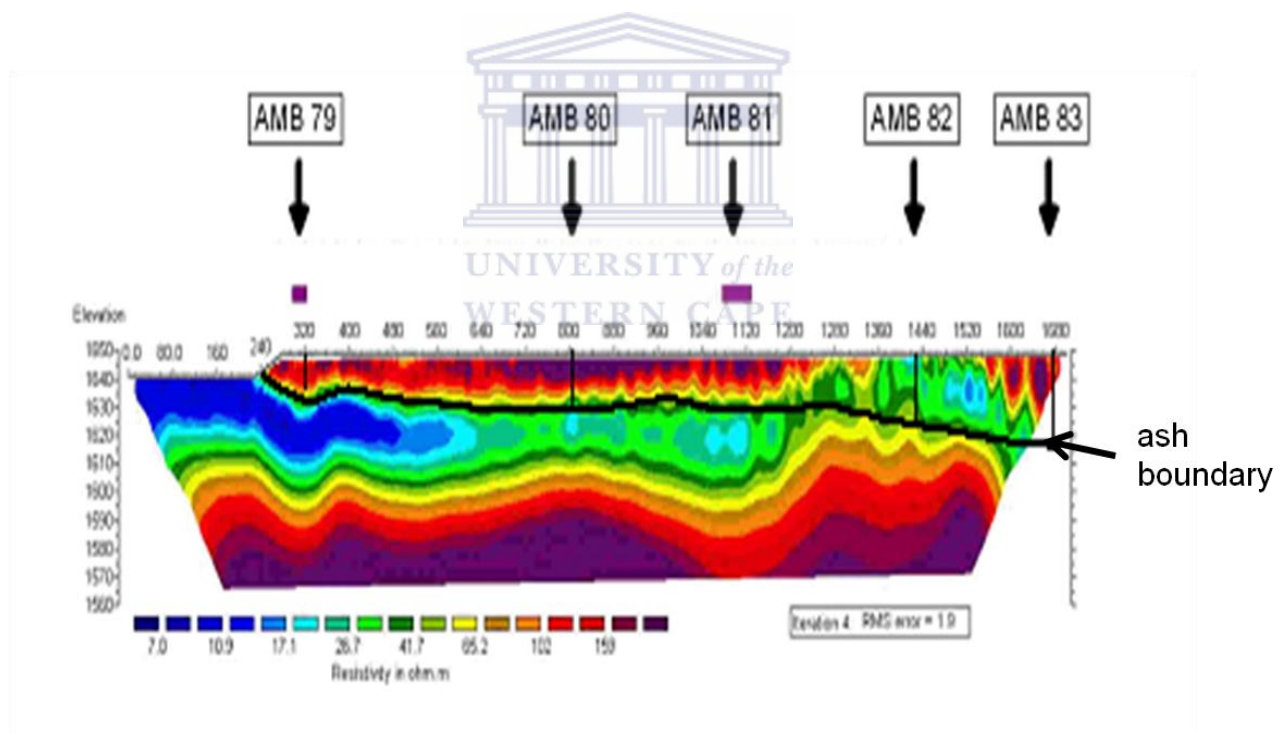


Figure 4.13. Approximate borehole positions in relation to the electrical resistance profile results. The black line represents the inferred ash/bedrock contact (adopted from Nel et al., 2007).

Table 4.1 presents a summary of the drilling results of each of the boreholes in Figure 4.13.

**Table 4.1 Summary of ash and bedrock characteristics at the core sites (Adopted from Nel et al., 2007).**

	<b>AMB 79</b>	<b>AMB 80</b>	<b>AMB 81</b>	<b>AMB 82</b>	<b>AMB 83</b>
<b>Ash Age</b>	20 Years	15 Years	8 Years	4 Years	1 Year
<b>Ash depth</b>	11	23	>13	24	32
<b>Ash Characteristic</b>	Unsaturated, Consolidated	Unsaturated, Consolidated	Dry ash, unconsolidated	High salt content; Hard & fractured	Recently rehabilitated; Hard & highly fractured
<b>Bedrock Characteristic</b>	Deep weathered – different rock from rest of site	Shallow bedrock	Very deep weathered	Deep weathered	Deep weathered
<b>Water used for dust suppression</b>	Fresh	Fresh	Brine	Brine	Brine

As summarized in Table 4.1, the borehole cores showed sections consisting of very hard coarse ash, then very hard fine ash that was fractured, soft fine powdery ash and clay, and mudstone or dolomite material where the bedrock was sampled. The same information is also inferred from the geophysical interpreting geophysical results based on pre-existing geological knowledge of the study area. The borehole logs also shows that the ash column is successively underlain by the clay, dolomite weathered dry and dolomite fresh moist, as had been inferred by the geophysical methods. The 2D

electrical resistivity tomography results clearly showed the thickness of the ash heap without probing the ash medium. Thus the geophysical methods provided a quick and convenient ash dump characterization tool that is relatively inexpensive and does not create unwanted preferential flow through coring the medium. The increasing height of the ash dump was indicated by the geophysical results (Figure 4.13) was confirmed by the borehole logs on the ash dump as summarized in Table 4.1. Zones of high salinity/potential contamination identified by the electrical resistivity results and discussed in earlier sections of the chapter (e.g. around borehole ABM82) were also confirmed by studies done by Getari et al., (2011). In their assessment of the chemical properties on the core samples from boreholes, Gitari et al., (2011) reported very high salinity levels for core AMB82, a phenomenon which had been observed by the geophysical results without probing the medium under investigation. Overmore, the geophysical results could infer the structural extend of this plume, together with the direction with which it is progressing in the underlying aquifer system.

#### **4.7 Summary**

A new cementation parameter for the coal ash was experimentally determined and can be used in any future electrical resistivity characterisation of pulverised coal ash.

Changes in resistivity were used to correlate changes in moisture contents during moisture and salt leachate ingress in ash dumps with a sufficient accuracy. Since Archie's law was successfully used to evaluate the conductivity of fluid through the ash dump. The application of ERT type measurements assisted in the elucidation of flow paths and brine dispersion in the ash dump. The flow rates through the ash dump were

estimated by considering the rate of brine injection, and considering the distance travelled by the brine plume over the time spanned by the investigations. Vertical infiltration is more pronounced than horizontal infiltration indicating due gravitational force, especially when the field capacity of the ash dump has been exceeded. The results suggest no evidence of macro-pore preferential flow, suggesting that the unsaturated zone of dry ash dumps is homogeneous. However, in such media, unstable flow may still be possible because of the spatial variability of hydraulic properties that are attributed to the pozzolanic nature of the ash medium. The issue of spatial variability will be discussed in the next chapter.

The more conductive nature (lower resistivity) of the ash in that area could result from surface irrigation (this is feasible as this is the fresh ash being deposited and conditioned with brine and has not yet reached equilibrium with the atmospheric CO<sub>2</sub> for mineral formation). The more conductive (less resistive) layer (blue-yellow contours) below the ash layer is associated with the entrapment and saturation of salts at the lower base of the ash dump. These results are useful in the conceptualization and development of suitable hydrologic models which could be used to obtain estimates of the spatial progression of any salt plumes through the unsaturated zone of the ash medium.

There is no doubt that the geology of a dumping site will play a vital role in managing the impact of waste disposal on the environment of the site (Theis *et al.*, 1987 and Adriano *et al.*, 1983), and in particular the underlying aquifer system at Tutuka. This vital information of the subsurface structure of underlying geology could be inferred from the electrical resistivity results and thereby ensuring that the knowledge of the geology of



such a site when starting to investigate the effects that a waste dump has on its environment is known. Ideally, natural soils at the base of the dumpsite with a high proportion of clay (from the weathered dolomite) are associated with a low permeability barrier to force the salt to leach to the subsurface beneath the ash dump.

Electrical resistivity geophysical method has thus proved to be very effective method for unsaturated zone characterisation. Contrary to traditional methods of measurements and observations from drilled sampling holes which perturb the medium, electrical resistivity is non-destructive and can provide continuous measurements over a large range of scales. The study showed that temporal variables such as water and solute transport can be effectively monitored and quantified without altering the soil structure.



## CHAPTER 5

### NUMERICAL SIMULATION OF CONTAMINANT TRANSPORT IN THE UNSATURATED ZONE OF DRY COAL ASH DUMP.

#### 5.1 Introduction

An understanding of the movement of moisture fluxes in unsaturated zone of the ash dumps often has a critical role in terms of potential contaminant transport through the ash dump. The unsaturated zone plays an inextricable role in many aspects of hydrology, including soil moisture storage, evaporation, and acting as groundwater recharge buffer. Vulnerability to contaminant transport can be associated with surface and subsurface flows of water through a site which are mainly influenced by the hydraulic characteristics of the site. As such, any quantitative analysis of contaminant transport must first evaluate water fluxes into and through the vadose zone. These fluxes typically enter the vadose zone in the form of precipitation or irrigation at the ash dump. As most contaminant fluxes and leachates are transported as solutes, a description of water flow in the vadose zone is necessary to understand contaminant transport in the unsaturated zone. However, accurate measurement of the hydraulic properties is difficult because of the highly nonlinear nature and the heterogeneity of the subsurface environment (Leij and van Genuchten, 1992). Hence, there is a need to apply methods which can reliably provide measurements of the unsaturated soil-hydraulic properties are critical in solving moisture and salt transport in ash medium. This can be achieved by using numerical models to solve for unsaturated hydraulic parameters as presented in the Richards equation (5.1).

Numerical models have often been used in the simulation of water and solute movement in the subsurface for a variety of applications, including contaminant transport modelling. This has even been made possible by the development of sophisticated computer programs for simulation water flow and contaminant transport in the subsurface (Šimůnek et al., 2011). One type of numerical based program that has been widely used as suitable tool for solving unsaturated water and solute flow is the HYDRUS2D (Šimůnek et al., 1999), which solves the Richard's unsaturated flow equation using the Galerkin-type linear finite element scheme (Mendoza et al., 1991) and provides a 2 dimensional solution of unsaturated zone solute transport. In this study HYDRUS2D is used to simulate water and salt movement in the unsaturated zone of the dry ash dump at Tutuka ash dump site. The main objective of this work is to determine the flux dynamics within the unsaturated zone of the coal ash medium, so as to develop a conceptual understanding of water flow and salt transport through the unsaturated zone of the coal ash medium.

## 5.2 Solute flow in the vadose zone of the ash dump

Solute and water flux in the vadose zone has a great influence on contaminant transport through the unsaturated zone of the ash dump. Water flow in the vadose zone is predominantly vertical and is simulated using unsaturated transport hydrologic models which describe solute flow and transport in the unsaturated zone based on the Richards equation (Equation 5.1).

$$\frac{\partial \theta(h)}{\partial t} = \frac{\partial}{\partial z} \left[ K_s(h) \frac{\partial h}{\partial z} + K(h) \right] - S(h, x, y, z, t) \dots \dots \dots (5.1)$$

where  $\theta(h)$  the volumetric water content,  $z$  is the vertical coordinate, and  $S(h)$  is the sink factor which represents the capillary rise.

The Richard equation requires knowledge of the unsaturated soil hydraulic functions, i.e., the soil water retention curve,  $\theta(h)$ , describing the relationship between the water content  $\theta$  and the pressure head  $h$ , and the unsaturated hydraulic conductivity function,  $K(h)$ , defining the hydraulic conductivity  $K_s$  as a function of  $h$ . A detailed analysis of the Richards equation is presented in Chapter 3.

The Richards' equation is based solely on Darcy's law and the continuity equation and can be used for fundamental research and scenario analysis since it is related to physical phenomenon. A reasonable description of the hydraulic conductivity structure is therefore a prerequisite for modelling moisture and transport through the unsaturated zone of the ash dump. Variably saturated zones are fundamental to understanding many aspects of hydrology, including infiltration, soil moisture storage and groundwater recharge. The software has the ability to simulate the movement of water, solute in both saturated & unsaturated areas.

### **5.3 Materials and Methodology**

The methodology was divided into two stages, namely field experiments and the numerical simulation using HYDRUS2D. The field experiments were done at the ash dump with a primary purpose of obtaining an input data set for the field parameters for the HYDRUS numerical models. The experiments included constant head infiltration tests using the Guelph permeater for estimation of saturated hydraulic conductivity and pressure heads, and collecting samples for the determination of the residual moisture content for the ash dump.

### **5.3.1 Determination of saturated hydraulic parameters using infiltration methods**

Modelling of water and solute transport in the ash dump requires the knowledge of medium properties that have to be estimated with sufficient precision. Hydrologic properties often control the potential movement of salt leachates in the vadose zone and help to diagnose the hydrodynamic functioning of the medium in relation to the natural infiltration processes in the vadose zone of the dump.

As the transport of salts is closely linked with the movement of water fluxes in the ash making up the vadose zone, any quantitative analysis of salt transport must therefore evaluate water fluxes into and through the vadose zone of the medium. However, the hydraulic parameters often exhibit spatial variation across the medium due to different levels of compaction and ash handling procedures at the dump, and in most cases the an average field parameter under consideration would need to be established for the medium under investigation. Thus the accuracy of numerical simulations used for unsaturated zone transport largely depends upon the accuracy with these model input parameters can be estimated. One such parameter which is critical in defining the progression of any plume in the unsaturated zone is the saturated hydraulic conductivity, whose values and variability is often provided through infiltration experiments such as auger-hole permeability methods.

The auger-hole method, involves preparation of a cavity extending into the medium structure with minimum disturbance of the medium matrix (Amoozegar and Warrick, 1986) and the constant head Guelph permeater (Figure 5.1) is usually used for the infiltration experiments.

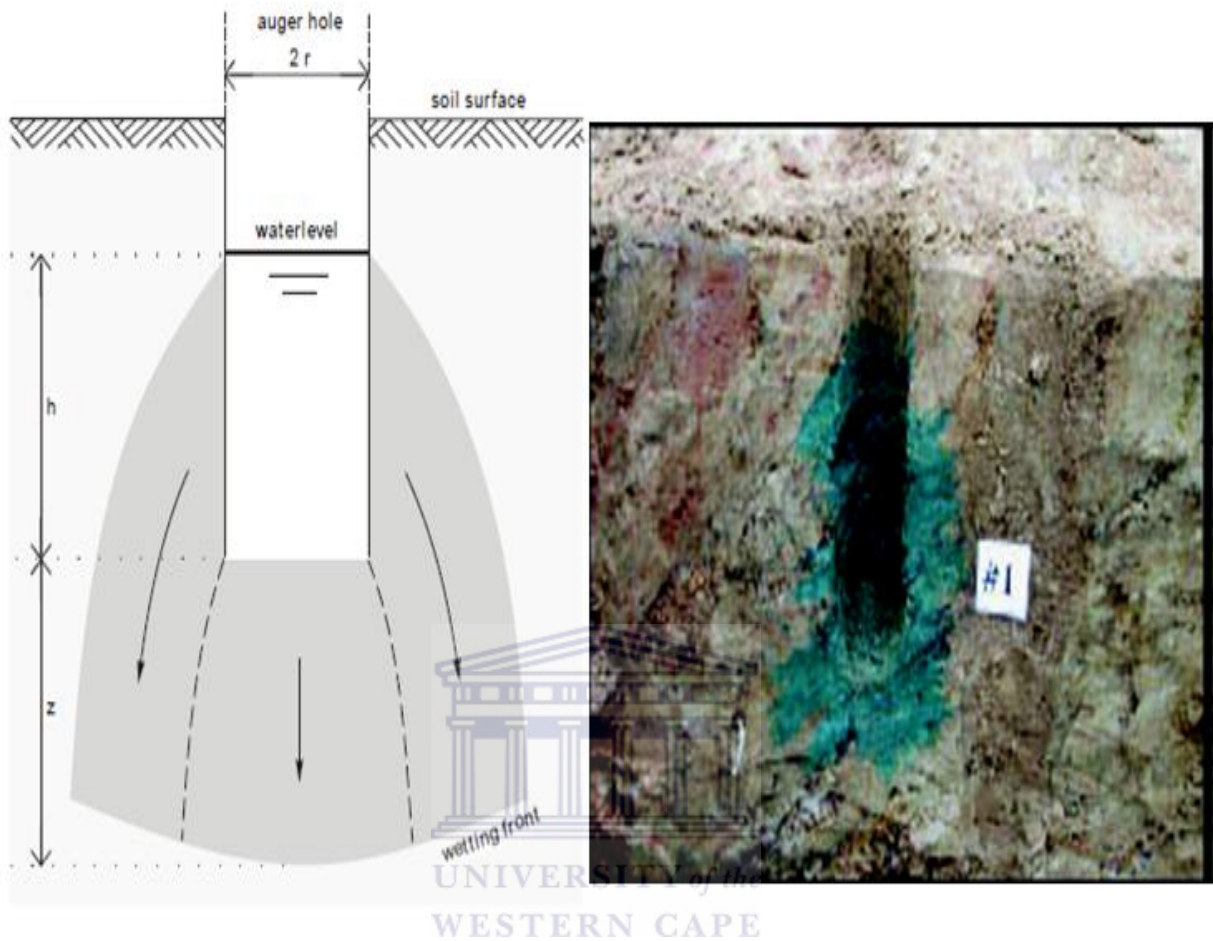


**Figure 5.1. Principle of infiltration in auger-hole methods (Amoozegar and Warrick, 1986).**

The Guelph permeameter (Reynolds et al., 1983, 1985) consists of a mariotte bottle that maintains a constant water level inside a hole augured in the soil. The practical procedure involved the preparation of a cavity extending into the medium structure with minimum disturbance of the medium matrix as suggested in Amoozegar and Warrick, (1986). At equilibrium, the water level in the hole will be at a constant level. The depth of water in the hole,  $H$ , the diameter of the hole,  $2r$ , and the distance between the bottom of the hole and the underlying impermeable layers,  $s$ , must be determined (Figure 5.1),

(Amoozegar and Warrick, 1986). Several methods have been developed to determine the saturated conductivity in the field. The constant head Guelph infiltrometer (Figure 5.2) has remained one of the famous methods for measuring the saturated hydraulic conductivity using the auger-hole technique.

The simultaneous approach for solving the Richard's based steady-state equation (Philip, 1985; Elrick and Reynolds, 1992). Steady-state infiltration measurements were made at the specific constant head and the saturated hydraulic conductivity  $K_s$  was calculated based on the calibrated empirical relationship (Equations 5.2 and 5.3).

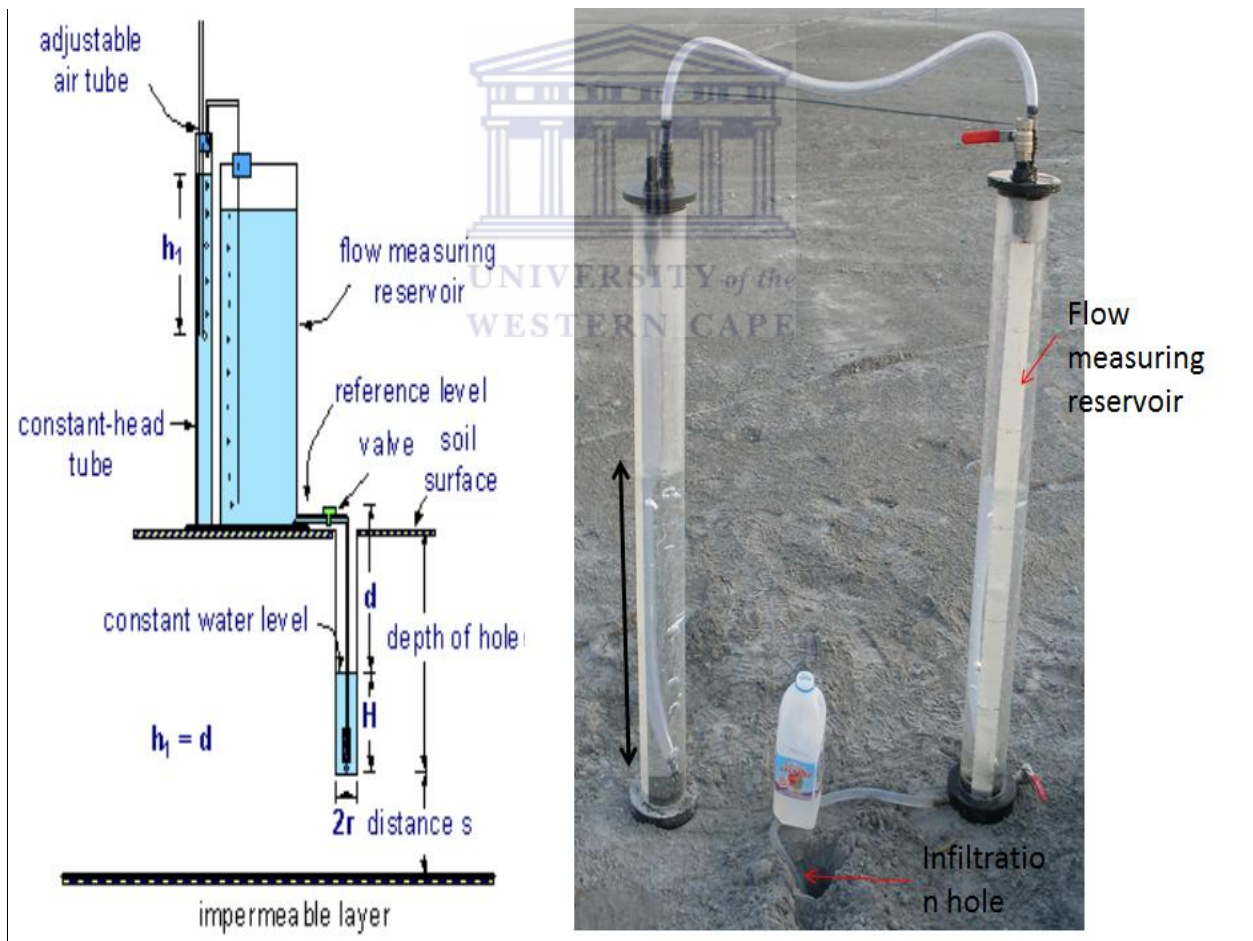
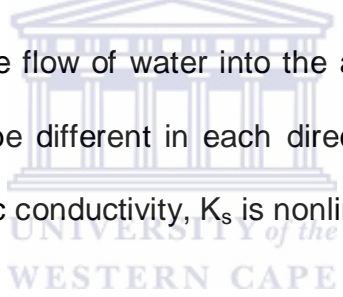


**Figure 5.2. The principle and general construction of the Guelph infiltrometer used for determining hydraulic conductivity.**

The practical procedure followed was as described in Amoozegar and Warrick, (1989) for different infiltration sites of the ash dump. Ten 1-metre deep infiltration holes were hand augured at randomly selected sites on the ash dump. The infiltrometer reservoir chamber was then filled with water. The negative pressure head was maintained at a fixed value of -55.0 cm throughout the experiment by keeping the volume of water in the constant head pipe at the specified level of 55.0cm. The internal diameter of the hole,  $2r$ , the depth of water in the hole,  $H$ , was also measured before the tap to the reservoir tank was opened. The volume flow rate was measured by determining the rate of water drop in the reservoir chamber and was later used to calculate the saturated hydraulic conductivity. Since the flow of water into the auger hole is three-dimensional and the flow properties could be different in each direction, the equation that is used to calculate the saturated hydraulic conductivity,  $K_s$  is nonlinear (Equation 2 and 3).



$$K_s = AQ \dots\dots\dots 5.2$$

Where  $K_s$  – Hydraulic conductivity

$A$  – Is a factor in the Glover equation is given by:

$$A = \left[ \sinh^{-1} \left( \frac{H}{r} \right) - \left( 1 + \frac{r^2}{H^2} \right)^{\frac{1}{2}} + \frac{(r/H)}{2\pi H^2} \right] \dots\dots\dots 5.3$$

$Q$  is the steady-state flow rate of water from the bottom of the hole into the soil.



Ash samples were also collected at the surface, 0.5m and 1m depths for all the infiltration points and were analysed for moisture content so as to assess the dependence of hydraulic properties on moisture content (See Photo 4.1). The average depth to the water level of the underlying aquifer, which needed to be specified on the deep drainage lower boundary condition selected for the simulation, was also determined from pre-existing boreholes which had been drilled in the previous years. Photo 5.1 presents a summary of the main field experimental procedures which were done at the study site.



**Photo 5.1. A photographic summary of the field work done at the study site.**

A and B describes the drilling of the whole and the carrying out of the infiltration experiment respectively. C shows the experimental determination of the groundwater level of the underlying aquifer being measured using a dip meter while D shows the collection of undisturbed samples for bulk density and moisture analysis.

Results of the calculated saturated hydraulic conductivity values; together with the average saturated hydraulic conductivity value that was calculated for the ash dump are presented in Table 5.1, together with the values for the geometric mean values used as inputs to the model. The sensitivity of predictions using numerical water flow models may be evaluated by the spatial variation in the hydraulic conductivity  $K$  between nodes.

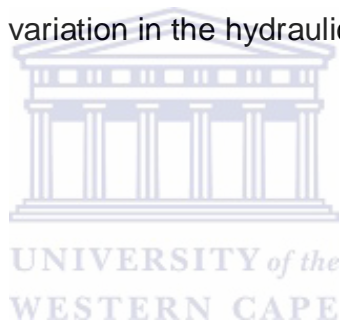


**Table 5.1. Results of the moisture content, density and saturated hydraulic conductivities.**

Site	$K_s$ (m/day)	$\theta_i(h)(\%)$	Density (kg/m <sup>3</sup> )
1	0.51	19.5	930
2	0.83	22.2	910
3	0.93	21.5	920
4	0.90	21.7	850
5	0.62	19.0	1030
6	0.97	21.7	804
7	0.57	19.0	680
8	0.62	23.7	800
9	0.83	21.8	783
10	0.98	20.5	950
<b>Arithmetic mean</b>	<b>0.78</b>	<b>22.1</b>	<b>866</b>
<b>Geometric mean</b>	<b>0.76</b>	<b>21.0</b>	<b>860</b>

The average saturated hydraulic conductivity, moisture content and the bulk density values were used as initial inputs to the Rosetta Lite (section 5.3.2) program which is coupled to the HYDRUS2D program and is used in predicting the soil textural class for complicated medium, like the ash dump.

The average depth to the groundwater level of 35.11m was obtained from routine monitoring of boreholes on borehole which were drilled around the ash dump (Photo 5.2).



**Photo 5.2. Measuring groundwater level at a monitoring borehole A85. The average groundwater level was used as an input parameter for the deep drainage lower boundary condition that was used for the simulations.**

The finite element variable saturated flow model was used to solve the Richard's equation in 2D. The depth of the studied layer was 45 m and single layer conditions were used as the estimated extend of the unsaturated zone. Initial soil moisture was measured and an averaged value was used for the three different sites under study.

The initial total head was set to 0.65 and the right boundary cells were constrained to the estimated position of the saturated zone for all the simulations. The grid was discretized into uniform cells of 0.1-m width and 0.05-m depth. In HYDRUS2D, flow and transport can occur in the horizontal plane, vertical plane, or asymmetrical vertical region (a three-dimensional region exhibiting radial symmetry about the vertical axis).

### **5.3.2 HYDRUS2D modelling unsaturated zone transport in the unsaturated zone of the ash dump**

A numerical simulation was used to model potential solute transport in the unsaturated zone of the ash dump. The aim of the simulation was to determine the flux dynamics within the unsaturated zone of the coal ash medium, which would be useful in managing water flow and salt transport through the unsaturated zone of the ash dump. The total period of simulation was approximately 20 years, corresponding to the approximate age of the ash dump at the time of the study.

The model that was used for the simulation, HYDRUS2D is an interactive graphics-based user interface that runs in Windows and executes HYDRUS2D, which is a Fortran code and has a two-dimensional finite element model used for the analysis of solute transport in an unsaturated porous media (Šimůnek et al., 2011). The software numerically solves the Richards' equation for saturated-unsaturated water flow and the Fickian-based advection-dispersion equations for solute transport and is used to analyse water and solute movement in unsaturated, partially saturated, or fully saturated porous media.

The unsaturated hydraulic functions were determined from the Rosetta Lite Dynamically linked library (Schaap et al., 2001) which implements the pseudo transfer functions that

can predict the van Genuchten (1980) water retention parameters and the soil textural classification for the medium using quasi-empirical models using a neural network. Field infiltration data (Table 1) were used as inputs to the library.

### **5.3.2.1 Model Validation and calibration**

Model calibration is generally involves the process of tuning a numerical or inverse through the use of particular input parameters, (for instance , the established soil hydraulic parameters, initial conditions and /or boundary conditions until the simulated model results matches the observed model results. Model calibration is often referred to also as history matching since the ultimate goal of model calibration is to optimize unknown parameters in the model so as to ensure that the model output of the long term simulations were done to sufficient precision. In this study, the results from the geophysical time lapse experiments were used to calibrate the HYDRUS 2D model. Model calibration was achieved by simulating a 2D infiltration test and adjusting the input parameters until the observed simulated results were optimised results of a 2D brine infiltration survey that was monitored using electrical resistivity tomography as reported in Chaper 4 of the study and published in Muchingami et al., (2013), (Figure 5.3). The adjustable parameters were tuned until the time lapse infiltration simulation of the HYDRUS 2D model matched the results from the geophysical time lapse experiments.

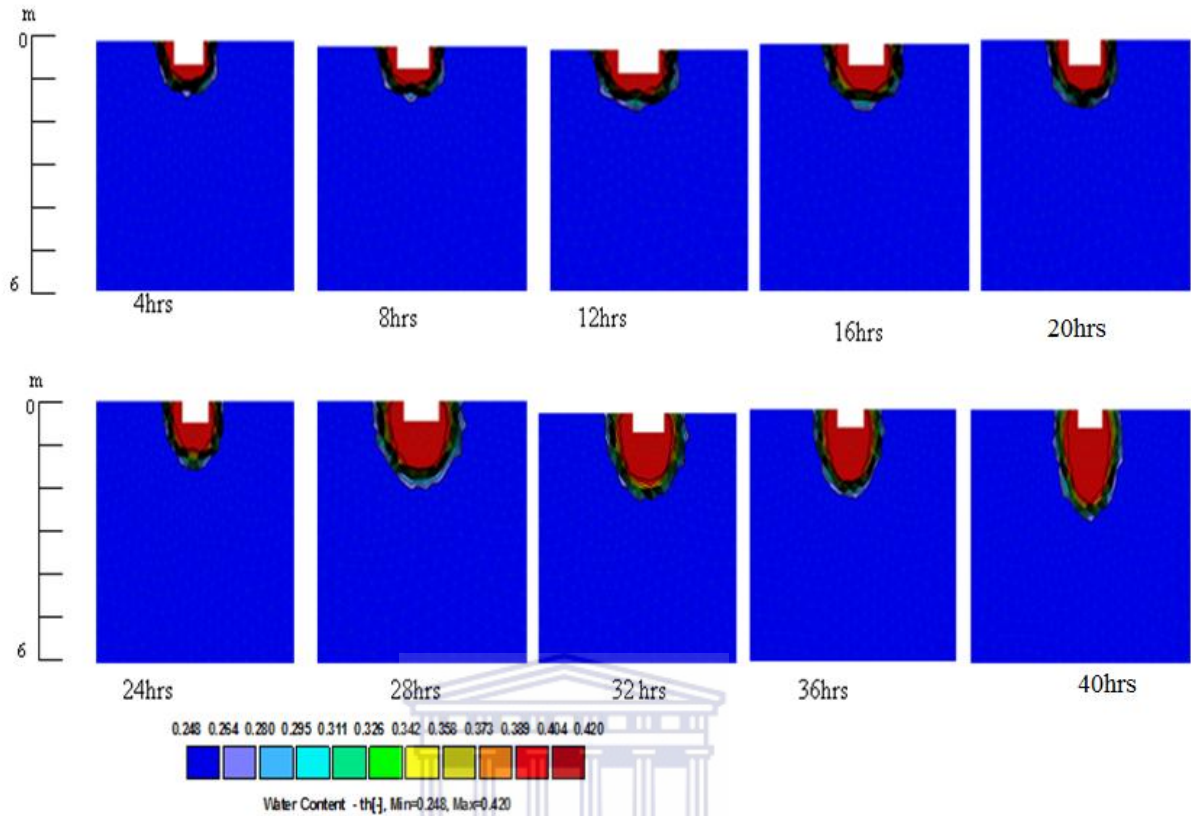


**Figure 5.3. Results of the HYDRUS2D model using parameters obtained from the time lapse infiltration experiments.**

#### 5.4 Long term simulations of solute transport within the ash dump

After the model calibration, a long term simulation for a cross section of the ash dump was done to estimate the unsaturated flow of solutes in the ash dump, thereby providing a tool for managing solute transport in the ash dump. The finite element variable saturated flow model was used to solve the Richard's equation in 2D through iteration methods. The model reached the answer with 10 iterations. In time step stage, optimal range of iteration is considered in both upper and lower limit of 3 and 7. In order to give accuracy to the model and selecting the most appropriate value of  $\Delta t$ , in time step control section, the values 3 and 10 were assigned as specifications for minimum and

maximum optimal iterations respectively. The flow domain section considered for the study was a rectangular cross section of 100 m length and 45 m depth on the non-rehabilitated part of the ash dump. HYDRUS2D has the ability to generate a finite element mesh of irregular elements improving discretization for the domain. As such the domain was discretized into a finite element mesh of irregular elements, where boundary conditions, initial conditions, and parameter values discussed previously were assigned. The mesh was generated using the automatic features of the model. For the simulation, the mesh had a total of 766 mesh points with 1438 mesh triangles, which were created of irregular sizes and shapes (Figure 5. 4).

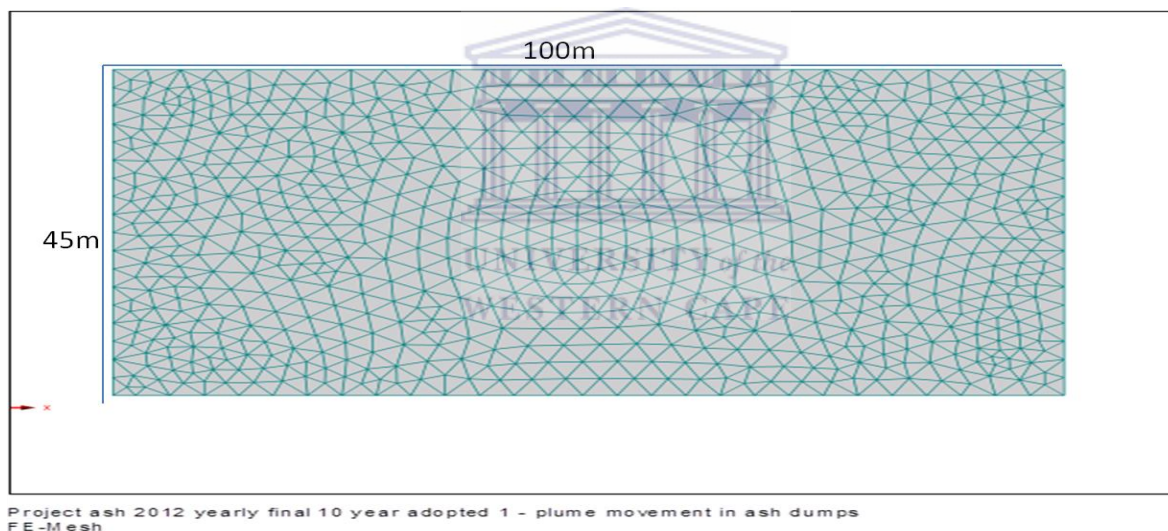


**Figure 5.4. The FE- Mesh generated for the plume movement model.**

Boundary conditions at the top surface were defined as “atmospheric boundary” at the top of the ash dump to simulate natural rainfall falling uniformly over the domain during rainfall, and normal waste water irrigation during the routine dust suppression sessions. The relation between storage and ground level changes depends on geologic factors, thus the change in groundwater level will level also affect the flow rates. The average depth to the groundwater level of 35m was obtained from monitoring boreholes around



the ash dump. The depth of the studied layer was 45 m and single layer conditions were used as the estimated extend of the unsaturated zone. The grid was discretized into uniform cells of 0.1-m width and 0.05-m depth. The selected time –lapse models are presented in Figure 5.5 (a-h).

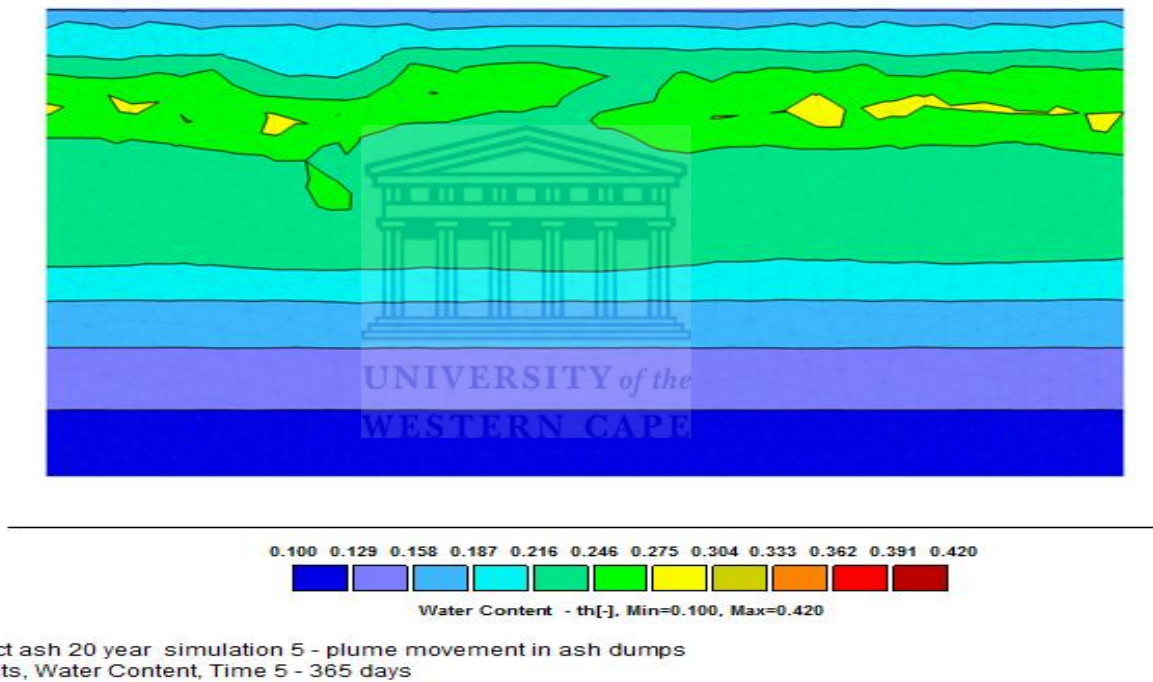
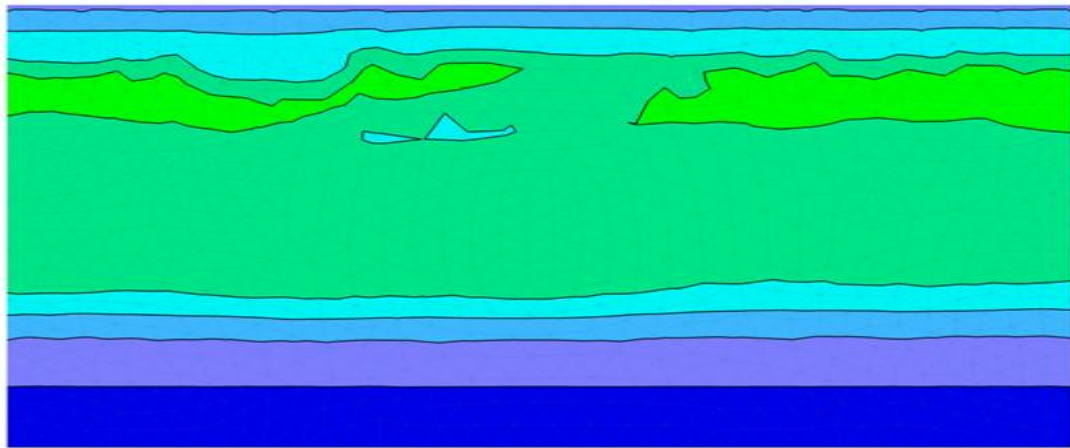
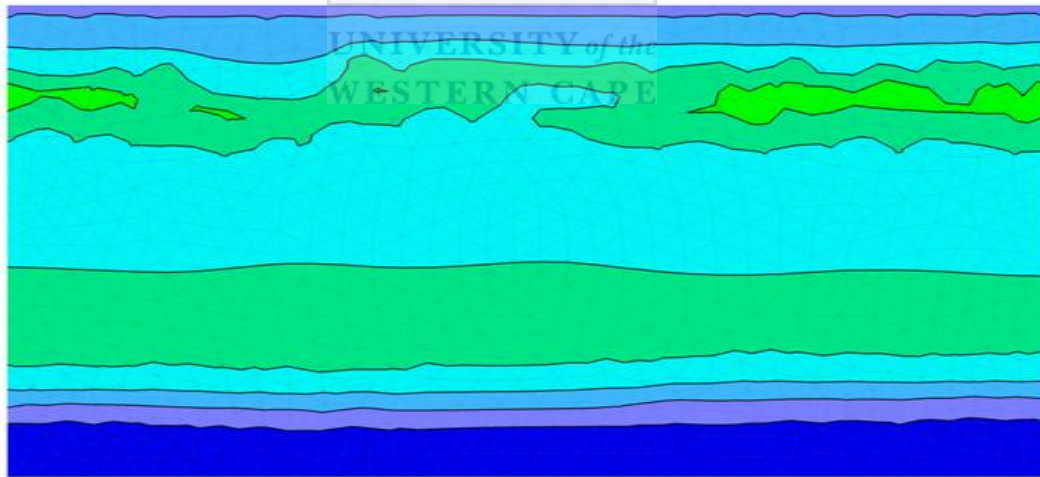


Figure 5.5 (a)



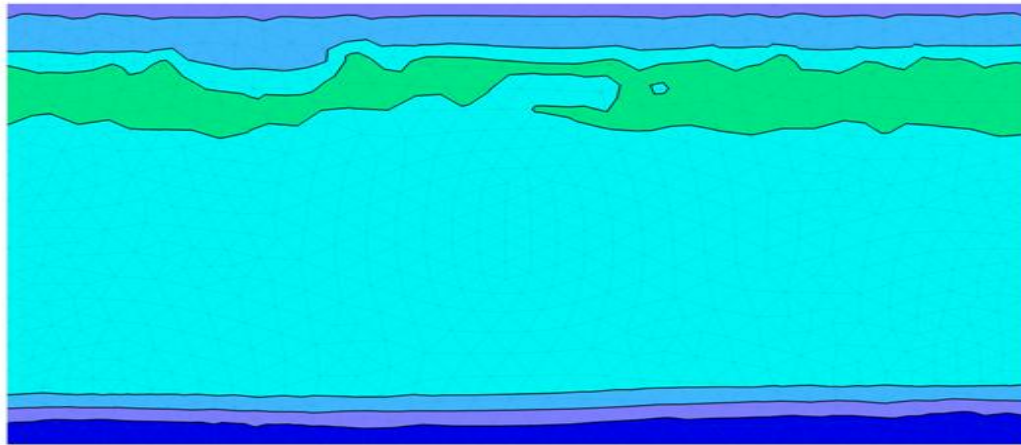
Project ash 20 year simulation 5 - plume movement in ash dumps  
Results, Water Content, Time 10 - 731 days

Figure 5.5 (b)



Project ash 20 year simulation 5 - plume movement in ash dumps  
Results, Water Content, Time 20 - 1461 days

Figure 5.5 (c)



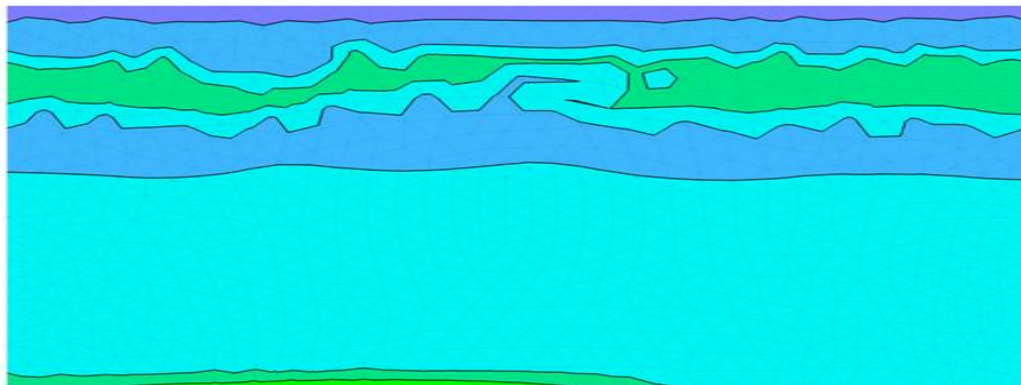
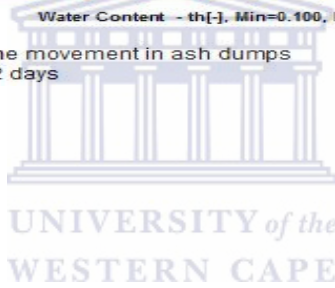
0.100 0.129 0.158 0.187 0.216 0.246 0.275 0.304 0.333 0.362 0.391 0.420



Water Content - th[-], Min=0.100, Max=0.420

Project ash 20 year simulation 5 - plume movement in ash dumps  
Results, Water Content, Time 30 - 2192 days

Figure 5.5 (d)



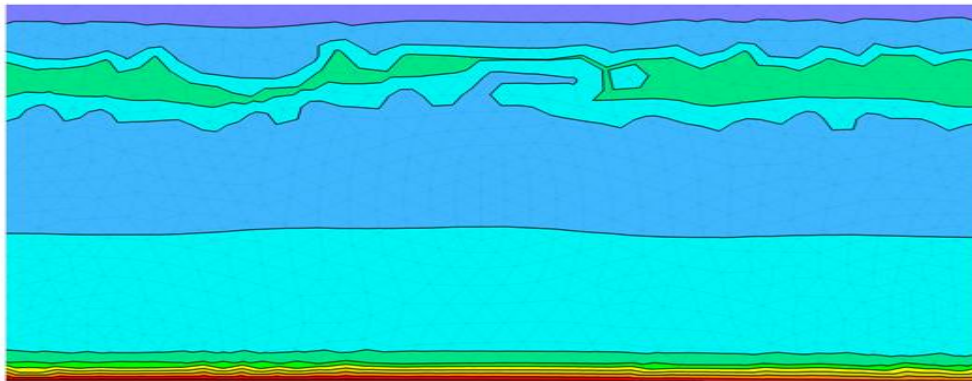
0.100 0.129 0.158 0.187 0.216 0.246 0.275 0.304 0.333 0.362 0.391 0.420



Water Content - th[-], Min=0.100, Max=0.420

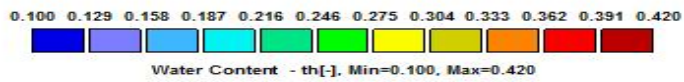
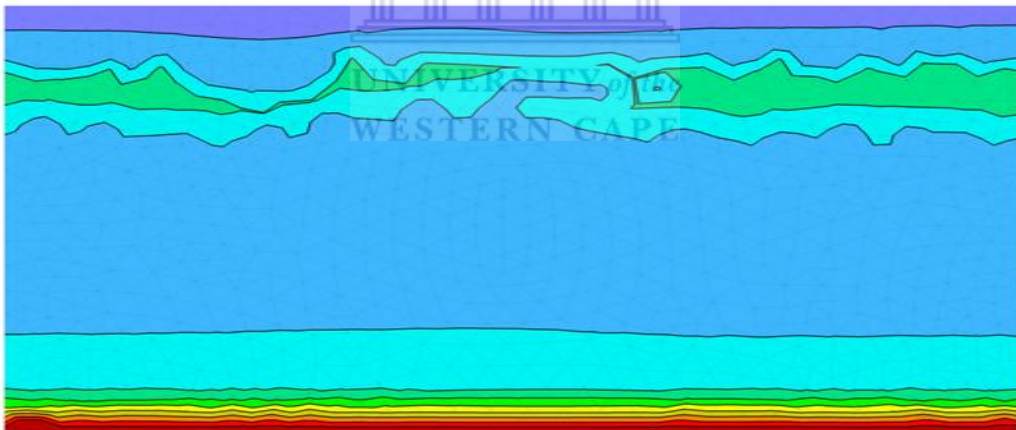
Project ash 20 year simulation 5 - plume movement in ash dumps  
Results, Water Content, Time 50 - 3653 days

Figure 5.5 (e)



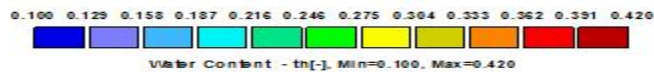
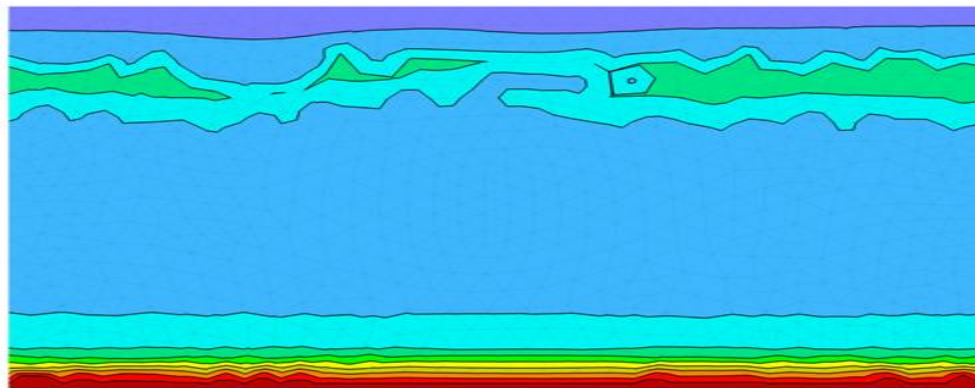
Project ash 20 year simulation 5 - plume movement in ash dumps  
Results, Water Content, Time 70 - 5114 days

Figure 5.5 (f)



Project ash 20 year simulation 5 - plume movement in ash dumps  
Results, Water Content, Time 90 - 6575 days

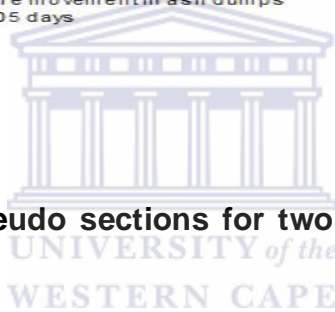
Figure 5.5 (g)



Projectash 20 year simulation 5 - plume movement in ash dumps  
Results, Water Content, Time 100 - 7305 days

Figure 5.5 (h)

**Figure 5.5 (a-h). Selected pseudo sections for two dimensional solute transport within the ash dump.**



The models suggest a reduced rate of solute transport through the unsaturated zone of the ash dump, mainly attributed to the pozzolanic properties of coal ash. Results from the current study could suggested a chance for the potential for immediate percolation of pore water through ash dumps and thus proper ash management practices need to be maintained at the ash dump.

The HYDRUS model proved to be an efficient tool in the simulation of moisture and solutes transport in the ash dump. These models also showed that the ash dump consists of spatially variable hydraulic properties that are causing the inhomogeneities within the ash dump transport model. The models were useful in predicting any chances

of potential contaminant transport and the plume attenuation in the unsaturated zone through adsorption. The model also managed to clearly show the accumulation of solutes as observed at the base of the ash dump. Thus the models seem to suggest a general a gradual increase in the % moisture and salt content of the ash dumps as a function of sample depth as observed on the ash dump. This is more pronounced in long term simulations of the ash dump where the plume has had sufficient time to progress through the ash dump (see photo 5.3).



**Photo 5.3. Field evidence of a saturated bottom layer as a result of accumulation of the solute fluxes. The mechanism of the accumulation is as suggested by the HYDRUS2D models.**

A proper scientific evaluation of any hydrological problem related to salt movement in the unsaturated zone of the ash dump needed to take into account the processes

affecting flow through the vadose zone. Since the ash dump is a complex mixture of anthropogenic deposits, their physical properties would show a wide range of variation in texture and will thus have substantial internal permeability. As such the knowledge about water flow and solute transport in the unsaturated zone is important in understanding mechanisms for groundwater and surface-water systems (pollution) and sustainable management of salt transport in the unsaturated zone.

From the simulations, subsurface solute transport through the unsaturated zone is a generally slow process, and there is evidence of the salt and solute trapping within the ash dump as suggested by the relatively high solute flux (between 20-24% water content) being observed at depths ranging from 5-12 m. The evidence of this higher moisture zone is observed as being relatively constant for long term profiles (Figures 5.5 (a-d)). This could suggest the presence of a salt entrapment mechanism which could be explained in terms of the pozzolanic action of the ash media, and will tend to reduce the rate of solute transport. This is also suggested by the long solute travel times that are observed, and evident in the fact that the base saturation of the flow domain was observed after 17 years. The evidence the saturated base of the ash dump (observed after 20 years) is also presented by photo 5.2 which shows the physical observation of the saturated base being observed on the ash dump itself and will thus validate the models. If this approach is adopted the optimal period of rehabilitation of the active deposit area would be just before the saturated excess front reaches the bottom of the ash dump, which is any time before the 16 year period for such an ash heap of a nominal height of 45 m height used in this study.

The active deposit area refers to the area where fresh ash is deposited. This is often a much smaller area than the total ash area, with the remaining area rehabilitated by covering with a layer of top soil and planting suitable vegetation. It was assumed that the leachate generated from the rehabilitated area is negligible since a solid and impermeable layer is often formed on the surface.

### **5.5 Correlation of Hydrus2D simulations with lithostratigraphic sections of the ash dump.**

The current Chapter demonstrated the effectiveness in characterizing potential solute transport in the ash medium. Although the observed simulations have already been correlated to the field observations, the numerical simulations were also linked to the lithostratigraphic cores from boreholes drilled on the ash dump (as described in section 4.6). Since the simulations were done on the unrehabilitated part of the ash dump, lithologic log from boreholes ABM81 and ABM82 (Figure 5.6) which were cored from the fresher side of the ash dump was used for this correlation. It should nevertheless be known that this section of the ash dump had been recently rehabilitated, and thus is covered by a soil layer.



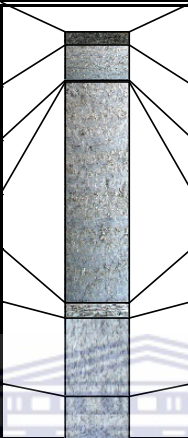
Well ID	AMB 81	Well Log: Lithology and Construction					
		Tutuka Ash Dump					
Drilling method:		Air Flush Core		Contract No.		8 Year old ash	
Coordinate		X	E29.40131	Scale		H	23
		Y	S26.77104			V	200
Surface Elevation (m)		0		Diameter (mm)		215	
Well depth (m)		13		Commencing date		20061130	
Casing depth (m)		0		Ending date		20061130	
Layer No.	Strata	Thick (m)	Elev. (m)	Depth (m)	Column map	Lithology	Remark
1	ASH	0.4	-0.4	0.4		top soil	
2	ASH	1.1	-1.5	1.5		hard ash	
3	FRAC	0.05	-1.55	1.55		Fracture	
4	ASH	6.95	-8.5	8.5		hard ash	
5	ASH	0.5	-9	9		brittle ash, core loss	
6	ASH	2.5	-11.5	11.5		No Core, unconsolidated ash	No water level
7	ASH	1.5	-13	13		layers to soft to drill	

Figure 5.6. The Graphic Log and Physical Sample Description of Core AMB81.

UNIVERSITY of the  
WESTERN CAPE

Well Log: Lithology and Construction				
Tutuka Ash Dump				
Air Flush Core		Contract No.	4 Year old ash	
E29.40349		Scale	H	23
S26.77030			V	200
0		Diameter (mm)	215	
25.1		Commencing date	20061130	
0		Ending date	20061130	
Elev. (m)	Depth (m)	Column map	Lithology	Remark
-0.5	0.5		top soil	
-2.85	2.85		coarse ash	
-2.9	2.9		2.9m fracture	
-10.45	10.45		coarse ash	
-10.5	10.5		10.5m fracture	
-12.85	12.85		coarse ash	
-12.9	12.9		12.9m fracture 45deg	
-22	22		coarse ash	
-23	23		hard fine ash	Depth to water level: 23.07 mbc
-24	24		brittle ash	EC: 571.4 mS/m
-25.1	25.1		clay soil , weathered dolorite	

**Figure 5.7. The Graphic Log and Physical Sample Description of Core AMB82.**

The lithological section of the borehole core describes an ash medium consisting of several alternate layers of loose, unconsolidated and friable ash sections. This indicates that pozzolanic reactions discussed earlier (Chapter 3, section 3.2) had taken place over time. Hard and soft layers were found directly adjacent to each other and control

the solute flow within the ash medium. Figures 5.6 and 5.7 indicate that at various ages and depths, differences in the ash were found varying from very hard coarse ash, to very hard fine ash, soft fine powdery ash and clay, mudstone or dolorite material where the bedrock was sampled. Some of the sections above it had layers and zones which were still unconsolidated, friable and loose, indicating that no or few pozzolanic reactions had taken place over time and hard and soft layers were found directly adjacent to each other. The electrical conductivities of core water sampled from the borehole samples varied from 315 to 571 mS/m indicating differences in conductivity/resistance, as had been suggested using the non-invasive electrical resistivity methods (Chapter 4), and are likely attributed to the differences in brine irrigation regime practiced on different areas of the dump.

The presence of a layered medium observed on the lithostratigraphic sections explains the solute entrapment within some sections of the ash dump. The borehole logs indicated that there is not much homogeneity in solute distribution and that solute movement is likely to be vertically downwards from one layer to the next, a phenomenon that was also observed from the numerical simulations. The depth to the saturated section of the ash dump as at August 2006 (20 years) was at a depth of 23.07m, a depth of approximately 2m from the base of the ash dump. This was in total agreement with the 20 year numerical simulations which showed moisture saturation to a height of 1.9m from the base of the ash dump. Therefore, numerical modeling techniques provides a quick and efficient tool for estimating and predicting unsaturated zone transport in dry ash dumps without probing the ash dump. The simulations are

thus a useful convenient method for predicting the future behaviour of the current and future behaviour of the ash medium.

## **5.6 Summary.**

The main objective of the chapter was to demonstrate the use of numerical methods in predicting unsaturated zone flow in the ash dump. Overall, the accuracy of the HYDRUS-2D simulations is considered to be very good, and certainly accurate enough to justify using HYDRUS-2D as a tool for in simulating unsaturated zone transport in dry ash dumps. The models managed to provide a better understanding of the processes that occur in the ash dump at the field scale, such as the mechanism of contaminant transport and the pozzolanic action which forms the basic control for modelling solute transport within the ash medium. The atmospheric upper boundary condition and the deep drainage lower boundary condition used in the in HYDRUS-2D simulations maintain the present scenario of the models and hence they also validate the results. The ROSETTA pedotransfer function software package offers a quick and easy way to estimate the soil hydraulic parameters that are needed for the simulations with minimum field inputs, thereby ensuring that the medium being investigated is undisturbed and hence no preferential flow pathways are generated. The borehole logs also and the field observations could also relate well with the Hydrus2D simulations for the study area. In conclusion, the simulations managed to sufficiently predict the hydraulic and transport properties of the ash dump by considering input data obtained from the study area.

## CHAPTER 6

### A CONCEPTUAL MODEL FOR THE TUTUKA ASH DUMP SITE

#### 6.1 Introduction

The main purpose of the current study was to investigate the extent to which non-intrusive methods can be used to provide an acceptable conceptual model of the unsaturated zone transport model in dry ash dumps so as to enable scientifically valid conclusions to be made concerning the potential for the environmental impact of disposal materials. To achieve this, the unsaturated zone solute transport in the ash dump as described and observed from the geophysical results and numerical simulations techniques have to be integrated to produce an acceptable and accurate conceptual model of the ash medium. The understanding the movement of water and chemicals into and through the unsaturated zone will be of vital importance in managing, using and protecting the underlying aquifer system. The management of a disposal system must include both its present and future conditions. Nevertheless, it may sometimes be necessary to include other anticipated events even less probable events as well.

To properly evaluate the potential impact of the disposal of coal combustion by-products on groundwater quality, the physical and chemical properties of these by-products, transport processes in groundwater, and the solution techniques of mathematical models must be understood. This means that the contributions of many different factors must be consistently, considered and evaluated, often in the absence of quantitative data. As suggested in earlier chapters, the ash has the potential to adsorb some of the

elements in the contaminated wastewater thereby making coal ash to act as a sink. However, the desorption of the adsorbed elements, desorption is defined as a phenomenon whereby a substance is released from or through a surface, from the coal ash over time at the ash disposal sites could have negative impacts on the ground and surface water resources.

## **6.2 Conceptual Model development**

A major advantage of a conceptual model is that it can provide considerable physical insight into the features events and processes that should be included in more site-specific transport models. Although the historical modelling methodology is still in use today, the operators of waste sites are experiencing increased pressure from the critical group of stakeholders to ensure that future management methodologies for waste disposal sites will have to demonstrate that the waste will never affect human health and the environment adversely and also ensure that the disposal system satisfies any regulatory framework. A good management methodology should allow management to make such assessments based on accurate scientific conclusions and recommendations made on the disposal system characteristics and timeframes of sustainable disposal.

### **6.2.1 Conceptual understanding of the input and output streams of the ash dump**

The starting stage in the development of the conceptual model for solute transport in the ash dump and the evaluation of the potential for groundwater contamination is to consider the potential sources of the solutes. This procedure involves identification of all possible scenarios which influences the input and output streams of the ash dump. The

scenario development in then incorporated into the experimental observations from the electrical resistivity surveys and the numerical models so that a detailed conceptual model for the potential solute transport model for the ash dump can be developed. Figure 6.1 presents the scenario diagram for the input and output streams around the Tutuka ash dump.

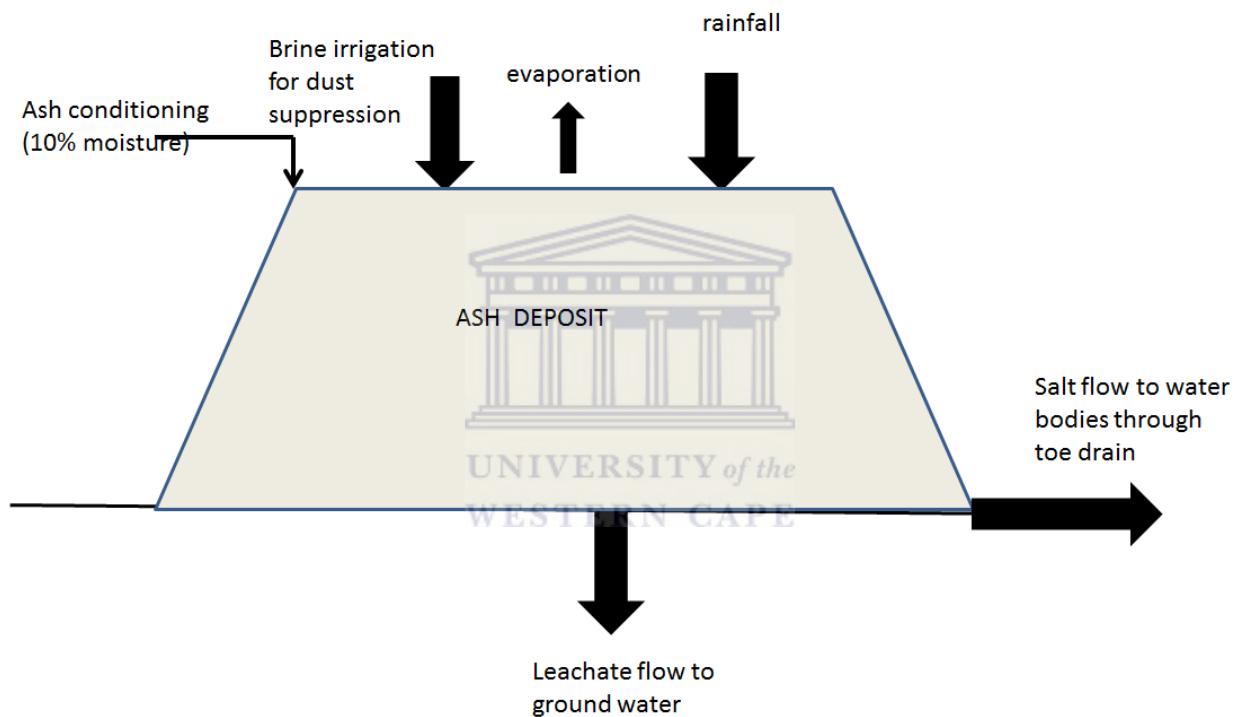


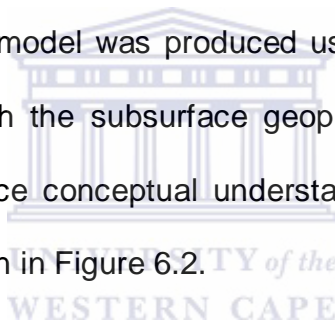
**Figure 6.1. The conceptual diagram of the input and output streams around Tutuka ash deposit.**

In the current scenario, the major source of potential solute generation is from part of the water applied on the surface of the ash, be it in the form of rain or through brine irrigation that infiltrates into the unsaturated zone of the ash dump. For solute transport and evaluation of potential pollution of groundwater by ash dumps, three basic conditions must exist, these include:

- The ash dump must be located over, adjacent to or in an aquifer;
- Ash dump be able to act as a solute transport medium, this may occur due to percolation of irrigation; and
- Leachate must be produced and this leached fluid must enter the aquifer.

### **6.2.2 Development of the conceptual model for the ash dump-aquifer system**

Data from the topographic models was combined with geophysical data to infer the nature of the underlying aquifer system in the ash dump. The digital elevation model data for the study site was imported into the Surfer model developing program where a three dimensional topographic model was produced using a unit elevation of 5m. The model was then combined with the subsurface geophysical results and pre-existing geologic information to produce conceptual understanding of the ash dump and its hydro-geologic system as shown in Figure 6.2.





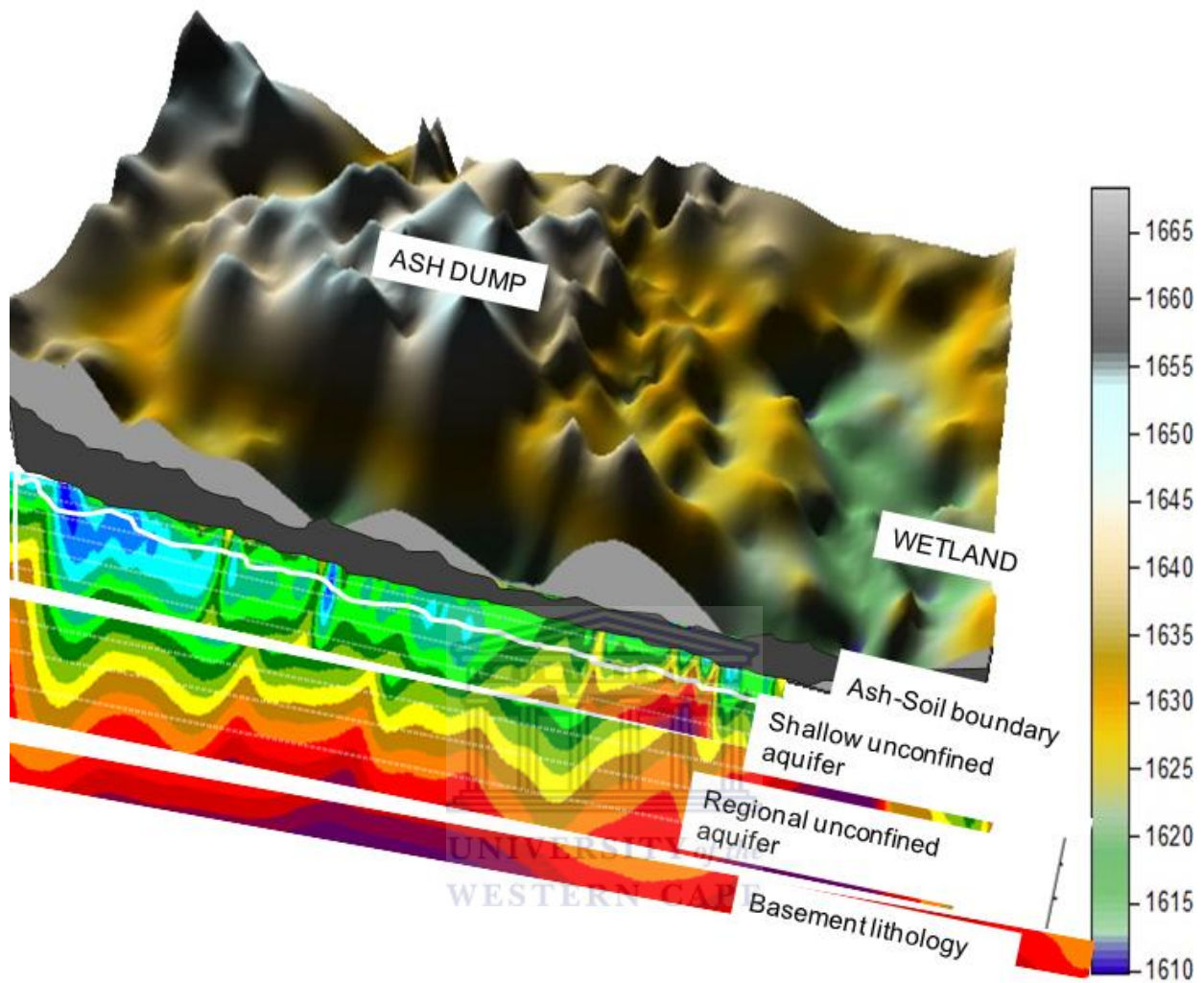


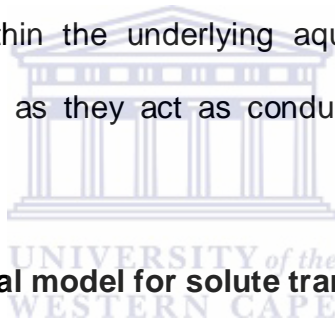
**Figure 6.2. Conceptual model of the major hydro-geologic features in the study area.**

Deductions from Figure 6.2 suggest that the Tutuka ash dump site is underlain by multiple aquifer system that includes:

- Unconfined aquifers present within soil horizons that have developed within colluvial and alluvial environments and the weathered upper levels of Ecca Formation sediments.

- Unconfined shallow aquifer along the trend of dolomite dykes. These may also act as recharge points for confined aquifers within the Ecca Formation at depth. Evidence from geophysical surveys and some previous studies by Van Niekerk and Staats (2010) suggests that salt contamination has already reached this aquifer system has already reached the shallow aquifer
- Regional unconfined aquifers within the Ecca Formation. These aquifers are commonly confined along essentially horizontal bedding interfaces between different lithologies.
- Deeper confined aquifers within basement lithologies.

The presence of fractures within the underlying aquifer system has an increased potential for pollutant transport as they act as conduits between the ash dump and underlying aquifer system.



### **6.3 The generalised conceptual model for solute transport at Tutuka ash dump.**

The best scenario of the ash dump transport model is developed by screening all historical and currently available information on the characteristics of the ash dump (e.g. the existing conceptual models, management practices, climate, hydrogeological conditions, and any other natural or human induced condition). Personal judgment is then used to develop scientifically sound but hypothetical descriptions of the transport model.

Because of the close linkage between water flow and solute transport, the physics and mathematical description of water flow in the vadose zone was used to develop a conceptual model of the unsaturated zone transport parameters for dry ash dumps. To

enable this conceptualisation, the numerical and geophysical interpretation of the models should be critical components of any effort to optimally understand and quantify site-specific subsurface water flow and solute transport processes. These have been combined to come up with the most acceptable conceptualisation of the vadose zone transport of the ash dump that could be used in hazard assessment and mitigation against water pollution. Earlier studies which sought to study the hydrological behaviour of ash dumps have mostly concentrated on the development of conceptual models for the overall and concentrated mainly on the underlying aquifer systems. Whilst many of the previous studies managed to develop conceptual models of hydrologic systems characterising the study area, (e.g. October, 2010, and Mengusthu, 2011), an in-depth understanding of the unsaturated zone transport mechanism in the ash dump was critical since it formed the basis for assessing any potential ground-water contamination in the underlying aquifer system. The model developed here-in seeks not only to provide evidence of a smart and non-invasive way for characterisation waste disposal sites, but also to develop a dual conceptual model which will be able to present in detail the unsaturated zone transport model and the full hydrologic model of the study site. Figure 6.3 presents a conceptual model for the solute transport system developed for the Tutuka ash dump.

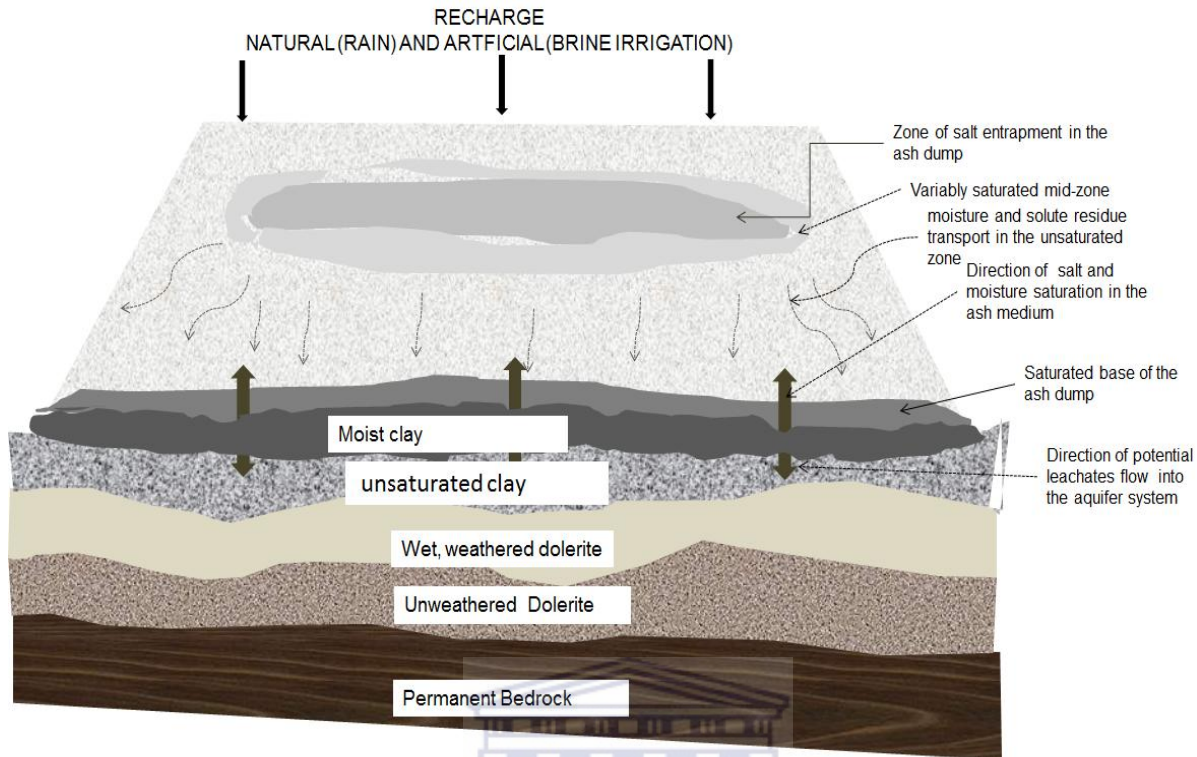


**Figure 6.3. Conceptual model for the solute transport of the Tutuka ash dump and its underlying environment.**

Results from the current study suggested that the potential for immediate groundwater contamination by downward percolation of pore water through ash dumps is quite significant and cannot be neglected in management practices. However, the numerical simulations and the long term geophysical profiles suggested a region of salt entrapment in the ash dump. This is also supported in literature by the presence of a compacted zone in the ash dump that will result in the formation of a pozzolanic crust also help to limit leaching as a wetting front must first penetrate through a mass of dry ash before the underlying groundwater can be contaminated.

Continuous rehabilitation of dry ash dumps is becoming common practice and involves covering the ash with a layer of soil and establishing suitable vegetation (Carlson and Adriano, 1993) further limiting leaching. As such the hydrodynamic regime in a dry ash

deposit is more complex, as the system is “gas phase continuous”. The ash medium also depicts the existence of static and dynamic regions where the ash particles can be completely wetted, partially wetted or completely dry (Hunsen et al., (2002). Hodgson et al. (1997) suggested that the observed hydrodynamic behaviour is further complicated through pozzolanic or cementation reactions resulting in areas of decreased permeability within the ash dump. This would therefore imply a reduction in the volumes of salt fluxes reaching the base of the ash dump. However, once these potential contaminants reach the successfully reach the base of the ash dump they will ultimately seep through the vadose zone of the underlying medium and ultimately seep through under natural groundwater to the underlying aquifer as dissolved solids.

As suggested by the numerical models, the changes in volumetric water content, between dry and wet seasons, are generally small (on the order of a few percent), which is consistent with experimental data reported by Smith et al. (1995). These results also suggests that the ash dump is characterized by complex material composition, non-uniform compaction within each layer, whose hydrodynamic behaviour is site specific as suggested by the time-lapse infiltration experiments , and presented in the conceptual model in Figure 6.2. The hydraulic conductivity and moisture retention characteristics of the fly/coarse ash will depend, among other things, on the degree of change that the ash has undergone in the ash dump, through pozzolanic crystallization (Hodgson and Krantz, 1998), the way the ash is placed and the engineering of the ash dump. Also, as mentioned above, fly ash in an ash dump is not a homogeneous medium because of grain size variations and crystallization. The heterogeneity of the size of the particles contributes to the difference in hydraulic conductivity.

The environmental impact of fly ash has been investigated by many researchers with the use of laboratory leaching tests and field sampling. Previous studies were able to identify typical elements leaching from ash disposal sites which could contaminate the surrounding ground and surface water environment (Baba et al., 2004, Gitari et al., 2011). The current study managed to give an understanding of the possible fate and mechanism of solute transport in and through the ash medium and how leaching is influenced under these conditions. In this regard, a clear understanding of the interaction between the ash dump and the underlying natural environment was of critical importance as it enables informed decisions to be made on any mitigation procedures. Once the potential leachates filter through the base of the ash dump, they are most likely to percolate the underlying aquifer through capillary flow between the ash dump and the clay layer which forms the natural soil environment.

#### **6.4 Conceptual site model for the potential hydrological interaction between the ash dump and the wetland.**

The conceptual models presented in Figure 6.2 and Figure 6.3 described the interaction between the ash dump and the underlying aquifer and demonstrated the potential of solute transportation through the unsaturated zone into the underlying aquifer system. Van Niekerk and Staats (2010) established that the main water bearing aquifers underlying the ash dump are basement fractured rocks. These fractures often serve as potential conduits that may influence the interconnection between the ash dump and the surface hydrological features such as the wetland located on the eastern side of the study area (Photo 6.1). The major shortfall on the assessment of potential wetland contamination from the ash dump has been the traditional conception that the ash

dump, groundwater and the wetland are independent hydrological units. As a matter of fact, nearly all surface-water features, including wetlands interact with groundwater. In dry seasons wetlands are frequently charged from groundwater, therefore any contamination that may have progressed through to the underlying aquifer may contaminate the wetland that is on the eastern side of the ash dump.



**Photo 6.1 Photographic setting of showing the ash dump and the wetland in the eastern side of the study area.**

In this study, knowledge from the developed conceptual models were combined to used discuss the scenario of potential wetland contamination by the ashing activities. The topographic map described by Figure 2.3 (Chapter 2) showed that the slope of the study area deeps towards the eastern side where the wetland exists. As such potential contaminants to the wet are most likely to be transported directly from the ash dump, and the underlying soil medium through local flow. Since the flow of groundwater in

unconfined aquifers is mostly influenced by the topographic gradient, another possible scenario is that the shallow unconfined aquifer may act as an interconnecting medium between the dump and the wetland. This may therefore result in wetland contamination by the solutes which will have progressed through the ash dump to the underlying aquifer system and will be transported via water's ambient flow (advection) and diffusion. The potential for contaminant transport will thus be through groundwater-surface water interaction described by three flow regions; local flow, intermediate flow and regional flow. Figure 6.4 presents a schematic flow conceptual model developed for the potential contaminant flow between the ash dump and the wetland.

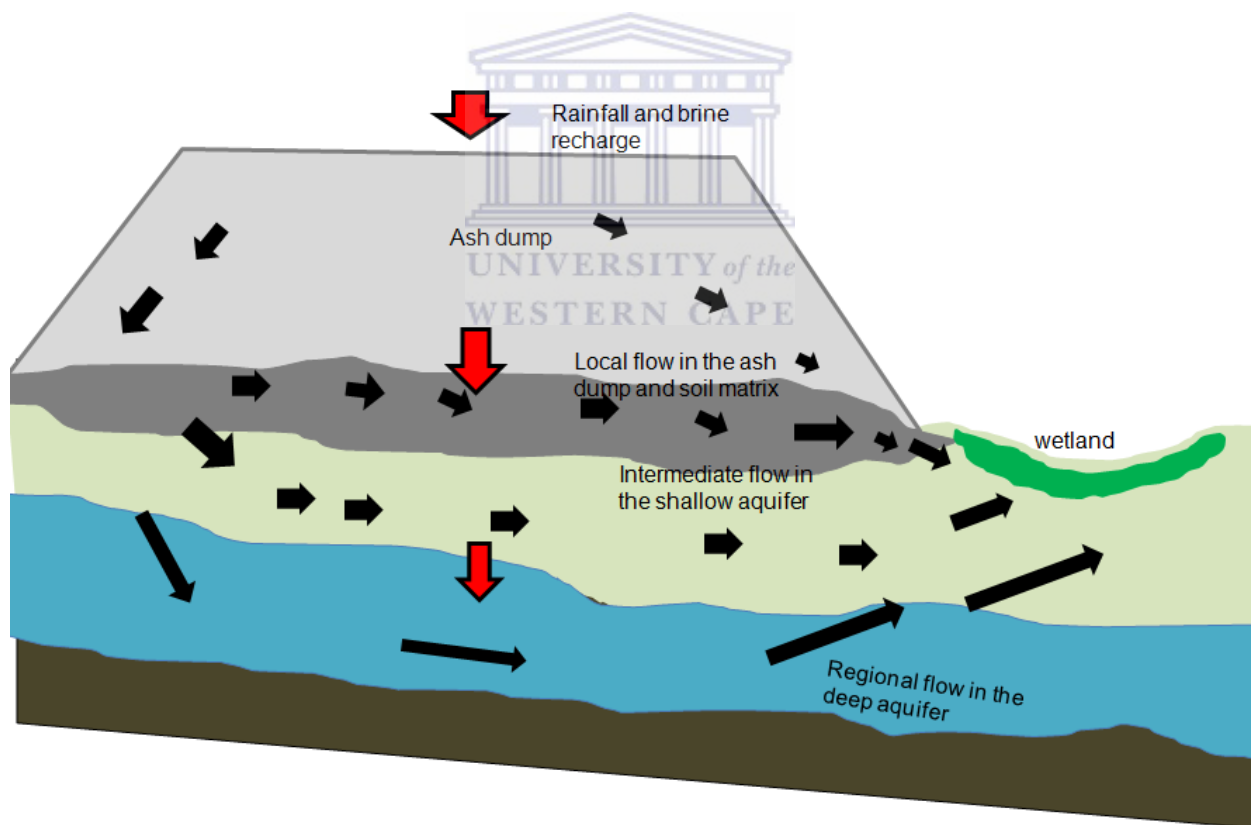


**Figure 6.4. A site conceptual model describing potential contaminant flow between the ash dump and the wetland.**



The developed conceptual model describes a system where interaction between the wetland and the ash dump is linked by groundwater-surface water interaction driven by both capillary action and potential gradients (usually described by hydraulic heads). The potential contaminant transport starts from the top of the ash dump which defines the recharge zone of the system through brine irrigation and rainfall recharge zone. Leaching will then be initiated by these ingressing fluids as they progress through the ash dump as described by the numerical models, until they reach the base of the ash dump where some solutes are likely to seep through the ash-soil boundary. Intermediate and local flow systems are the most dynamic and the shallowest and therefore have the greatest interaction with the wetland. The intermediate flow describes the potential transport of contaminants through interaction between the unconfined aquifer and the wetland. Regional flow describes the interaction between the deep aquifer and the wetland and is governed by the slope of the water table.

## **6.5 Summary**

The purpose of the current study was done under the context of developing a detailed proposal for a framework with a view to increasing the competency of both organizations in the management of the co-disposal of ash and brine and the dissemination of knowledge with regard to the impacts of the sites. The conceptual model developed in this chapter managed to describe the transport mechanism in both the ash dump and the underlying aquifer system, as well as suggest mechanisms for the interaction between the two sub-systems. The two-dimensional transport model was developed by considering results from the non-invasive numerical and geophysical techniques for this study (Chapters 4 and 5). As such this model can be regarded as an

accurate generic model for the Tutuka ash dump site. However, this conceptual is not an attempt to predict the future of a given waste site, but is an aid to assess how effectively the site is managed and controlled.

The conceptual models presented in Figure 6.3 and 6.4 are useful in providing information regarding the sources and receptors of potential contaminants in the ash dump system. It therefore explains the impact of the ash dump to the eco-hydrologic environment. In this regard, wetland managers may need to develop remedial action objectives specifying the contaminants in the ash medium and evaluate the groundwater surface water exposure pathways in both the shallow aquifer and the deep aquifer system, and then take mitigation measures that permit a range of alternatives for both the ash dump and the wetland.



## CHAPTER 7

### CONCLUSIONS AND RECOMMENDATIONS

#### 7.1 Conclusions

An understanding of the components of the conceptual transport model was done through the use non-intrusive geophysical and numerical modelling techniques of the unsaturated zone and the surrounding hydrological environment surrounding the ash dump. The investigation of ash dumps established percolation of natural precipitation, or the movement of groundwater through the ash dump and its environment.

Electrical resistivity tomography (ERT) proved to be an efficient non-intrusive method for characterizing and mapping the time and spatial variability in salt distribution and water content within the ash dump, thereby eliminating the need to drill boreholes which could cause additional preferential pathways through the ash dump to the underlying aquifer system. The empirical determination of the cementation factor for the ash dump provided the basis for linking the electrical resistivity to salt and moisture contents in the ash dump with a sufficient accuracy. Considering the fact that the variations in electrical conductivity in the invaded substrate are known to correspond with changes in the total dissolved solids and/or chloride concentration in such environments, it was thus possible to predict some hydro-chemical parameters and fluid migration patterns from accurate electrical conductivity models of the subsurface and time-lapse studies. The ERT profiles were efficient tools in monitoring of moisture variation and relative plume progressions can easily be detected and modelled.

Measuring the unsaturated conditions of the ash dump system can assist and enhance estimation of the saline water movement through the ash dump system and the effect of wet and dry cycles on the movement of water and salts. The change in properties is dependent on the time the ash is exposed to the process water. The flow conceptualization of the ash dump system suggested that the ash dump plays a significant role on the impact the saline water has on the underlying aquifer.

The Richards' equation is a partial differential equation which is highly non-linear due to the non-linear physical relationships in the hydraulic head and the moisture capacity. Nevertheless, the numerical methods could solve the Richards' equation to ensure that the solute transport and distribution in the ash medium was done with sufficient accuracy. The characterisation of solute transport in the unsaturated zone of the ash provided the understanding to predict future site behaviour based on past and present ash dump conditions and operations. It was also critical in the assessment of the solute transport mechanisms as well as evaluating the existence of transport pathways within the medium under study.

Coal ash disposal is considered to be a major environmental issue because of its potential to contaminate groundwater with salts from brine irrigation for dust suppression and any potential trace elements which maybe entrapped within the ash dump itself. Leaching is the most likely means by which these metals and other constituents in fly ash would become mobile, environmental contaminants. The main leachates of the disposed ash are rainwater, mostly acidic due to gaseous power plant emissions and the slurry which carries the ash from the plant to the pond (Praharaj et al., 2002). Rain water discharge and run off from the ash mound areas into surface

water bodies are a source of water pollution. The leaching of contaminant species contained in coal ash when in contact with water/aqueous solution has been widely observed to negatively impact the environment.

The hydraulic parameters and moisture retention characteristics of the unsaturated zone of the ash dump also depend, among other things, on the degree of change that the ash has undergone in terms of its compaction and its pozzolanic crystallization. The conceptual model developed showed that solute transport in the unsaturated zone of the ash dump is more pronounced in non-compacted ash which is also characterised by a lesser pozzolanic action. As the ash goes through different stages during dumping processes, mineral precipitation and pozzolanic crystallization of the ash particles could be the reason for the reduced hydraulic conductivity at the ash dump.

As discussed in Chapter 5, predictions of unsaturated flow are complex, even without the addition of ash residues, and research on unsaturated flow through coal combustion residues (ash dumpsites) is extremely limited. Nevertheless, the current study suggest that the unsaturated flow will depend on a number of factors, including the degree of contrast in hydraulic properties between the ash dumpsite and the surrounding spoil or geologic strata, the moisture content, the procedure that was followed in ash dump placement, and the length of the period to which a particular section of the ash dump is active for ash emplacement before final rehabilitation.

The conceptual model discussed in this study was discretized into a two dimensional model consisting of two layers. The upper layer represented the unsaturated zone of the ash dump which was the source of any potential contaminant transport that could be of concern. The lower layer describe the underlying the subsurface environment to the

ash dump which include the perched aquifer and the lower layer of the fractured rock aquifer.

## **7.2 Management of Ash Dump**

The management of the ash dumps is a very important parameter to be considered to reduce the impact of the ash disposal on the environment, as it has been shown that the disposal technique have the tendency of releasing contaminants to the surrounding soils and subsequently into the groundwater system. Despite the fact that the study has suggested that dry ash disposal facilities have the capacity to retain most salt fluxes in the ash matrix, this does not imply less environmental impact, as he solute fluxes which manage to seep through the ash medium are capable of contaminating large volumes of the underlying groundwater. The study showed that solute migration through the ash dump and the underlying shale and weathered dolorite is generally very slow. However, these potential groundwater contaminants will eventually reach the underlying aquifer and it may take many years after land disposal of the waste for contaminants to be detected in groundwater. Another detrimental effect would be due to the fact that groundwater flows naturally towards any nearby surface streams or rivers. As such the surrounding surface water sources may also be polluted by groundwater through groundwater surface water interaction mechanism or through drainage from the base of the ash dump into the toe drain. In the present scenario, there is evidence of salt contamination in surface water bodies downstream of the ash dump. This scenario is most probable for the study area under consideration, as it is surrounded by various water bodies such as streams (e.g. the Koornfonteinspruit and its tributary) and dams that are utilized by local livestock farmers. Over-more the eastern part of the study area

also houses a wetland, suggesting strong evidence for groundwater-surface water interaction for the study area.

The leaching of contaminant species contained in coal ash when in contact with water/aqueous solution has been widely observed to cause a negative impact on the environment. As mitigation, some authors suggested the implementation of drastic measures such as lining the bottom of the ash mound, stabilization of the ash mound and covering of the completed mound with vegetation are required to minimize environmental damage (e.g. Vidya and Snigdha, 2006). The safe disposal and adequate management of the ash disposal sites will reduce the negative environmental impact of coal ash disposal irrespective of the type of ash disposal techniques employed. As such it is very important to implement a proper and informed ash management framework to prevent the coal ash disposal site from polluting its natural environment and any groundwater resources underlying the disposal site.

Several of the potential remedial alternatives may include innovative technologies. The availability of services and materials to implement certain technologies may be limited. Substantial uncertainty may exist regarding the technical implementation ability of in situ technologies under actual Site conditions. The remedial action that is often implemented in the ash dump is the in-situ capping process, where by the ash dump is rehabilitated by covering it with ordinary soil and planting grass on the surface. The level of risk reduction associated with this remedy generally depends on the action level selected for capping and the level of contamination that may continue to enter the groundwater system from the ash medium. From the geophysical results, it is also evident that the water table is at the bottom or below the ash stack and that very little

water exists in the ash stack itself where the brine irrigation has stopped. Due to this the leaching of pollutants from the ash is greatly reduced when excessive irrigation stops and the in-situ cap is placed on the ash dump.

Promoting the utilization of fly ash in the form of an alternative to another industrial resource, process such as an additive to cement and concrete products, structural fill and cover material, roadway and pavement utilization, addition to construction materials as a light weight aggregate, infiltration barrier and underground void filling, and soil, water and environmental improvement (Halstead, 1986; Ahmaruzzaman, 2010) can also be considered as a way of averting the accumulation of these coal combustion products.

Fly ash may also be used in the manufacture of lightweight aggregate, in road base construction, landfill liners, sewage sludge treatment and in the ceramics industry and in the manufacture of bricks and tiles. Utilization of fly ash will certainly minimize negative environmental impacts and the chemical and leaching of its trace elements into the underlying groundwater system and thus can be implemented as a mitigating procedure.



## References

Aaltonen, J. (2001). Ground monitoring using resistivity measurements in Glaciated terrains. Unpublished PhD thesis, Royal Institute of Technology, Stockholm.

Abdullahi, N.K., Osazuwa, I. B. and Sule P.O., (2011). Application of integrated geophysical techniques in the investigation of groundwater contamination: a case study of municipal solid waste leachate. *Ozean Journal of Applied Sciences*, Vol. 4 (1), 7-25.

Adriano, D.C., Page, A.L., Elseewi, A.A., Chang, A.C. and Straughan, I. (1980). Utilization and disposal of fly ash and other coal residues in terrestrial ecosystems: A review. *Journal of Environmental Quality* , Vol. 9 (3), 333–344.

Ahmaruzzaman, A., (2010). A review on the utilization of fly ash. *Progress in Energy and Combustion Science*, Vol. 36, 327–363.

Akinyemi S. A., (2010). Geochemical and mineralogical evaluation of toxic contaminants mobility in weathered coal fly ash: as a case study, Tutuka dump site, South Africa. Unpublished PhD thesis, University of the Western Cape, South Africa.

Al, T.A., and Blowes D.W., (1996). Storm-water hydrograph separation of runoff from a mine tailings impoundment formed by thickened tailings discharge at Kidd Creek, Timmins, Ontario. *Journal of Contaminant Hydrology*, Vol.180, 55-78.

Amoozegar, A., (1992). Compact constant head permeameter: A convenient device for measuring hydraulic conductivity, pages 31–42. In G.C. Topp et al. (ed.) *Advances in measurement of soil physical properties: bringing theory into practice*. SSSA Spec. Publ. 30. SSSA, Madison,WI.

Amoozegar, A. 1989a. A compact constant-head permeameter for measuring saturated hydraulic conductivity of the vadose zone. *SSSA Journal*. Vol 53(5), 1356-1361.

Amoozeger , A. and A.W. Warrick, (1986). Hydraulic conductivity of saturated soils. In Klute, A., ed. *Methods of Soil Analysis Part I: Physical and Mineralogical Methods*, 2<sup>nd</sup> edition. Monograph 9 (Part 1), American Society of Agronomy, Inc., Soil Science Society of America, Inc. publisher, Madison, WI.

Anon A. (1952). Report on the investigation of leaching of the ash dumps. State of California water Pollution Control Board Pub. No 2.

Archie, G.E. (1942). The electrical resistivity log as an aid in determining some reservoir characteristics, *Transactions of the American Institute of Mining and Metallurgical Engineers*, Vol.146, 54-61.

Arora T. and Shakeel A., (2010). Electrical structure of an unsaturated zone related to hard rock aquifer, *Research Communications in Science*, Vol. 99(2), 216-220.

Arora, T., Krishnamurthy, N. S. and Ahmed S., (2005). TLERT to decipher the unsaturated zone. Published and presented in the International Conference on Hydrological Perspectives for Sustainable Development, IIT, Roorkee, Allied Publishers Pvt Ltd, Vol. II, 846–852.

Asch T.H. and Morrison H.F. (1989), Mapping and monitoring electrical resistivity with surface and sub-surface electrode arrays. *Geophysics*, Vol. 54, 235–244.

Asokan, P., Saxena, M., Asolekar, S.R., (2005). Coal combustion residues- environmental implications and recycling potentials. *Resources, Conservation and Recycling*, Vol. 43, 239-262.

ASTM C618-08 Standard Specification for Coal fly ash and Raw or Calcined Natural Pozzolan for use in Concrete.

Atekwana, E. A., Sauck, W. A. and Werkema J., (2000). Investigations of electrical signatures at a contaminated site. *Journal of Applied Geophysics*, Vol. 44 (2-3), 167-180.

Baba, A. Kavdir, Y., Deniz, O., (2004). The impact of open waste disposal site on groundwater, *International Journal of Environment and Pollution*, Vol. 22 (6), 76-687.

Babcock and Wilcox Company, (1978). *Steam. Its Generation and Use*. New York, NY.

Banton, O., Seguin, M.K., Cimon, M.A., 1997. Mapping field scale physical properties of soil with electrical resistivity. *Soil Sci. Soc. Am. J.* 61, 1010–1017.

Baran, E. and Dziembowski, Z.M. (2003). An explanation of the 1:500 000 general hydrogeological map: Kroonstad 2725. Department of Water Affairs and Forestry, Pretoria, Republic of South Africa.

Barker R. and Moore J. (1998). The application of time-lapse electrical tomography in groundwater studies. *The Leading Edge*, Vol. 17, 1454–1458.

Barker, R. D. (1996), Application of electrical tomography in groundwater contamination studies: 61st Mtg. Eur. Assoc. Expl Geophys., Extended Abstracts, European Association Of Geophysical Exploration, Session, p.082.

Barker, R. D. (1992). The Offset System of Resistivity Sounding and its use with a Multicore Cable. *Geophysical Prospecting*, Vol. 29, 128-143.

Barker R.D., (1990). Investigation of groundwater salinity by geophysical methods. In Ward, S. H. (ed.). Geotechnical and environmental geophysicists, Tulsa, USA, 201-212.

Bauer P., Supper R., Zimmerman S. and Kinzelbach W., (2006). Geoelectrical imaging of groundwater salinization in the Okavango Delta, Botswana journal of applied geophysics, Vol. 60 (2), 126-141.

Beer, J.M., (2000). Combustion technology developments in power generation in response to environmental challenges. Progress in Energy and Combustion Science, Vol. 26, 301-327.

Belmans, C., Wesseling J. G. and Feddes R. A., (1983). Simulation model of the water balance of a cropped soil: SWATRE, Journal of Hydrology., Vol. 63, 271- 286.

Benson, A. K., Payne, K. L., and Stubben, M. A., (1997). Mapping groundwater contamination using DC resistivity and VLF geophysical methods – A case study. Geophysics, Vol. 62, 80–86.

Bernston C., and Dahlin T., (1998). D.C. resistivity mapping of old landfills. Two case studies. European Journal of Environmental and Engineering geophysics. Vol. 2, 121-136.

Borner, F. D., and J. H. Schön, (1991) A relation between the quadrature component of electrical conductivity and the specific surface area of sedimentary rocks, Log Anal., 32: 612–613.

Sudha K. , Israil M., Mittal S., Rai J. , (2009). Soil characterization using electrical resistivity tomography and geotechnical investigations. Journal of Applied Geophysics , Vol. 67 , 74–79.

Bevan, B.W., (2000). An early geophysical survey at Williamsburg, USA. Archae. Prospecting 7, 51– 58.

Bevc D. and Morrison H.F. (1991). Borehole-to-surface electrical resistivity monitoring of a salt water injection experiment. Geophysics, Vol. 56, 769–777.

Bilski, J. J., Alva, A. K., and Sajwan, K. S., (1995). Fly ash. In: Rechcigl, J.E. (Ed.), Soil Amendments and Environmental Quality. Lewis, Boca Raton, 237–363.

Binley A., Cassiani, G., Middleton, R. and Winship P., (2002). Vadose zone model parameterization using cross-borehole radar and resistivity imaging. Journal of Hydrology, Vol. 267, 147–159.

Bishop, P.L. (2000). Pollution Prevention: Fundamentals and Practice. Boston, MA: McGraw-Hill Higher Education.

Blowes D.W., and R.W. Gillham, (1988). The generation and quality of streamflow on inactive uranium tailings near Elliot Lake, Ontario. *Journal of Hydrology* Vol. 97,1-22.

Botha, W. J. and Vorster, A. R., (1993). Geophysics applied to groundwater exploration in the Kalahari regions of southern Africa: 61st Mtg. Eur. Assoc. Expl Geophys., Extended Abstracts, European Association Of Geophysical Exploration, Session:D046.

Bradshaw, A. D., Chadwick, M. J., (1980). *The Restoration of Land*, University of California Pres, Berkeley, California.

Belmans, C., Wesseling, J.G. and Feddes, R.A., 1983. Simulation model of the water balance of a cropped soil: SWATRE. *Journal of Hydrology*, 63 (3/4), 271-286. Concepts and dimensionality in modeling unsaturated water flow and solute transport.

Bras R.L. and Rodriguez-Iturbe I.; (1993). *Random functions and hydrology*. Dover publications, New York.

Brassington R, (1988). *Field Hydrogeology*. Geological Society of London, Handbook Series. Open University Press.

Brooks, R. H. and Corey, A. T. (1966). Properties of porous media affecting fluid flow. *Proceedings of the American Society of Civil Engineers*. Vol. 92 (IR2), 61–87.

Brown, H.S., S. Raymond, and Kasperson R.E. (1990). Trace pollutants in the global environment: A three hundred year perspective. In *The earth as transformed by human action*, ed. B. Turner et al., 437-454. Cambridge: Cambridge University Press.

Brunet, P., Clement, R., and Bouvier C. (2009). Monitoring soil water content and defeciet using electrical resistivity tomography- A case study in the Cevennes area, France. *Journal of Hydrology*, Vol. 380, 146-153.

Buselli., G., Davis G. B., Barber, C. Height G.B., and Howard S.H. D., (1992). Time application of electromagnetic and electrical methods to groundwater problems in urban environments. *Exploration Geophysics*.

Cardarelli, E. and Bernabini M., (1997). Two case studies of the determination of parameters of urban waste dumps. *Journal of Applied geophysics*, Volume 36(4), 167-174.

Carlson, C. L., and Adriano, D. C. (1993). Environmental impacts of coal combustion residues, *Journal of Environmental Quality*, Vol. 22, 227-247.

Carpenter P. J., Kaufman R. S., and Price B., (1990). Use of resistivity soundings to determine landfill structures. *Groundwater*, Vol. 28 (4), 569-575.

Cassiani G., Binley A.M. and Ferré T.P.A (2006). Unsaturated Zone Processes. Applied Hydrogeophysics IV, Earth and Environmental Sciences, Nato Science Series.

Cassiani, G., V. Bruno, A. Villa, N. Fusi, and A. Binley (2006), A saline trace test monitored via time-lapse surface electrical resistivity tomography, Journal of Applied Geophysics, Vol. 59, 244–256.

Cassiani, G., C. Strobbia, and L. Gallotti (2004), Vertical radar profiles for characterization of deep vadose zones, Vadose Zone Journal, Vol. 3, 1093–1105.

Celia, M. A., and Bououtas E. T., R. L. Zarba, (1990). A general mass-conservative numerical solution for the unsaturated flow equation, Water Resour. Res., Vol. 26, 1483-1496.

Chevallier, L. Goedhart, M. and Woodford, A.C. (2001). The influence of dolomite sill and ring complexes on the occurrence of groundwater in Karoo fractured aquifers: a morpho-tectonic approach. WRC Report no 937/1/01. Water Research Commission, Pretoria

Chindaprasirt P., S. Homwuttiwong, and V. Sirivivatnanon, (2005). Influence of fly ash fineness on strength, drying shrinkage and sulfate resistance of blended cement mortar, Cement and Concrete Research, Vol. 34 (7), 1087-1092.

Dahlin, T. (2001). "The development of DC resistivity imaging techniques." Computers & Geosciences, Vol. 27 (9), 1019-1029.

Dahlin T., and M. H. Loke, (1998). Resolution of 2D Wenner resistivity imaging as assessed by numerical modelling, Journal of Applied Geophysics .Vol. 38 (2001), 237-249.

Dahlin T., (1996). 2D resistivity surveying for environmental and engineering applications. First Break, Vol.14, 275–284.

De la Vega, M., Osella, A., and Lascano, E, (2003). Joint inversion of Wenner and dipole-dipole data to study a gasoline-contaminated soil. Journal of Applied Geophysics, Vol. 54 (1-2), 97-109.

Deiana R., Cassiani G., Kemna A., Villa A., Bruno V. and Bagliani A., (2007). An experiment of non-invasive characterization of the vadose zone via water injection and cross-hole time-lapse geophysical monitoring. Near Surface Geophysics, 183-194.

Dienhart, G.J., B.R. Stewart, and Tyson S.S., (1998). Coal Ash: Innovative Applications of Coal Combustion Products. American Coal Ash Association: Alexandria, VA.

Digioia, Anthony, M., Jr. and William, L. N., (1997). "Fly ash as Structural Fill". Proceedings of the American Society of Civil Engineers. Journal of the Power Division, New York, NY.

Dolmar D. C., (2001). Transport of anthropogenic and natural solutes near a prehistoric native american pueblo, Socorro, Master of Science in Hydrology , New Mexico Institute of Mining and Technology , Department of Earth and Environmental Science Socorro, New Mexico.

Eary, L. E., Dhanpat, R., Mattigod, S. V., and Ainsworth, C. C., (1990). Geochemical factors controlling the mobilization of inorganic constituents from fossil fuel combustion residues: II. Review of the minor elements. Journal of Environmental Quality, 19,202–214.

Elrick, D. E. and Reynolds, W. D. (1992a). Methods for analyzing constant- head well permeameter data. Soil Science Society Amamerica Journal, Vol. 56: 320–323.

Elrick,D.E.,and W.D.Reynolds (1992b). Infiltration from constant-head well permeaters and infiltrmeters. In: Advances in Measurements of Soil Physical Properties: Bringing Theory into Practice. G.C. Topp, W.D. Reynolds, and R.E. Green (eds.). SSSA Spec. Publ. No. 30. SSSA, Madison,WI, p. 1–24.

EPA (environmental protection agency), (1997). Electrical resistivity evaluations at solid waste disposal facilities. Report SW -729 USA.

Fatoba, O.O., (2011). Chemical Interactions and mobility of species in fly ash-brine co-disposal systems, Unpublished PhD thesis, University of the Western Cape, Cape Town, South Africa.

Fatoba, O.O., (2007). Chemical compositions and leaching behaviour of some South African fly ashes, Unpublished M.Sc thesis, University of the Western Cape, Cape Town, South Africa.

Feddes, R. A., Bresler E., and Neuman S. P., (1974). Field test of a modified numerical model for water uptake by root systems, Water Resour. Res., Vol.10(6), 1199-1206.

Ferguson, G. and Levorson S.M., (1999). Soil and Pavement Base Stabilization with Self-Cementing Coal Fly Ash. American Coal Ash Association: Alexandria, VA.

Foner, H. A., Robl, T. L., Hower, J. C., Graham, U. M., (1999). Characterization of fly ash from Israel with reference to its possible utilization. Fuel, Vol. 78, 215–223.

Fukue, M., Minatoa, T., Horibe, H., Taya, N., 1999. The microstructure of clay given by resistivity measurements. Eng. Geol. 54, 43–53.

Gardner, W. R., (1958). Some steady-state solutions of the unsaturated moisture flow equation with application to evaporation from a water table. *Soil Science*, Vol 58, 228–232.

GHT Consulting Scientists. (2004) Groundwater Modeling at Hendrina Power Station. Unpublished Report. Report no.: RVN 396.1/574.

GHT Consulting Scientists. (2007a) Routine Monitoring Phase 20 Site Assessment and Audit Report at Taaibosch and Highveld Power stations. Unpublished Report. Report no.: RVN 511.2/822.

GHT Consulting Scientists. (2002) Site Hydrology, November at Kriel and Matla Power Station. Unpublished Report. Report no.: RVN 264.4/467.

Gitari, M.W., Petrik, L.F. and Reynolds, K. (2011) Chemical Weathering in a Hypersaline Effluent Irrigated Dry Ash Dump: An Insight from Physicochemical and Mineralogical Analysis of Drilled Cores *Energy Science and Technology* Vol. 2, No. 2, 2011, pp. 43-55

Gitari, M. W., Petrik, L. F., Etchebers, O., Key, D. L., Iwuoha, E., Okujeni, C., (2006). Treatment of acid mine drainage with fly ash: removal of major contaminants and trace elements. *Journal of Environmental Science and Health – Part A*, Vol. 41, 1729–1747.

Glover P. W. J., (2010). A generalized Archie's law for n phases. *Geophysics*, Vol. 75 (6), 85-91.

Greenhouse, J. P., Monier-Williams, M. E., Ellert N. and Slaine, D. D., (1987). Geophysical methods in groundwater contamination studies. *Proceedings of Exploration '87, Applications of Geophysics and Geochemistry*, 666-677.

Greenhouse, J. P. and Slaine, D. D. (1986). Geophysical modelling and mapping of contaminated groundwater around three waste disposal sites in Southern Ontario. *Canadian Geotechnical Journal*, Vol. 23 (3), 372-384.

Greenhouse, J.P. and Harris R.D. (1983). DC, VLF and Inductive Resistivity surveys, in Cherry, J.A. (ad.), *Migration of Contaminants in Groundwater at a Landfill: A Case Study*. *Journal of Hydrology*, Vol. 63, 177-197.

Grellier S., Reddy K. R., Gangathulasi J., Adib R., and Peters C. C., (2007). Correlation between Electrical Resistivity and Moisture Content of Municipal Solid Waste in Bioreactor Landfill. *Geotechnical Special Publication No. 163*, ASCE Press, Reston, Virginia, 2007, 2-15.

Grellier, S., Bouyé, J.M., Guérin, R., Robain, H., and Skhiri, N. (2005). Electrical Resistivity Tomography (ERT) applied to moisture measurements in bioreactor:

principles, in situ measurements and results. International Workshop “Hydro-Physico-Mechanics of Landfills”, Grenoble (France), 21-22 March.

Griffiths D.H., Turnbull J. and Olayinka A.I. 1990, Two-dimensional resistivity mapping with a computer- controlled array. *First Break* 8, 121-129.

Guerin, R. (2004). Leachate recirculation: moisture content assessment by means of a geophysical technique. *Waste Management*, 24(8): 785-794.

Hajarnavis, M.R and Bhide. A. D., (1999). Leacheability and toxicity of heavy metals from fly ash. *Indian Journal of Environmental Health* 41: 326-332.

Halstead, W. J. 1986. Use of Fly Ash in Concrete. National Highway Research Program Synthesis of Highway Practice #127. Washington, DC: Transportation Research Board.

Haverkamp, R. and Vauclin, M., 1979. A note on estimating finite difference interblock hydraulic conductivity values for transient unsaturated flow problems. *Water Resources Research*, 15 (1), 181-187.

Haynes, R. J., (2009). Reclamation and revegetation of fly ash disposal sites – Challenges and research needs. *Journal of Environmental Management*, Vol 90, 43–53.

Hazell, J. R. T., Cratchley, C. R. and Preston, A. M., (1988). The location of aquifers in crystalline rocks and alluvium in Northern Nigeria using combined electromagnetic and resistivity techniques. *Quarterly Journal of Engineering Geology*, Vol. 21, 159-175.

Hazell, J. R. T., Cratchley, C. R. and Jones, C. R. C., (1992). The hydrogeology of Crystalline Aquifers in Northern Nigeria and Geophysical Techniques used in their Exploration. In: E. P. Wight and W. G. Marin, L.E., Steinich, B., Jaglowski, D. and Barcelona, M.J. 1998. *Hydrogeologic Site Characterization Using Azimuthal Resistivity Surveys*, p. 179.

He, F., and Qin, D. (2006). China’s Energy Strategy in the Twenty-First Century. *China and World Economy*, Vol. 14, 93-104.

Hillel, D., (1998). *Environmental Soil Physics*. Academic Press, San Diego, CA, p.771.

Hodgson, F.I.D and Krantz, R.M. (1998a). Investigation into groundwater quality deterioration in the olifants river catchment above the Loskop Dam with specialized investigation in the Witbank dam sub-catchment. WRC Report No. 291/1/98. Water Research Commission, Pretoria.

Hodgson, F., (1998b). *Groundwater Quality and Pollution Plume Modelling at Duvha Power Station*. Unpublished Report.



Hornung, U. and Messing, W., 1983. Truncation errors in the numerical solution of horizontal diffusion in saturated/unsaturated media. *Advanced Water Resources*, 6, 165-168.

Hulett L. D. and Weinberger, A. J. 1980. Some etching studies of the microstructure and composition of large aluminosilicate particles in fly ash from coal-burning power plants. *American Chemical Society*, Vol. 14, 965-970.

Iyer, R. 2002. The surface chemistry of leaching coal fly ash. *Journal of Hazardous Materials*.

B93: 321–329. Johnson T. M., Keros C., and R. M.Schuller, (1976). Monitoring leachate migration in the vicinity of a sanitary landfill. *Groundwater monitoring and remediation Journal*, Vol.1 (3), 55-63.

Joshi, R.C. and R.P. Lohtia. (1997). *Fly Ash in Concrete: Production Properties and Uses*. Gordon and Breach Science Publishers: Amsterdam.

Joshi R. C., Langan B. W., and M. A. Ward (1990). Strength and Durability of Concrete Containing 50 percent Portland Cement Replacement by Fly Ash and Other Materials, *Canadian Journal of Civil Engineering*, Vol. 17, 19-27.

Kean W.F., Walter M.J. and Layson H.R. (1987), Monitoring moisture migration in the vadose zone with resistivity. *Groundwater*, Vol. 25, 562–571.

Kearey, P., Brooks, M., Hill, I., 2002. *An introduction to geophysical exploration*. Blackwell Science.

Kemna A., J. Vanderborght, B. Kulesa and Vereecken H. (2002), Imaging and characterisation of subsurface solute transport using electrical resistivity tomography (ERT) and equivalent transport models, *Journal of Hydrology*. Vol. 267, 125–146.

Keller, G.V. and Frischknecht, F.C., (1966). *Electrical Methods in Geophysical Prospecting*. Pergamon, Oxford University Press.

Kelly, W. E. and Asce A. M., (1997). Resistivity methods and flow around landfills. *Proceedings of the conference on geotechnical practice for disposal of solid waste materials*, June 13-15. Michigan , USA, 744-755.

King, G.M. (2003). *An Explanation of the 1:500 000 General Hydrogeological Map: Vryheid 2730*. Department of Water Affairs and Forestry, Pretoria.

Kirby, C.S. and Rimstidt, J. D., (1994). Interaction of municipal solid waste ash with water, *Environmental Science Technology*, Vol. 28 443 – 451.

Klass, L.D. (2003). A Critical Assessment of Renewable Energy Usage in the USA. Energy Policy, Vol.31, 353-367.

Kobr M. and Linhart , I., (1994). Geophysical survey as a basis for regeneration of waste dump Halde 10, Zwickau, Saxony. Journal of applied geophysics. Journal of Applied Geophysics, Vol. 54, 107-116.

Kruger R. A. and Krueger E., (2005). Historical development of coal ash in South Africa. Ash Resources (research paper).

Lam L., Y.L. Wong and C.S. Poon, (1998). Effect of fly ash and silica fume on compressive and fracture behaviors of concrete, Cem-Concr Res., Vol. 28, 271–283.

Lasher, C., J. M. Nel, Y. Xu, A. October, L. Dlamini and Reynolds, K., (2009). The use of Geophysics to determine salt capturing and fluid transport properties of ash dumps. Proceedings of the World of Coal Ash Conference. Lexington USA.

Ledesma, R. and L.L. Isaacs., (1990). "Thermal properties of coal ashes," Fly Ash and Coal Conversion By-Products: Characterization, Utilization and Disposal VI. Robert L. Day and Fredrik P. Glasser, eds., Materials Research Society: Pittsburgh, Pennsylvania.

Leij, F. J., Skaggs T. H., and van Genuchten M. T., 1991. Analytical solutions for solute transport in three-dimensional semi-infinite porous media, Water Resources. Res., Vol. 27(10), 2719-2733.

Lile , O. B., Morris, M., and Ronning J.S., 1997. Estimating groundwater flow velocity from flow changes in contact resistance during a salt water tracer experiment. Journal of Applied Geophysics, Vol. 38, 105-114.

Lohtia R. P., Joshi, R. C. (1995). Mineral admixtures. In Concrete Admixtures Handbook- Properties, Science, and Technology, edn 2. Edited by Ramachandran VS. Park Ridge, N J: Noyes Publications; 657- 739. London.

Loke M.H., (2000a). Electrical Imaging Surveys for Environmental and Engineering Studies. A Practical Guide to 2D and 3D Surveys. [www.heritagegeophysics.com/images/lokenotepdf](http://www.heritagegeophysics.com/images/lokenotepdf).

Loke M.H., (2000b). Rapid 2-D Resistivity & IP inversion using the least squares method. Geo-electrical Imaging 2D & 3D GEOTOMO SOFTWARE practical manual, [www.geoelectrical.com](http://www.geoelectrical.com).

Loke M.H. and Barker R.D., (1996a). Rapid least-squares inversion of apparent resistivity pseudosections using quasi-Newton method. Geophysics Prospectus, Vol. 44, 131-152.

Loke M.H. and Barker R.D., (1996b). Practical techniques for 3D resistivity surveys and data inversion. *Geophysics Prospectus*, Vol. 44, 499–523.

Loke MH, Barker RD (1995) Improvements to the Zohby method for the inversion of resistivity sounding and pseudosection data. *Computing Geosciences*, Vol. 21(2), 321–332.

Macfarlane, D .S. Cherry, J.A., Gillham, R.W. & Sudicky E.A., (1983) Migration of contaminants in groundwater at a landfill: a case study. 1. Groundwater flow and plume delineation. *Journal of Hydrology*, Vol. 63, 1-29.

Malin H. E. Olin and Chester S., (1992). Evaluation of Geological and Recharge Parameters for an Aquifer in Southern Sweden Chalmers Univ. of Technology and Goteborg Univ., Goteborg, Sweden *Nordic Hydrology*, Vol. 23, 305-314.  
<http://www.iwaponline.com/nh/023/0305/0230305.pdf>

Marescot, L., R. Monnet, and D. Chapellier, 2009. Resistivity and induced polarization surveys for slope instability studies in the Swiss Alps. *Engineering Geology*, Vol. 98,18-28.

Mattigod, S. V., Dhanpat, R., Eary, L. E., Ainsworth, C. C. (1990a). Geochemical factors combustion residues: I. Review of the major elements. *Journal of Environmental Quality*, Vol.19, 188–201.

Mattigod, S. V., Rai, D., Eary, L. E. and Ainsworth, C. C., (1990b). 'Geochemical factors controlling the mobilization of inorganic constituents from fossil fuel combustion residues: 1. Review of the major elements', *Journal of Environmental Quality*, Vol. 19, 188–201.

Mattuck, R. and Nikolaidis, N.P., (1996). Chromium mobility in freshwater wetlands, *Journal of Contaminant Hydrology*, 23, 213-232.

Mazac, O., Kelly, W.E., and Landa., I., (1987). Surface geo-electrics for groundwater pollution and protection studies. *Journal of Hydrology*, Vol. 93., 277-294.

McCarter, W.J., 1984. The electrical resistivity characteristics of compacted clays. *Geotechnique*, Vol. 34, 263–267.

Meju M. A., (2000) Geoelectrical characterization of covered landfill sites: a process-oriented model and investigative approach. *Applied Geophysics*, Volume 44, 115-150.

Mendoza, C. A., Therrien R., and Sudicky E. A., (1991). *ORTHOFEM User`s Guide*, Version 1.02. Waterloo Centre for Groundwater Research, University of Waterloo, Waterloo, Ontario, Canada.

Menghistu, M. T., (2010). Development of a numerical model for unsaturated/saturated hydraulics in Ash/Brine systems. Unpublished PhD Thesis, University of Free State, South Africa.

Metts, B.S., K.A. Buhlmann, D.E. Scott, T.D. Tuberville, W.A. Hopkins. 2012. Interactive effects of maternal and environmental exposure to coal combustion wastes decrease survival of larval southern toads (*Bufo terrestris*). *Environmental Pollution* 164: 211-218.

Meyer, P.S., (2003). An explanation of the 1:500 000 general hydrogeological map: Bloemfontein 2924. Department of Water Affairs and Forestry, Pretoria.

Meyer de Stadelhofen, C., (1991). Application de la géophysique aux recherches d'eau. Ed. Lavoisier, Paris.

Michot, D., Benderitter, Y., Dorigny, A., Nicoulaud, B., King, D., Tabbagh, A., 2003. Spatial and temporal monitoring of soil water content with an irrigated corn crop cover using electrical resistivity tomography. *Water Resour. Res.* Vol. 39, 1138.

Mills, W.B., Loh, J. Y., Bate M.C., Johnson, K.M., (1999). Evaluation of potential risks from ash disposal site leachate. *Journal of Environment Engineering* 125, 306-313.

Moreau, S., Bouye, J. M., Barina, G. and Oberty, O., (2003). Electrical resistivity survey to investigate the influence of leachate recirculation in a MSW landfill. In: E. S. E. Centre (Editor), Ninth International Waste Management and landfill Symposium, Calgliari, Italy.

Mualem, Y. (1976). A new model for predicting the hydraulic conductivity of unsaturated porous media, *Water Resour. Res.*, Vol. 12(3), 513-522.

Muchingami, I, Nel J., Xu, Y., Steyl, G., and K Reynolds, (2013). On the use of electrical resistivity methods in monitoring infiltration of salt fluxes in dry coal ash dumps in Mpumalanga, South Africa. *Water SA*, Vol 39 (3), pp 491-498.

Muchingami, I., Nel J., Steyl G. and Reynolds K., (2011). Using electrical resistivity tomography in monitoring brine infiltration at a dry coal ash dump. Proceedings of the Biannual International Groundwater Conference, 18-22 September, Pretoria, South Africa.

Mudd G. M., (2002). Solute transport modelling of Latrobe valley ash disposal sites. Unpublished PhD thesis. School of the Built Environment Faculty of Engineering & Science Victoria University.

Mukhtar A. L., W. N. Sulaiman, S. Ibrahim, P. A. Latif and M.M. Hanaf,(2000). Detection of groundwater pollution using resistivity imaging at Seri Petaling landfill, Malaysia *Journal of environmental hydrology*, Vol 8, paper 3.

Nathan, Y., Dvorachek, M., Pelly, I., and Mimran, U., (1999). Characterization of coal fly ash from Israel. *Fuel*, Vol 78, 205–213.

Nel, J.M., K. Reynolds and Xu Y., (2009). Comparison between geohydrological properties of wet and dry ash dump disposal sites. *Proceedings of the World of Coal Ash Conference*. Lexington USA.

Nel, J.M., Lasher, C., October, A., Dlamini, L. and Nel, M. (2007). *Integrated Hydraulics Report for Tutuka and Secunda: Contribution to SASOL ESKOM collaborative Project: Towards the Development of Sustainable Salt Sinks: Fundamental Studies on the Co-Disposal of Brines within Inland Ash Dams and Dumps*. Unpublished ESKOM Internal Report.

Nel J. M., M. de Klerk, K. Reynolds, L. Petric, Y. Xu, and Batelaan, (2007). The use of electrical resistivity to map water flow paths through ash dumps and the underlying fractured aquifer in Mpumalanga, South Africa. *Conference paper. 2007 World of Coal Ash Conference*.

Neuman, S. P. (1975), Galerkin approach to saturated-unsaturated flow in porous media, Chapter 10 in 225 *Finite Elements in Fluids*, Vol. I, Viscous Flow and Hydrodynamics, edited by R. H. Gallagher, J. T. Oden, C. Taylor, and O.C. Zienkiewicz, John Wiley & Sons, London, pp. 201-217,.

Neuman, S. P., Feddes R. A., and Bresler E., (1974). Finite element simulation of flow in saturated-unsaturated soils considering water uptake by plants, *Third Annual Report, Project No. A10-SWC-77, Hydraulic Engineering Lab., Technion, Haifa, Israel*.

Neuman, S. P., (1973). Saturated-unsaturated seepage by finite elements, *J. Hydraul. Div., ASCE*, 99 (HY12), 2233-2250.

Neuman, S. P., (1972). Finite element computer programs for flow in saturated unsaturated porous media, *Second Annual Report, Project No. A10-SWC-77, Hydraulic Engineering Lab., Technion, Haifa, Israel*.

Nielsen, D.M. (1991), *Practical handbook of ground-water monitoring*, Lewis, Chelsea, MI.

Nikolaidis N. P. and Shen H. (2000). *Conceptual site model for evaluating contaminant mobility and pump-and-treat remediation* conceptual site model for evaluating contaminant mobility and pump-and-treat remediation.

Nobes C., (1996). *Troubled water: environmental applications of electrical and electromagnetic methods*. *Surveys in geophysics* Vol 363-454.

October G. A., (2010). Development of a conceptual model for ash dump system using hydraulic and tracer test techniques, Unpublished Master's thesis, Department of Earth Sciences, University of the Western Cape , Cape Town , South Africa.

Olayinka, A.I. and Yaramanci, U., 2000, Use of block inversion in the 2-D interpretation of apparent resistivity data and its comparison with smooth inversion: Journal of Applied Geophysics, 45, 63-82.

Olayinka, A. and Barker, R., (1990). Borehole Siting in Crystalline Basement Areas of Nigeria with a Microprocessor Controlled Resistivity Traversing System. Groundwater, vol. 28, pp. 178-183.

Osiensky J. L., and P. R. Donaldson, (1995). Electrical flow through an aquifer for contaminant source leak detection and delineation of plume evolution. Journal of Hydrology, Vol. 169, 243-263.

Page, A. L., Elseewi, A. A., and Straughan, I. R., (1979). Physical and chemical properties of fly ash from coal-fired power plants with special reference to environmental impacts. Residue Rev., Vol. 71, 83-120.

Pares J.M., Querol X., Plana F., Fernandez-Turiel J.L., Lopez A, (1993). Fly ash content and distribution in lake sediments around a large power station: inferences from magnetic susceptibility analysis. Environ Geochem Health; Vol. 15(4), 9–18.

Park, S.K. and Van, G.P. 1991. Inversion of pole-pole data for 3-D resistivity structures beneath arrays of electrodes. Geophysics, Vol. 56, 951-960.

Petersen R.C., Wagener, Hemphill –Haley, M. A., Weller, L. N., Kilburg R, and Champlin J. B. F., (1987). Resistivity mapping of a complex aquifer system at a hazardous waste site in the Salinas Walley, California. Proceedings of the Geophysical methods and groundwater instrumentation conference, October 15-17, Denver USA, 187-202.

Petrik, L., Hendricks, N., Ellendt, N. and Burgers, C., ( 2007). Toxic element removal from water using Zeolite adsorbents made from solid waste residues. Water Research Commission, WRCReport No. 1546/1/07, University of the Western Cape, South Africa.

Petrik, L., White, R., Klink, M., Somerset, V., Key, D., Iwuoha, E., Burgers, C., Fey, M.V., (2005). Utilization of fly ash for Acid Mine Drainage remediation. WRC Report No. 1242/1/05

Petrik, L.F., White, R.A., Klink, M.J, Somerset, S.V., Burgers, L.C. and Fey, V.M., (2003). Utilization of South African fly ash to treat acid coal mine drainage, and

production of high quality zeolites from the residual solids. International Ash Utilization Symposium, Lexington, Kentucky, USA.

Philip, J. R., (1985). Approximate analysis of the borehole permeameter in unsaturated soil, *Water Resour. Res.*, Vol. 21, 1025-1034.

Philip, J. R. 1969. Absorption and infiltration in two- and three-dimensional systems. Pages 503–525 in R. E. Rijtema and H. Wassink, eds. *Water in the unsaturated zone*. 1966, Vol. 1. Proceedings of ASH/UNESCO Symposium, Wageningen, The Netherlands.

Philip, J. R., and de Vries D. A., (1957). Moisture movement in porous media under temperature gradients, *Eos Trans. AGU*, Vol. 38(2), 222-232.

Porsani L, Filho W.M, Ellis V.R, Shimlis J.D, and Moura H.P (2004). The use of GRR & VES in delineating a contamination plume in a landfill site; A case study in SE Brazil. *Journal of Applied Geophysics*. Vol. 55, 199 – 209.

Praharaj T, Powell MA, Hart BR, Tripathi S., (2002a). Leachability of elements from sub-bituminous coal fly ash from India. *Environment International*, Vol. 27(8), 609–615.

Praharaj, T., Swain, S.P., Powell, M.A., Hart, B.R., Tripathy, S., (2002b). Delineation of groundwater contamination around an ash pond. Geochemical and GIS approach. *Environment International*, Vol. 27, 631-638.

Prasad, B., Banerjee, N. N., and Dhar, B. B., (1996). Environmental assessment of coal ash disposal: a review. *Journal of Sci Ind Res India*, Vol. 55, 772–780.

Raghavendra S. C., S. Khasim, M. Revanasiddappa, M. V. N. Ambika, and A. B. Kulkarni (2003). Synthesis, characterization and low frequency a.c. conduction of polyaniline/fly ash composites. *Bulletin of Material Sciences*, Vol. 26 (7), 733–739.

Reynolds, W. D., Elrick, D. E. and Clothier, B. E., (1985). The constant head well permeameter: Effect of unsaturated flow. *Soil Science*, Vol. 139, 172–180.

Reynolds, W. D., Elrick, D. E. and Topp, G. C., (1983). A re-examination of the constant head well permeameter method for measuring saturated hydraulic conductivity above the water table. *Soil Science*, Vol. 136, 250–268.

Richards, L. A. (1931). Capillary conduction of liquids in porous mediums. *Physics*. 1, 318–333.

Rubin Y.; 2003: Applied stochastic hydrogeology. Oxford University Press, New York, p.391.

Robin E. N., (2002). Direct current and self-potential monitoring of an evolving plume in partially saturated fractured rock. *Journal of Hydrology*, Vol. 267, 258-272.

Robinson, H. D. and Lucas, J. L., (1985). Leachate attenuation in the unsaturated zone beneath landfills: instrumentation and monitoring of a site in southern England. *Water Science Technology*, Vol. 17, 477-492.

Rodgers, R. B. and Kean W. F., (1980). Monitoring groundwater contamination at a fly ash disposal site using surface electrical resistivity methods: *Groundwater*, Vol. 18, 472-478.

Rosqvist, H. Dahlin, T., and Lenhe, C., (2005). Investigation of water flow in a bioractor landfill using geoelectrical imaging techniques. In E. S. E. Centre (Editor), 10<sup>th</sup> International Waste Management and landfill Symposium, Cagliari, Italy.

Rushton, K.R., (2003). *Groundwater Hydrology Conceptual and Computational Models*, Chichester: John Wiley & Sons Inc.

Sasaki, Y. 1992. Resolution of resistivity tomography inferred from numerical simulation. *Geophysical Prospecting*, Vol. 40, 453-464.

Sauck, W.A., and Zabik, S.M., (1992). Geophysics for Glacial/Unconsolidated Deposits Azimuthal Resistivity Techniques and the Directional Variations of Hydraulic Conductivity in Glacial Sediments, Symposium on the Application of Geophysics to Environmental and Engineering Problems.

Schaap, M.G., Leij, F.J. and van Genuchten, M.T., (2001). Rosetta: A computer program for estimating soil hydraulic parameters with hierarchical pedotransfer functions. *Journal of Hydrology*, Vol. 251, 163–176.

Scheetz, B. E. and Earle, R., (1998). Utilisation of fly ash. *Current Opinion in Solid State and Material Science*, Vol. 3, 510-520.

Šejna, M., Šimůnek J., and van Genuchten M. T., (2011). The HYDRUS Software Package for Simulating Two- and Three-Dimensional Movement of Water, Heat, and Multiple Solutes in Variably-Saturated Media, User Manual, Version 1.0, PC Progress, Prague, Czech Republic.

Šimůnek, J., Van Genuchten M. T., and Šejna M., (2011). The HYDRUS Software Package for Simulating Two- and Three Dimensional Movement of Water, Heat, and Multiple Solutes in Variably-Saturated Media, Version 2.0. Technical Manual, PC Progress, Prague, Czech Republic.

Šimůnek, J., M. Sejna, and van Genuchten. M.T., (1999). The HYDRUS-2D software for simulating the two-dimensional movement of water, heat, and multiple solutes in



variably-saturated media. 251 p. International Groundwater Modeling Center, Colorado School of Mines, Golden, Colorado, USA.

Šimůnek, J., M. Šejna, and M. Th. van Genuchten, (1996a). The HYDRUS-2D software package for simulating water flow and solute transport in two-dimensional variably saturated media. Version 1.0, IGWMC - TPS - 53, International Groundwater Modeling Center, Colorado School of Mines, Golden, Colorado, 167pp.

Šimůnek, J., and M. Th. van Genuchten, (1996b). Estimating unsaturated soil hydraulic properties from tension disc infiltrometer data by numerical inversion, *Water Resour. Res.*, Vol 32(9), 2683-2696.

Šimůnek, J., and van Genuchten M. T., (1995) Numerical model for simulating multiple solute transport in variably-saturated soils, *Proc. "Water Pollution III: Modelling, Measurement, and Prediction*, Ed. L. C. Wrobel and P. Latinopoulos, Computation Mechanics Publication, Ashurst Lodge, Ashurst, Southampton, UK, p. 21-30,.

Šimůnek, J., T. Vogel and van Genuchten M. T. (1994). The SWMS\_2D code for simulating water flow and solute transport in two-dimensional variably saturated media, Version 1.1, Research Report No. 132, U. S. Salinity Laboratory, USDA, ARS, Riverside, California.

Šimůnek, J., and Suarez D. L., (1993). Modeling of carbon dioxide transport and production in soil: 1. Model development, *Water Resour. Res.*, Vol. 29(2), 487-497.

Sinha, K.S and Basu, K., (1998). Mounting fly ash problems in growing coal based power stations – few pragmatic approaches towards a solution. In: Verma, C.V.J., Lal, P.K., Kumar, V., Lal, R., Krishnamurthy, R. (Eds.), *Proceedings of the International Conference on Fly ash Disposal and Utilization*, Vol.1. Central Board of Irrigation and Power, New Delhi, India, 15-27.

Sivakumar D.S., and Datta M., (1996). Assessment of groundwater contamination potential around ash ponds through field sampling: a review. In: Raju VS, editor. *Ash ponds and ash disposal systems*. New Delhi: Narosa Publishing House, 311–325.

Slater, L. (2007). Near surface electrical characterization of hydraulic conductivity: From petro-physical properties to aquifer geometries—A review, *Surveys in Geophysics*, Vol. 28, 169–197.

Slater L., A. Binley and D. Brown, (1997) Electrical imaging of fractures using ground-water salinity change, *Groundwater* Volume 35, 436–442.

Smith, L.A., Means, J.L., Chen, A., Alleman, B., Chapman, C.C., Tixier, J.S., Jr., Brauning, S.E., Gavaskar, A.R., and Royer, M.D. (1995). Remedial Options for Metals Contaminated Sites, Lewis Publishers, Boca Raton, FL.

South African Weather Services ([www.weathersa.co.za](http://www.weathersa.co.za)).

Spears, D. A., Lee, S. (2004). Geochemistry of leachates from coal ash. In: Gieré R, Stille P, editors. Energy, waste and the environment: a geochemical perspective. Geological Society of London, Special Publications, Vol. 236, 619–639.

Spears, D. A., (2000). Role of clay minerals in UK coal combustion. Applied Clay Science, Vol.16, 87–95.

Splajt T, Ferrier G, and Frostick L. E., (2003). Application of ground penetrating radar in mapping and monitoring landfill sites. Journal of Environmental Geology, Vol. 44, 963–967.

Steenari, B. M., Schelander, S., O. and Lindqvist, O., (1999a). Chemical and leaching characteristics of ash from combustion of coal, peat and wood in a 12 MW CFB – a comparative study. Fuel, Vol. 78, 249-258.

Steenari, B.-M., Karlsson, L. G., Lindqvist, O., (1999b). Evaluation of the leaching characteristics of wood ash and the influence of ash agglomeration. Biomass and Bioenergy, Vol.16, 119-136.

Steyl, G., Nel J.M., Dustay S., Muchingami I., October A., Dlamini L., Gomo M., Teboho S., and Leketa K., (2010). Deliverable 2: Tutuka Field Report ESKOM-SASOL PHASE II Sustainable Salt Sinks. Unpublished Eskom internal report.

Steyl, G., Nel J.M., Muchingami I., Dustay S., October A., Dlamini L., Gomo M., Teboho S., and Leketa K., (2010b). Deliverable 4: Link to Electrical Resistivity Data at Tutuka and Secunda. Unpublished ESKOM-SASOL PHASE II Sustainable Salt Sinks report.

Steyl, G., Nel J.M., Muchingami I., Dustay S., October A., Dlamini L., Gomo M., Teboho S., and Leketa K., (2010c). Deliverable 6: Tutuka field experiments linked to saturated and unsaturated hydraulic conductivity. Unpublished ESKOM-SASOL PHASE II Sustainable Salt Sinks report.

Tarantola A., (1984). Inversion of seismic reflection data in the acoustic approximation Geophysics 49 1259-66 - 1987 hwm Problem Theory (New York Elsevier Sharma P.V., (1997). Environmental and Engineering geophysics. Cambridge University Press, UK.

Tsadilas, C., Tsantilas, E., Stramatiadis, S., Antoniadis, V., Samaras, V., (2006). Influence of fly ash application on heavy metal forms and their availability. In: Presad,

M.N.V., Sajwan, K.S and Naidu, R, Editors, "Trace Elements in the Environment, Biotechnology and Bioremediation", CRC Press, Boca Raton, 63-75.

Telford W.M., Geldart L.P. and Sheriff R.E., (1990). Applied Geophysics. 2<sup>nd</sup> Edition Cambridge University Press, UK.

Tiab, D. and Donaldson, E.C. (1996). Petrophysics: Theory and practice of measuring reservoir rock and fluid transport properties, Gulf Publishing Company, Houston, Texas.

Theis, T. L., Richter, R. O. (1979). Chemical Speciation of Heavy Metals in Power Plant Ash Pond Leachate. Environ. Science and Tech., Vol.13: 219-224.

Theis, T.L and Gardener, K.H., (1990). Environmental assessment of ash disposal. Critical Review on Environmental Control 20: 21-42.

Townsend, W. N. and D. R. Hodgson, (1973). Edaphological problems associated with deposits of pulverized fuel ash. In R. J. Hutnik and G. Davis (ed.) Ecology and reclamation of devastated land, Gordon and Breach, New York, Vol.1, 45-56.

U.S. Environmental Protection Agency (U.S. EPA), (2000). "Regulatory determination for wastes from the combustion of fossil fuels." EPA 530-F-025, Washington, D.C.

U.S. Environmental Protection Agency (U.S. EPA), (2003a). "Emissions data & compliance reports." Clean Air Markets-Progress and Results. Washington, D.C: <<http://www.epa.gov/airmarkets/emissions/index.html>>.

Van Genuchten, M. T., (1980). A Closed-form equation for predicting the hydraulic conductivity of unsaturated Soils. Journal of the American Society of Soil Science. Vol. 44, 892–898.

Van Genuchten, M. T., (1978). Mass transport in saturated-unsaturated media: one-dimensional solutions, Research Rep. No. 78-WR-11, Water Resources Program, Princeton Univ., Princeton, New Jersey.

Van Niekerk L.J. and S. Staats (2010). Tutuka Power Station ash stack pollution plume model final report. Unpublished Eskom report.

Van Overmeeren R.A., (1989). Aquifer boundaries explored by geo-electrical measurements in the coastal plain of Yemen: a case of equivalence. Geophysics, Vol. 54 (1), 38-48.

Vassileva, C. G., and Vassilev, S. V. (2006). Behaviour of inorganic matter during heating of Bulgarian coals 2. Sub bituminous and bituminous coals Fuel Processing Technology, Vol. 87, 1095–1116.

Vassileva, G. G., and Vassilev, S. V. (2005). Behaviour of inorganic matter during heating of Bulgarian coals 1. Lignites. *Fuel Processing Technology*. Vol. 86, 1297-1333.

Vidya, S.B and Snigdha S., 2006. Analysis of fly ash heavy metal content and disposal in three thermal power plants in India, *Fuel*, Vol. 85, 2676-2679.

Vilches, L.F., Otal E., Moreno N., Querol X., Vale J. and Fernández-Pereira C., (2005). Application of zeolitised coal fly ashes to the depuration of liquid wastes, *Fue Journal I*, Vol. 84 (11), 1440–1446.

Wan, X., Wang, W., Ye, T., Guo, Y., and Gao, X., (2006). A study on the chemical and mineralogical characterization of MSWI fly ash using a sequential extraction procedure *Journal of Hazardous Materials*, Vol. B134: 197–201.

White P. A., (1988). Measurement of groundwater parameters using salt-water injection and surface resistivity. *Groundwater*, Vol. 26(2), 192-201.

Whitely, R. J. and Jewel C., (1992). Geophysical techniques in contaminated land assessment- Do they deliver? *Exploration Geophysics*, Vol. 23, 557-565.

Whitfield, C. J. (2003). The production, disposal, and beneficial use of coal combustion products in Florida. Unpublished Master's thesis.

Willis, J. P. (1987). Variations in the composition of South African fly ash. Council for Science and Industrial Research, Vol. 3, 2-6.

Winter T.C., Harvey J.W. , Franke O.L. and W.M. Alley (1998). *Groundwater and Surface Water A Single Resource*, USGS Report.

Ramsar Convention Secretariat, 2010. Managing groundwater: Guidelines for the management of groundwater to maintain wetland ecological character. Ramsar handbooks for the wise use of wetlands, 4<sup>th</sup> edition, Vol. 11. Ramsar Convention Secretariat, Gland, Switzerland.

Woodford, A.C. and Chevallier, L., (2002). Regional characterization and mapping of Karoo fractured aquifer systems - An integrated approach using a geographical information system and digital image processing. WRC Report 653/1/02. Water Research Commission. Pretoria, South Africa.

Wu, Y.S., and Pruess, K., (2000). Numerical simulation of non-isothermal multiphase tracer transport in heterogeneous fractured porous media. *Advances in Water Resources*, Vol. 23, 699-723.

Wurmstich, B. and Morgan, F. D., (1994). Similarities in modeling groundwater flow and DC resistivity: Annual Meeting Abstracts, Society Of Exploration Geophysicists, 578-579.

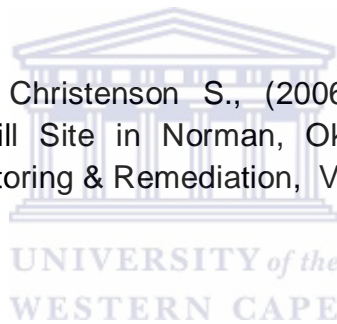
Yan, J., and Neretnieks, I., (1995). Is the glass phase dissolution rate always a limiting factor in the leaching processes of combustion residues? The Science of the Total Environment, Vol.172, 95-118.

Yang, C. and Lee, W., (1998). Using resistivity sounding and geostatistics to aid in hydrogeological studies in the Choshuichi alluvial fan, Taiwan: Annual Meeting Abstracts, Society Of Exploration Geophysicists, 832-835.

Yang, C., Tong, L. and Jeng, L., (1994). Locating groundwater at selected sites by geoelectric methods: Annual Meeting Abstracts, Society of Exploration Geophysicists, 652-654.

Zienkiewicz, O.C., (1977). The Finite Element Method, 3<sup>rd</sup> ed., McGraw-Hill, London, United Kingdom.

Zume J.T., A. Tarhule, and Christenson S., (2006). Subsurface Imaging of an Abandoned Solid Waste Landfill Site in Norman, Oklahoma National Groundwater Association. Groundwater Monitoring & Remediation, Vol. 62, 62–69.



## OUTPUT

**This thesis is based on the following manuscripts and internal reports:**

- ❖ Muchingami, I, Nel J., Xu, Y., Steyl, G., and K Reynolds, (2013). On the use of electrical resistivity methods in monitoring infiltration of salt fluxes in dry coal ash dumps in Mpumalanga, South Africa. *Water SA*, Vol 39 (3), pp 491-498.
- ❖ Muchingami, I., Xu, Y. and Nel, J. M., (2013). A numerical simulation of contaminant transport in the unsaturated zone of dry coal ash dumps with a case study in South Africa. *Proceedings 13<sup>th</sup> Biannual IAH/GSSA International Groundwater Conference, 17-19 September 2013, Durban South Africa*
- ❖ Muchingami I., Nel J., Steyl G. and K. Reynolds (2011). Using electrical resistivity tomography in monitoring brine infiltration at a dry coal ash dump. *Proceedings 12<sup>TH</sup> IAH/GSSA Biannual Groundwater Conference, 19 - 21 September 2011, Pretoria South Africa.*
- ❖ Steyl, G., Nel J.M., Dustay S., Muchingami I., October A., Dlamini L., Gomo M., Teboho S., and Leketa K., (2010). Deliverable 2: Tutuka Field Report ESKOM-SASOL PHASE II Sustainable Salt Sinks. Unpublished Eskom internal report.
- ❖ Steyl, G., Nel J.M., Muchingami I., Dustay S., October A., Dlamini L., Gomo M., Teboho S. , and Leketa K., (2010b). Deliverable 4: Link to Electrical Resistivity Data at Tutuka and Secunda; ESKOM-SASOL PHASE II Sustainable Salt Sinks report. Unpublished Eskom internal report.
- ❖ Steyl, G., Nel J.M.,. Muchingami I., Dustay S., October A., Dlamini L., Gomo M., Teboho S. , and Leketa K., (2010c). Deliverable 6: Tutuka field experiments linked to saturated and unsaturated hydraulic conductivity. ESKOM-SASOL PHASE II Sustainable Salt Sinks report. Unpublished Eskom internal report.

## APPENDICES

### APPENDIX 1A TIME INTERVALS FOR TIME LAPSE INFILTRATION SURVEYS

Site-1 (Schlumberger)

T1 = dry survey (15/03/2010)

Fill drainage trench 12:30 (16/03/2010). 2 m<sup>3</sup> Water EC = 1950mS/m

T2 = 13:00 – 15:00

T3 = 15:30 – 17:30

T4 = 09:30 – 11:30 (17/03/2010)

Fill drainage trench 11:45 (2m<sup>3</sup>)

T5 = 13:40 – 15:40

Site-1(Wenner)

T1 = dry survey (15/03/2010)

Fill drainage trench 12:30 (16/03/2010). 2 m<sup>3</sup> Water EC = 1950mS/m

Fill drainage trench 11:45 (2m<sup>3</sup>)

T2 = 12:35 – 13:40 (17/03/2010)

T3 = 15:45 – 16:45 (17/03/2010)

T4 = 07:00 – 08:00 (18/03/2010)



UNIVERSITY of the  
WESTERN CAPE

Site-2 (X direction, Wenner)

T1 = dry survey (18/03/2010)

Fill drainage pit 10:50 (18/03/2010). 1 m<sup>3</sup> Water EC = 24mS/m.

T2 = 12:50 – 13.20 (18/03/2010)

T3 = 16:00 – 16:30 (18/03/2010)

Site-2 (Y direction, Wenner)

T1 – dry survey (18/03/2010)

Fill drainage pit 10:50 (18/03/2010). 1 m<sup>3</sup> Water EC = 24mS/m.

T2 = 13:25 – 14:00 (18/03/2010)

T3 = 16:30 – 17:00 (18/03/2010)

## APPENDIX 1B

### Interpretation of initial resistivity model results for infiltration Site 1

Meaningful results can only be obtained if the apparent resistivity values themselves are accurate. For this reason the measuring protocols were limited to Schlumberger and Wenner. Figure 8 presents the initial survey results for both the Wenner and Schlumberger arrays.

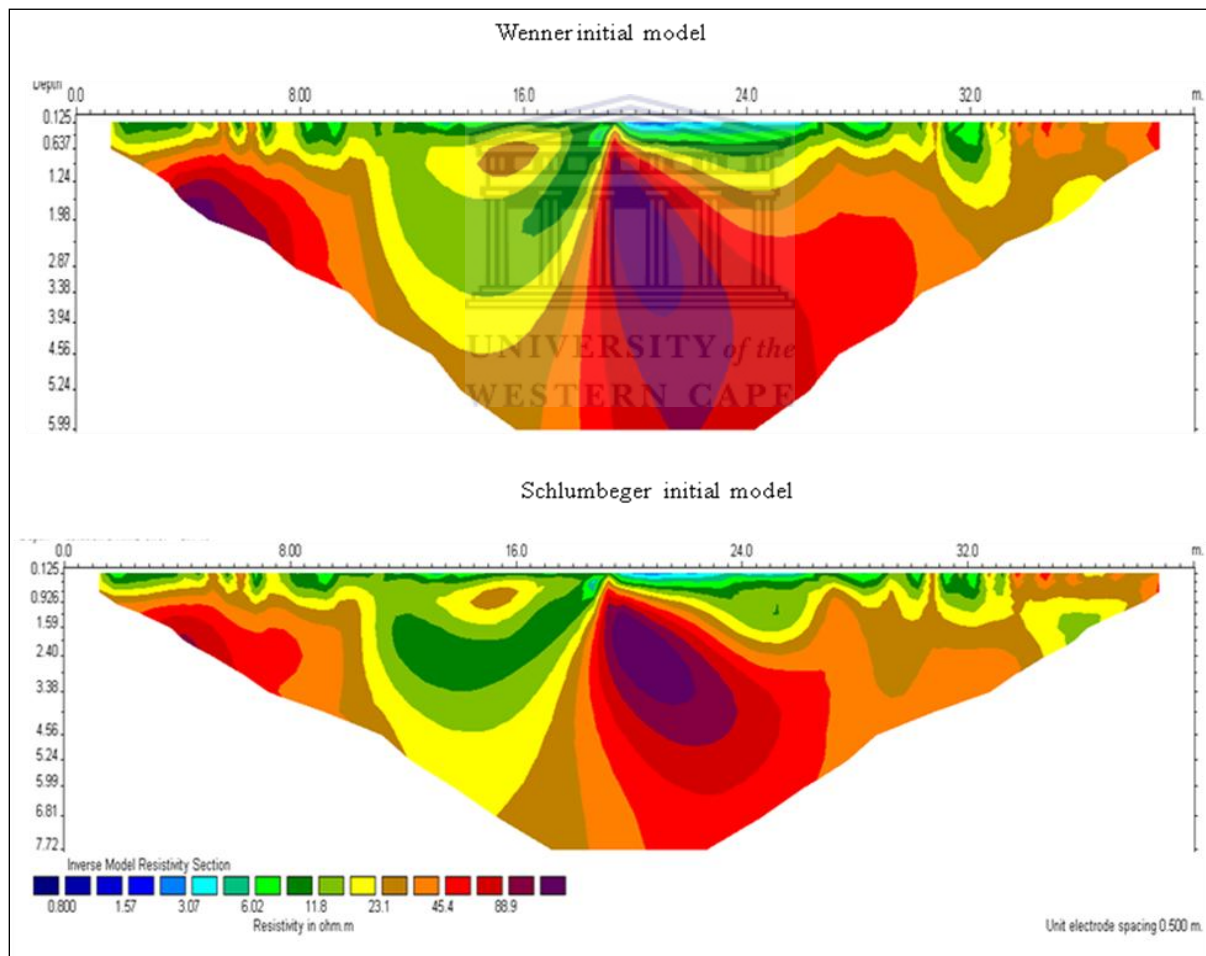
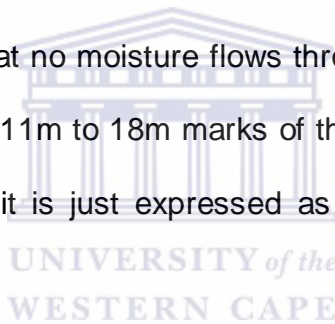


Figure A8. Initial resistivity pseudo sections for (a) the Wenner array and (b) Schlumberger array.



The resistivity distribution is indicative of the initial moisture and salt distribution of the study site, before the start of the survey. The resistivity scale for both pseudo sections is very small (0-120  $\Omega\text{m}$ ) compared to the normal resistivity values used in groundwater investigations (usually 0- over 1000 $\Omega\text{m}$ ), which suggests that the ash medium is generally a conductive medium that is full of salts which acts as electrolytic conductors. Resistivity values for the top 1m of the profile are lower suggesting that the top region is moist and contains a lot of salts entrapped in it.

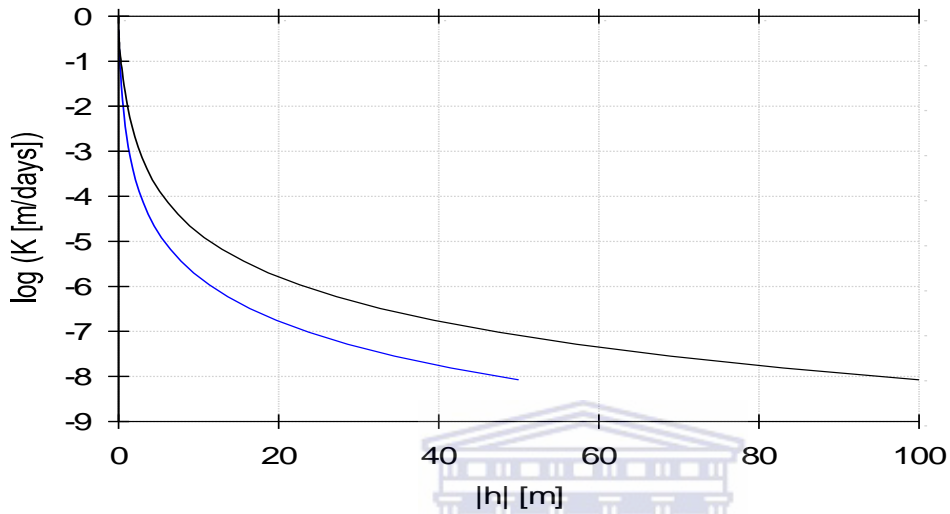
Both the Schulumberger and the Wenner arrays confirm the presence of a high resistivity region in the central section of the profile line. This is interpreted as a dry and with very low porosity such that no moisture flows through it. A low resistivity contrast on the subsurface between the 11m to 18m marks of the profile line is fully observed in the Schulumberger model but it is just expressed as a small vertical section by the Wenner model.



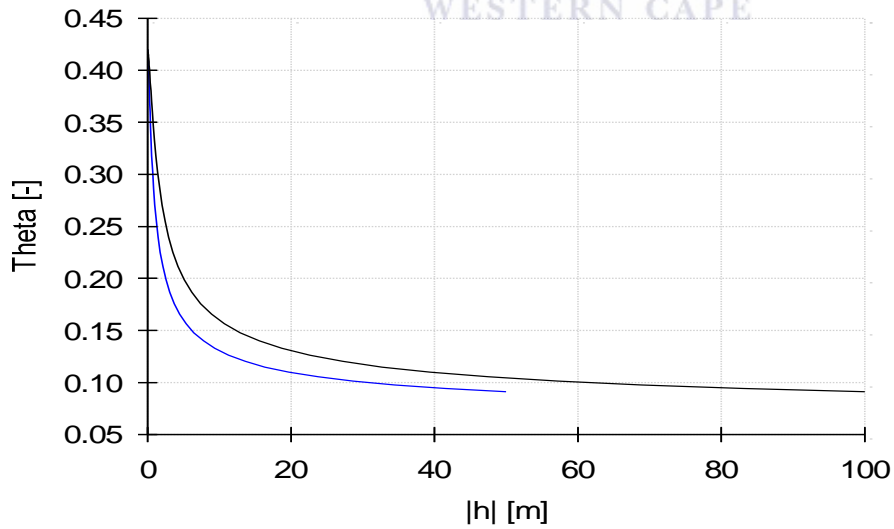
APPENDIX 2A.

VARIATION OF SOME OF THE SOIL HYDRAULIC PROPERTIES DEDUCED FROM HYDRUS2D

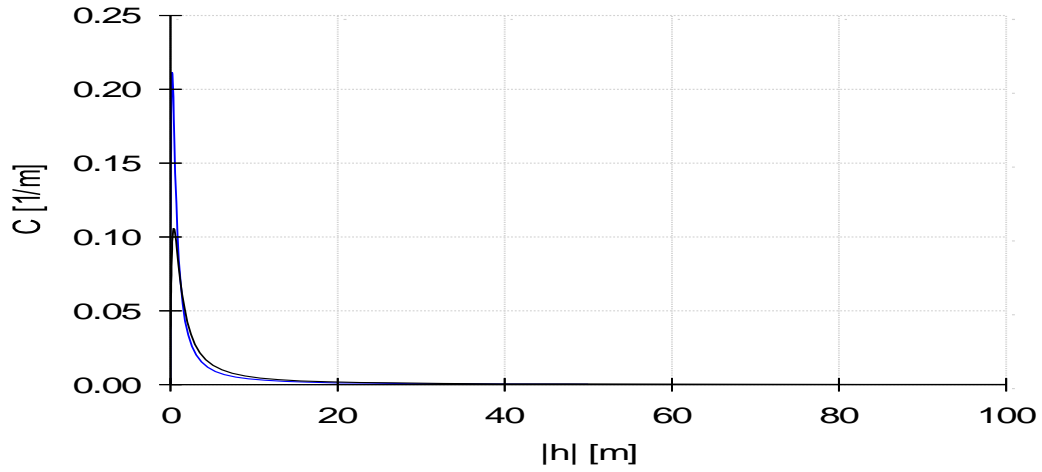
*Hydr. Prop.: log Conductivity vs. Head*



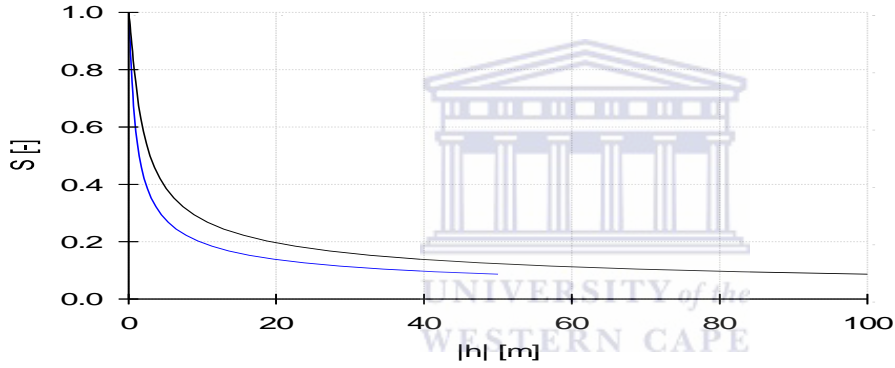
*Hydraulic Properties: Theta vs. Head*



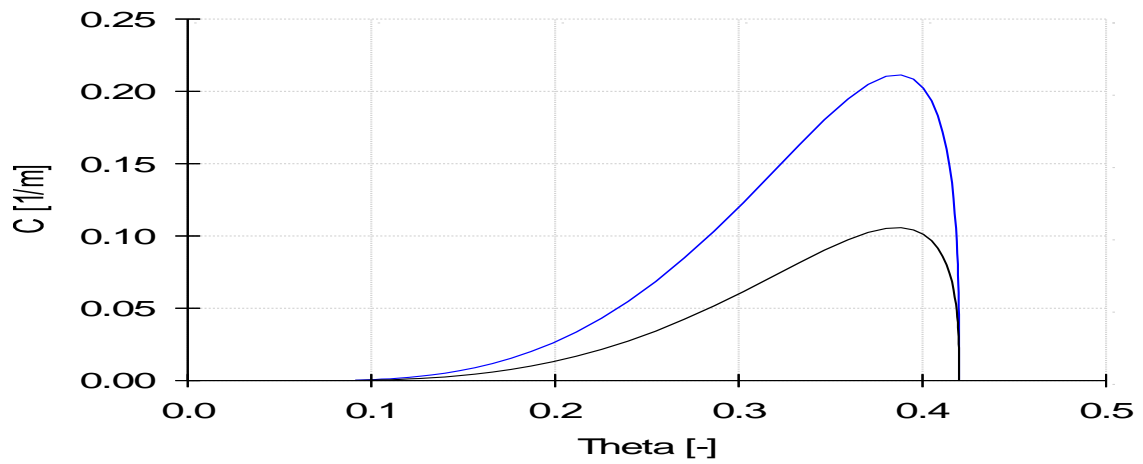
**Hydraulic Properties: Capacity vs. Head**



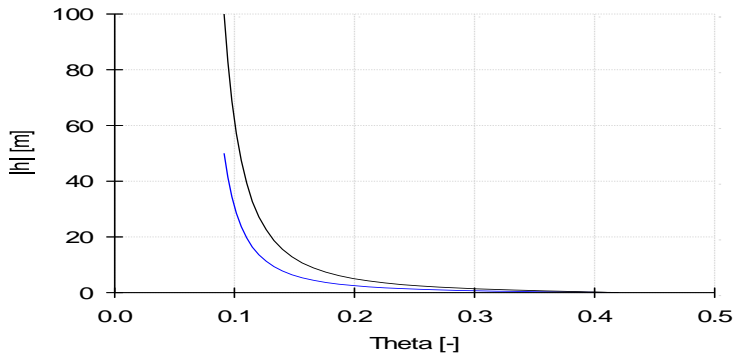
**Hydr. Prop.: Effective W.C. vs. Head**



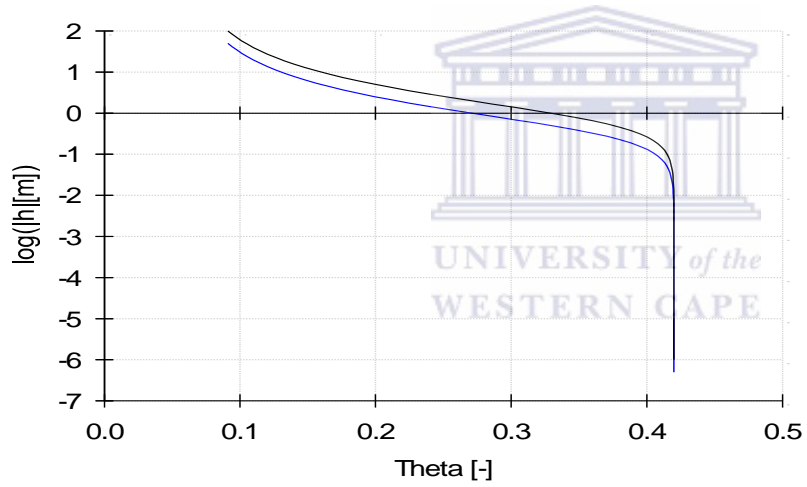
**Hydr. Properties: Capacity vs. Theta**



**Hydraulic Properties: Head vs. Theta**



**Hydraulic Properties: log h vs. Theta**



## APPENDIX 2B

### MASS BALANCE INFORMATION FOR THE HYDRUS2D MODEL

Welcome to HYDRUS

Program HYDRUS2

Date: 11.11. Time: 19:37:15

Time independent boundary conditions

Vertical plane flow,  $V = L \cdot L$

Units: L = m, T = days, M = mmol

-----  
 Time [T] 0.0000000E+00  
 -----

-----  
 Sub-region num.  
 1  
 -----

-----  
 Area [V] 0.45360E+04  
 0.45360E+04  
 Volume [V] 0.88786E+03  
 0.88786E+03  
 InFlow [V/T] 0.00000E+00  
 0.00000E+00  
 hMean [L] -0.11667E+02  
 -11.667

ConcVol [VM/L3] 1  
 0.00000E+00 0.00000E+00  
 cMean [M/L3] 1  
 0.00000E+00 0.00000E+00  
 -----

-----  
 Time [T] 73.0500  
 -----

-----  
 Sub-region num.  
 1  
 -----

-----  
 Area [V] 0.45360E+04  
 0.45360E+04  
 Volume [V] 0.88786E+03  
 0.88786E+03  
 InFlow [V/T] -0.82656E-04  
 -0.82656E-04  
 hMean [L] -0.10416E+02  
 -10.416

ConcVol [VM/L3] 1  
 0.00000E+00 0.00000E+00  
 cMean [M/L3] 1  
 0.00000E+00 0.00000E+00  
 WatBalT [V] -0.89256E-03  
 WatBalR [%] 0.004  
 CncBalT [VM/L3] 1  
 0.00000E+00  
 -----

-----  
 Time [T] 146.1000  
 -----

-----  
 Sub-region num.  
 1  
 -----

-----  
 Area [V] 0.45360E+04  
 0.45360E+04  
 Volume [V] 0.88785E+03  
 0.88785E+03  
 InFlow [V/T] -0.30082E-05  
 -0.30082E-05  
 hMean [L] -0.10373E+02  
 -10.373

ConcVol [VM/L3] 1  
 0.00000E+00 0.00000E+00  
 cMean [M/L3] 1  
 0.00000E+00 0.00000E+00  
 WatBalT [V] -0.11233E-01  
 WatBalR [%] 0.034  
 CncBalT [VM/L3] 1  
 0.00000E+00  
 -----

-----  
 Time [T] 219.1500  
 -----

-----  
 Sub-region num.  
 1  
 -----

-----  
 Area [V] 0.45360E+04  
 0.45360E+04  
 Volume [V] 0.88785E+03  
 0.88785E+03  
 InFlow [V/T] -0.32249E-04  
 -0.32249E-04  
 hMean [L] -0.10333E+02  
 -10.333

ConcVol [VM/L3] 1  
 0.00000E+00 0.00000E+00  
 cMean [M/L3] 1  
 0.00000E+00 0.00000E+00  
 WatBalT [V] -0.11680E-01  
 WatBalR [%] 0.029  
 CncBalT [VM/L3] 1  
 0.00000E+00  
 -----

-----  
 Time [T] 292.2000  
 -----

-----  
 Sub-region num.  
 1  
 -----

-----  
 Area [V] 0.45360E+04  
 0.45360E+04  
 Volume [V] 0.88784E+03  
 0.88784E+03  
 InFlow [V/T] -0.11117E-03  
 -0.11117E-03  
 hMean [L] -0.10293E+02  
 -10.293

ConcVol [VM/L3] 1  
 0.00000E+00 0.00000E+00  
 cMean [M/L3] 1  
 0.00000E+00 0.00000E+00  
 WatBalT [V] -0.15845E-01  
 WatBalR [%] 0.033  
 CncBalT [VM/L3] 1  
 0.00000E+00  
 -----

-----  
 Time [T] 365.2500  
 -----

-----  
 Sub-region num.  
 1  
 -----

-----  
 Area [V] 0.45360E+04  
 0.45360E+04  
 Volume [V] 0.88784E+03  
 0.88784E+03  
 InFlow [V/T] 0.61004E-06  
 0.61004E-06  
 hMean [L] -0.10254E+02  
 -10.254

ConcVol [VM/L3] 1  
 0.00000E+00 0.00000E+00  
 cMean [M/L3] 1  
 0.00000E+00 0.00000E+00  
 WatBalT [V] -0.18697E-01  
 WatBalR [%] 0.035  
 CncBalT [VM/L3] 1  
 0.00000E+00  
 -----

-----  
 Time [T] 438.3000  
 -----

-----  
 Sub-region num.  
 1  
 -----

-----  
 Area [V] 0.45360E+04  
 0.45360E+04  
 -----

Volume [V]	0.88784E+03	WatBalR [%]	0.029	Sub-region	num.
0.88784E+03		CncBalT [VM/L3]	1	1	
InFlow [V/T]	-0.19782E-04	0.00000E+00			
-0.19782E-04					
hMean [L]	-0.10215E+02			Area [V]	0.45360E+04
-10.215				0.45360E+04	
ConcVol [VM/L3]	1			Volume [V]	0.88784E+03
0.00000E+00	0.00000E+00			0.88784E+03	
cMean [M/L3]	1	Time [T]	657.4500	InFlow [V/T]	0.25815E-04
0.00000E+00	0.00000E+00			0.25815E-04	
WatBalT [V]	-0.19013E-01			hMean [L]	-0.10017E+02
WatBalR [%]	0.032	Sub-region	num.	-10.017	
CncBalT [VM/L3]	1	1		ConcVol [VM/L3]	1
0.00000E+00				0.00000E+00	0.00000E+00
				cMean [M/L3]	1
				0.00000E+00	0.00000E+00
		Area [V]	0.45360E+04	WatBalT [V]	-0.18368E-01
		0.45360E+04		WatBalR [%]	0.021
		Volume [V]	0.88784E+03	CncBalT [VM/L3]	1
		0.88784E+03		0.00000E+00	
Time [T]	511.3500	InFlow [V/T]	0.43895E-04		
		0.43895E-04			
		hMean [L]	-0.10099E+02		
		-10.099			
Sub-region	num.	ConcVol [VM/L3]	1		
1		0.00000E+00	0.00000E+00		
		cMean [M/L3]	1	Time [T]	876.6000
		0.00000E+00	0.00000E+00		
Area [V]	0.45360E+04	WatBalT [V]	-0.20240E-01		
0.45360E+04		WatBalR [%]	0.026	Sub-region	num.
Volume [V]	0.88784E+03	CncBalT [VM/L3]	1	1	
0.88784E+03		0.00000E+00			
InFlow [V/T]	-0.22718E-04			Area [V]	0.45360E+04
-0.22718E-04				0.45360E+04	
hMean [L]	-0.10177E+02			Volume [V]	0.88784E+03
-10.177				0.88784E+03	
ConcVol [VM/L3]	1	Time [T]	730.5000	InFlow [V/T]	-0.12721E-04
0.00000E+00	0.00000E+00			-0.12721E-04	
cMean [M/L3]	1			hMean [L]	-0.99745E+01
0.00000E+00	0.00000E+00	Sub-region	num.	-9.974	
WatBalT [V]	-0.19280E-01	1		ConcVol [VM/L3]	1
WatBalR [%]	0.029			0.00000E+00	0.00000E+00
CncBalT [VM/L3]	1			cMean [M/L3]	1
0.00000E+00				0.00000E+00	0.00000E+00
		Area [V]	0.45360E+04	WatBalT [V]	-0.18332E-01
		0.45360E+04		WatBalR [%]	0.019
		Volume [V]	0.88784E+03	CncBalT [VM/L3]	1
		0.88784E+03		0.00000E+00	
Time [T]	584.4000	InFlow [V/T]	-0.40891E-05		
		-0.40891E-05			
		hMean [L]	-0.10059E+02		
		-10.059			
Sub-region	num.	ConcVol [VM/L3]	1		
1		0.00000E+00	0.00000E+00	Time [T]	949.6500
		cMean [M/L3]	1		
		0.00000E+00	0.00000E+00		
Area [V]	0.45360E+04	WatBalT [V]	-0.19891E-01	Sub-region	num.
0.45360E+04		WatBalR [%]	0.024	1	
Volume [V]	0.88784E+03	CncBalT [VM/L3]	1		
0.88784E+03		0.00000E+00			
InFlow [V/T]	-0.14909E-04			Area [V]	0.45360E+04
-0.14909E-04				0.45360E+04	
hMean [L]	-0.10138E+02			Volume [V]	0.88784E+03
-10.138				0.88784E+03	
ConcVol [VM/L3]	1	Time [T]	803.5500	InFlow [V/T]	-0.20570E-05
0.00000E+00	0.00000E+00			-0.20570E-05	
cMean [M/L3]	1				
0.00000E+00	0.00000E+00				
WatBalT [V]	-0.20879E-01				

hMean [L] -0.99309E+01  
 -9.931  
 ConcVol [VM/L3] 1  
 0.00000E+00 0.00000E+00  
 cMean [M/L3] 1  
 0.00000E+00 0.00000E+00  
 WatBalT [V] -0.16086E-01  
 WatBalR [%] 0.016  
 CncBalT [VM/L3] 1  
 0.00000E+00

Time [T] 1022.7000

Sub-region num.  
 1

Area [V] 0.45360E+04  
 0.45360E+04  
 Volume [V] 0.88784E+03  
 0.88784E+03  
 InFlow [V/T] -0.48273E-05  
 -0.48273E-05  
 hMean [L] -0.98860E+01  
 -9.886  
 ConcVol [VM/L3] 1  
 0.00000E+00 0.00000E+00  
 cMean [M/L3] 1  
 0.00000E+00 0.00000E+00  
 WatBalT [V] -0.17092E-01  
 WatBalR [%] 0.016  
 CncBalT [VM/L3] 1  
 0.00000E+00

Time [T] 1095.7500

Sub-region num.  
 1

Area [V] 0.45360E+04  
 0.45360E+04  
 Volume [V] 0.88784E+03  
 0.88784E+03  
 InFlow [V/T] -0.20203E-04  
 -0.20203E-04  
 hMean [L] -0.98393E+01  
 -9.839  
 ConcVol [VM/L3] 1  
 0.00000E+00 0.00000E+00  
 cMean [M/L3] 1  
 0.00000E+00 0.00000E+00  
 WatBalT [V] -0.15265E-01  
 WatBalR [%] 0.014  
 CncBalT [VM/L3] 1  
 0.00000E+00

Time [T] 1168.8000

Sub-region num.  
 1

Area [V] 0.45360E+04  
 0.45360E+04  
 Volume [V] 0.88784E+03  
 0.88784E+03  
 InFlow [V/T] -0.18740E-04  
 -0.18740E-04  
 hMean [L] -0.97908E+01  
 -9.791  
 ConcVol [VM/L3] 1  
 0.00000E+00 0.00000E+00  
 cMean [M/L3] 1  
 0.00000E+00 0.00000E+00  
 WatBalT [V] -0.16633E-01  
 WatBalR [%] 0.015  
 CncBalT [VM/L3] 1  
 0.00000E+00

Time [T] 1241.8500

Sub-region num.  
 1

Area [V] 0.45360E+04  
 0.45360E+04  
 Volume [V] 0.88784E+03  
 0.88784E+03  
 InFlow [V/T] -0.16331E-04  
 -0.16331E-04  
 hMean [L] -0.97401E+01  
 -9.740  
 ConcVol [VM/L3] 1  
 0.00000E+00 0.00000E+00  
 cMean [M/L3] 1  
 0.00000E+00 0.00000E+00  
 WatBalT [V] -0.18052E-01  
 WatBalR [%] 0.015  
 CncBalT [VM/L3] 1  
 0.00000E+00

Time [T] 1314.9000

Sub-region num.  
 1

Area [V] 0.45360E+04  
 0.45360E+04  
 Volume [V] 0.88784E+03  
 0.88784E+03  
 InFlow [V/T] -0.36999E-05  
 -0.36999E-05  
 hMean [L] -0.96873E+01  
 -9.687  
 ConcVol [VM/L3] 1  
 0.00000E+00 0.00000E+00  
 cMean [M/L3] 1  
 0.00000E+00 0.00000E+00  
 WatBalT [V] -0.19376E-01  
 WatBalR [%] 0.016  
 CncBalT [VM/L3] 1  
 0.00000E+00

Time [T] 1387.9500

Sub-region num.  
 1

Area [V] 0.45360E+04  
 0.45360E+04  
 Volume [V] 0.88784E+03  
 0.88784E+03  
 InFlow [V/T] -0.22946E-04  
 -0.22946E-04  
 hMean [L] -0.96324E+01  
 -9.632  
 ConcVol [VM/L3] 1  
 0.00000E+00 0.00000E+00  
 cMean [M/L3] 1  
 0.00000E+00 0.00000E+00  
 WatBalT [V] -0.19057E-01  
 WatBalR [%] 0.015  
 CncBalT [VM/L3] 1  
 0.00000E+00

Time [T] 1461.0000

Sub-region num.  
 1

Area [V] 0.45360E+04  
 0.45360E+04  
 Volume [V] 0.88784E+03  
 0.88784E+03  
 InFlow [V/T] 0.19106E-04  
 0.19106E-04  
 hMean [L] -0.95762E+01  
 -9.576

ConcVol [VM/L3] 1  
 0.00000E+00 0.00000E+00  
 cMean [M/L3] 1  
 0.00000E+00 0.00000E+00  
 WatBalT [V] -0.20276E-01  
 WatBalR [%] 0.016  
 CncBalT [VM/L3] 1  
 0.00000E+00

Time [T] 1534.0500

Sub-region num.  
 1

Area [V] 0.45360E+04  
 0.45360E+04  
 Volume [V] 0.88784E+03  
 0.88784E+03  
 InFlow [V/T] -0.66423E-04  
 -0.66423E-04  
 hMean [L] -0.95166E+01  
 -9.517

ConcVol [VM/L3] 1  
 0.00000E+00 0.00000E+00  
 cMean [M/L3] 1  
 0.00000E+00 0.00000E+00  
 WatBalT [V] -0.20443E-01  
 WatBalR [%] 0.015  
 CncBalT [VM/L3] 1  
 0.00000E+00

Time [T] 1607.1000

Sub-region num.  
 1

Area [V] 0.45360E+04  
 0.45360E+04  
 Volume [V] 0.88784E+03  
 0.88784E+03  
 InFlow [V/T] 0.12816E-04  
 0.12816E-04  
 hMean [L] -0.94567E+01  
 -9.457

ConcVol [VM/L3] 1  
 0.00000E+00 0.00000E+00  
 cMean [M/L3] 1  
 0.00000E+00 0.00000E+00  
 WatBalT [V] -0.22202E-01  
 WatBalR [%] 0.016  
 CncBalT [VM/L3] 1  
 0.00000E+00

Sub-region num.  
 1

Area [V] 0.45360E+04  
 0.45360E+04  
 Volume [V] 0.88784E+03  
 0.88784E+03  
 InFlow [V/T] 0.11048E-04  
 0.11048E-04  
 hMean [L] -0.93943E+01  
 -9.394

ConcVol [VM/L3] 1  
 0.00000E+00 0.00000E+00  
 cMean [M/L3] 1  
 0.00000E+00 0.00000E+00  
 WatBalT [V] -0.21258E-01  
 WatBalR [%] 0.015  
 CncBalT [VM/L3] 1  
 0.00000E+00

Time [T] 1753.2000

Sub-region num.  
 1

Area [V] 0.45360E+04  
 0.45360E+04  
 Volume [V] 0.88784E+03  
 0.88784E+03  
 InFlow [V/T] -0.25515E-04  
 -0.25515E-04  
 hMean [L] -0.93299E+01  
 -9.330

ConcVol [VM/L3] 1  
 0.00000E+00 0.00000E+00  
 cMean [M/L3] 1  
 0.00000E+00 0.00000E+00  
 WatBalT [V] -0.21409E-01  
 WatBalR [%] 0.015  
 CncBalT [VM/L3] 1  
 0.00000E+00

Time [T] 1826.2500

Sub-region num.  
 1

Area [V] 0.45360E+04  
 0.45360E+04

Volume [V] 0.88783E+03  
 0.88783E+03  
 InFlow [V/T] -0.88273E-05  
 -0.88273E-05  
 hMean [L] -0.92642E+01  
 -9.264

ConcVol [VM/L3] 1  
 0.00000E+00 0.00000E+00  
 cMean [M/L3] 1  
 0.00000E+00 0.00000E+00  
 WatBalT [V] -0.23022E-01  
 WatBalR [%] 0.016  
 CncBalT [VM/L3] 1  
 0.00000E+00

Time [T] 1899.3000

Sub-region num.  
 1

Area [V] 0.45360E+04  
 0.45360E+04  
 Volume [V] 0.88784E+03  
 0.88784E+03  
 InFlow [V/T] 0.12899E-05  
 0.12899E-05  
 hMean [L] -0.91958E+01  
 -9.196

ConcVol [VM/L3] 1  
 0.00000E+00 0.00000E+00  
 cMean [M/L3] 1  
 0.00000E+00 0.00000E+00  
 WatBalT [V] -0.21664E-01  
 WatBalR [%] 0.015  
 CncBalT [VM/L3] 1  
 0.00000E+00

Time [T] 1972.3500

Sub-region num.  
 1

Area [V] 0.45360E+04  
 0.45360E+04  
 Volume [V] 0.88784E+03  
 0.88784E+03  
 InFlow [V/T] 0.10936E-04  
 0.10936E-04  
 hMean [L] -0.91249E+01  
 -9.125

ConcVol [VM/L3] 1  
 0.00000E+00 0.00000E+00  
 cMean [M/L3] 1  
 0.00000E+00 0.00000E+00  
 WatBalT [V] -0.21874E-01



WatBalR [%]	0.014	Sub-region	num.	hMean [L]	-0.87386E+01
CncBalT [VM/L3]	1	1		-8.739	
0.00000E+00		-----		ConcVol [VM/L3]	1
-----				0.00000E+00	0.00000E+00
-----		Area [V]	0.45360E+04	cMean [M/L3]	1
-----		0.45360E+04		0.00000E+00	0.00000E+00
-----		Volume [V]	0.88784E+03	WatBalT [V]	-0.19455E-01
-----		0.88784E+03		WatBalR [%]	0.012
Time [T]	2045.4000	InFlow [V/T]	0.28896E-04	CncBalT [VM/L3]	1
-----		0.28896E-04		0.00000E+00	
-----		hMean [L]	-0.89002E+01	-----	
Sub-region	num.	-8.900		-----	
1		ConcVol [VM/L3]	1	-----	
-----		0.00000E+00	0.00000E+00	Time [T]	2410.6500
-----		cMean [M/L3]	1	-----	
Area [V]	0.45360E+04	0.00000E+00	0.00000E+00	-----	
0.45360E+04		WatBalT [V]	-0.19322E-01	-----	
Volume [V]	0.88784E+03	WatBalR [%]	0.012	Sub-region	num.
0.88784E+03		CncBalT [VM/L3]	1	1	
InFlow [V/T]	0.18209E-04	0.00000E+00		-----	
0.18209E-04		-----		-----	
hMean [L]	-0.90524E+01	-----		Area [V]	0.45360E+04
-9.052		-----		0.45360E+04	
ConcVol [VM/L3]	1	-----		Volume [V]	0.88784E+03
0.00000E+00	0.00000E+00	-----		0.88784E+03	
cMean [M/L3]	1	Time [T]	2264.5500	InFlow [V/T]	0.17173E-04
0.00000E+00	0.00000E+00	-----		0.17173E-04	
WatBalT [V]	-0.21072E-01	-----		hMean [L]	-0.86543E+01
WatBalR [%]	0.014	Sub-region	num.	-8.654	
CncBalT [VM/L3]	1	1		ConcVol [VM/L3]	1
0.00000E+00		-----		0.00000E+00	0.00000E+00
-----		-----		cMean [M/L3]	1
-----		Area [V]	0.45360E+04	0.00000E+00	0.00000E+00
-----		0.45360E+04		WatBalT [V]	-0.17632E-01
Time [T]	2118.4500	Volume [V]	0.88784E+03	WatBalR [%]	0.011
-----		0.88784E+03		CncBalT [VM/L3]	1
-----		InFlow [V/T]	0.66780E-05	0.00000E+00	
-----		0.66780E-05		-----	
-----		hMean [L]	-0.88203E+01	-----	
Sub-region	num.	-8.820		-----	
1		ConcVol [VM/L3]	1	-----	
-----		0.00000E+00	0.00000E+00	-----	
-----		cMean [M/L3]	1	-----	
Area [V]	0.45360E+04	0.00000E+00	0.00000E+00	Time [T]	2483.7000
0.45360E+04		WatBalT [V]	-0.18015E-01	-----	
Volume [V]	0.88784E+03	WatBalR [%]	0.011	-----	
0.88784E+03		CncBalT [VM/L3]	1	Sub-region	num.
InFlow [V/T]	0.52870E-05	0.00000E+00		1	
0.52870E-05		-----		-----	
hMean [L]	-0.89766E+01	-----		-----	
-8.977		-----		Area [V]	0.45360E+04
ConcVol [VM/L3]	1	-----		0.45360E+04	
0.00000E+00	0.00000E+00	-----		Volume [V]	0.88784E+03
cMean [M/L3]	1	Time [T]	2337.6000	0.88784E+03	
0.00000E+00	0.00000E+00	-----		InFlow [V/T]	-0.49019E-05
WatBalT [V]	-0.20025E-01	-----		-0.49019E-05	
WatBalR [%]	0.013	Sub-region	num.	hMean [L]	-0.85661E+01
CncBalT [VM/L3]	1	1		-8.566	
0.00000E+00		-----		ConcVol [VM/L3]	1
-----		-----		0.00000E+00	0.00000E+00
-----		Area [V]	0.45360E+04	cMean [M/L3]	1
-----		0.45360E+04		0.00000E+00	0.00000E+00
-----		Volume [V]	0.88784E+03	WatBalT [V]	-0.18596E-01
-----		0.88784E+03		WatBalR [%]	0.011
Time [T]	2191.5000	InFlow [V/T]	0.22967E-04	CncBalT [VM/L3]	1
-----		0.22967E-04		0.00000E+00	
-----		-----		-----	



Time [T]	3068.1000	Sub-region	num.	Area [V]	0.45360E+04
-----					
Sub-region	num.	-----			
1		Area [V]	0.45360E+04	Volume [V]	0.88783E+03
-----					
Area [V]	0.45360E+04	0.88783E+03	InFlow [V/T]	0.58620E-05	hMean [L]
0.45360E+04			-0.30472E-04	-7.529	ConcVol [VM/L3]
Volume [V]	0.88783E+03	-0.30472E-04	hMean [L]	-0.75294E+01	0.00000E+00
0.88783E+03			-7.647	0.00000E+00	0.00000E+00
InFlow [V/T]	0.11025E-04	ConcVol [VM/L3]	1	0.00000E+00	0.00000E+00
0.11025E-04		0.00000E+00	0.00000E+00	0.00000E+00	0.00000E+00
hMean [L]	-0.77643E+01	cMean [M/L3]	1	0.00000E+00	0.00000E+00
-7.764		0.00000E+00	0.00000E+00	0.00000E+00	0.00000E+00
ConcVol [VM/L3]	1	WatBalT [V]	-0.27587E-01	WatBalR [%]	0.015
0.00000E+00	0.00000E+00	0.00000E+00	0.015	CncBalT [VM/L3]	1
0.00000E+00	0.00000E+00	0.00000E+00	0.015	0.00000E+00	
cMean [M/L3]	1	WatBalT [V]	-0.27587E-01	-----	
0.00000E+00	0.00000E+00	WatBalR [%]	0.015	-----	
0.00000E+00	0.00000E+00	CncBalT [VM/L3]	1	-----	
0.00000E+00	0.00000E+00	0.00000E+00		-----	
WatBalT [V]	-0.26824E-01	-----			
-0.26824E-01		-----			
WatBalR [%]	0.014	-----			
0.014		-----			
CncBalT [VM/L3]	1	-----			
0.00000E+00		-----			
-----					
-----					
Time [T]	3214.2000	Sub-region	num.	Area [V]	0.45360E+04
-----					
Sub-region	num.	-----			
1		Area [V]	0.45360E+04	Volume [V]	0.88783E+03
-----					
InFlow [V/T]	0.22811E-05	0.22811E-05		0.88783E+03	
0.22811E-05					
hMean [L]	-0.74088E+01	-7.409			
-0.74088E+01					
ConcVol [VM/L3]	1	0.00000E+00	0.00000E+00		
1	0.00000E+00	0.00000E+00			
cMean [M/L3]	1	0.00000E+00	0.00000E+00		
1	0.00000E+00	0.00000E+00			
WatBalT [V]	-0.28031E-01				
-0.28031E-01					
WatBalR [%]	0.015				
0.015					
CncBalT [VM/L3]	1	0.00000E+00			
1	0.00000E+00				
-----					
-----					
Time [T]	3360.3000	-----			
-----					
Sub-region	num.	-----			
1		-----			
-----					
Area [V]	0.45360E+04	0.45360E+04			
0.45360E+04					
Volume [V]	0.88783E+03	0.88783E+03			
0.88783E+03					
InFlow [V/T]	0.39303E-05	0.39303E-05			
0.39303E-05					
hMean [L]	-0.72885E+01	-7.288			
-0.72885E+01					